PFC/RR-86-1 UC20a,d

The Kinetics Of Liquid Lithium Reaction With Oxygen-Nitrogen Mixtures

by

T. K. Gil

M. S. Kazimi

Plasma Fusion Center
and the
Department of Nuclear Engineering
Massachusetts Institute of Technology
Cambridge, Massachusetts 02139

January 1986

Prepared for
EG&G Idaho, Inc.,
and
The U.S. Department of Energy
Idaho Operations Office
under
DOE Contract #DE-APO7-791DOO19

Abstract

A series of experiments have been conducted in order to characterize the kinetics of lithium chemical reaction with a mixture of oxygen and nitrogen. Three mixed gas compositions were used; 80% N_2 and 20% O_2, 90% N_2 and 10% O_2, and 95% N_2 and 5% O_2. The reaction rate was obained as a function of lithium temperature and the oxygen fraction. Liquid lithium temperature varied from 400 to 1100° C. By varying the composition, the degree of inhibition of the lithium-nitrogen reaction rate due to the presence of oxygen was observed. The results indicate that the lithium-nitrogen reaction rate depended on both the fraction of oxygen present and lithium temperature. The lithium nitride layer formed from the reaction also had a significant inhibition effect on the lithium-nitrogen reaction rate while the lithium-oxygen reaction rate was not as greatly hindered.

LITFIRE, a computer code which simulates temperature and pressure history in a containment building following lithium spills, was modified by including 1) an improved model for the lithium-nitrogen reaction rate and 2) a model for the lithium-CO_2 reaction. LITFIRE was used to simulate HEDL's LC-2 and LA-5 experiments, and the predicted temperatures and pressures were in a reasonable agreement. Furthermore, LITFIRE was applied to a prototypical fusion reactor containment in order to simulate the consequences of a lithium spill accident. The result indicated that if nitrogen was used as containment building gas during the accident, the consequences of the accident would be less severe than those with air. The pressure rise in the building was found to be reduced by 50% and the maximum temperature of the combustion zone was limited to 900 °C instead of 1200 °C in the case of air.

Acknowledgements

The authors would like to thank Mr. David Jeppson of HEDL who gave advise on several aspects of the experiments. The assistance from many individuals at the nuclear engineering machine shop is well appriciated. Also, continuous suggestions and assistance from Mr. P. Menedier and R. Childs are greatly appreciated. The authors are grateful to Bill Ijams who gave much time and assistance in the critical initial phase of this work. The cooperation of R. Rozier in the oxygen experiments is also acknowledged.

This work would not have been possible without the financial support of the Fusion Safety Program of INEL/EG&G, Idaho and the DOE Office of Fusion Energy.

Table of Contents

List of Figures

List of Tables

CHAPTER I Introduction

1.1 Background and Motivation for Current Work

In conceptual designs of fusion power plants for the production of electrical and thermal energy, liquid lithium has been found to be one of the preferred materials as a tritium breeder and primary coolant. Its low melting point, high boiling point, low vapor pressure, low density, high heat capacity, high thermal conductivity, good solubility of tritium, and low viscosity characterstics, all support liquid lithium as a desirable breeder and coolant.

Unfortunately, lithium, as a member of the alkali metals, is also highly corrosive at high temperatures and high fluid flow rates, particularly if it contains non-metallic impurities. A major safety concern of using lithium is the potentially large amount of energy that could be released into the containment from lithium-air or lithium-water chemical reactions. For a typical fusion reactor design, lithium reactions in air and concrete can amount to approximately 10^8 to 10^9 J available in chemical energy [1]. This energy may be sufficient to cause melting and/or volatilization of structural materials as well as substantial pressurization of the containment building. In consequence, the high temperature coupled with possible pressurization of the containment, may lead to failure of the containment integrity. Here, aside from the structural damage, a major concern is volatilization of radioactive structural materials such as the first wall of a tokamak torus. Indeed, lithium fires pose a potential danger of releasing radioactive nuclides outside the fusion reactors.

Due to these safety concerns with pure liquid lithium, concerned designers of fusion reactors have proposed replacing lithium as a breeder with other lithium based materials such as lithium-lead alloys (Li_7Pb_2, $Li_{17}Pb_{83}$, $LiPb_4$),

LiAl, Li_2O, and FLIBE. These materials are less reactive to use than pure lithium. However, lithium's excellent inherent characteristics as a breeder and coolant make lithium a strong candidate as both breeder and coolant, if chemical control in fusion reactors can be properly handled to prevent the contact with oxygen in free or compound forms [2]. A comparison of alternate coolants and breeders appears in Table 1.1 while a list of the important chemical reactions of lithium and LiPb compounds is shown in Table 1.2.

Due to the potentially large amount of hot flowing lithium in fusion reactors, one must be aware of the hazards of lithium leaks and spills. Presently, significant effort is dedicated to characterizing the reaction kinetics of both lithium and lithium-lead compounds. Starting in 1978, Handford Engineering Development Laboratory (HEDL) has been conducting a series of experiments to observe lithium interaction with various gases, water and ceramic compounds such as concretes and insulating materials. Along with HEDL's experiments, a computer code, LITFIRE, has been developed at MIT in order to predict pressures and temperatures generated inside a fusion reactor containment by a large lithium spill. Furthermore, lithium reaction kinetics experiments have also been conducted at MIT. In 1984, W. Ijams performed a series of experiments in order to obtain the lithium-nitrogen reaction rate as a function of the lithium pool temperature. These experiments have been performed to increase the state of knowledge concerning lithium and the effects of spills as well as to formulate an engineering database for the combustion of lithium. The results of all these experiments were used to calibrate many of the empirical relations found in LITFIRE.

TABLE 1.1

Comparison of Alternative Coolants and Breeders [2,15]

Material	(B = Breeder) (C = Coolant)	Advantage	Disadvantage
Lithium	B & C	Excellent heat transfer High boiling point Low melting point High specific heat Low viscosity Good neutron moderator No long-term activation products No neutron damage High breeding ratio possible Low density Low vapor pressure High thermal conductivity Tritium recovery demonstrated	Highly reactive with: air, water, concrete High electrical conductivity
Li17Pb83	B & C	Lower chemical reactivity than lithium High breeding ratio possible Lead is a good neutron shield for magnets Tritium recovery feasible	Poor database Low heat capacity High density Activation product Reactive with water or lithium coolant Low tritium solubility results in high leakage potential High electrical conductivity
Flibe (34 BeF2 : 66 LiF)	B & C	Good neutron moderator Low vapor pressure Low electrical conductivity Low chemical reactivity	Scarcity of beryllium Low thermal conductivity Relatively high melting temperature
LiAlO2	B	Chemical stability Highest melting temperature Low thermal conductivity Much more resistant of thermal expansion and swelling than LiO2	Requires neutron multiplication
Water	C	Substantial engineering experience and database	React with Li and LiPb alloys High pumping power High operating pressure Poor tritium control

TABLE 1.2

Lithium Reactions of Particular Interest [3]

			Heat of Reaction ΔH_{298} Kcal/mole of product
In Air:			
$4Li + O_2$	⟶	$2Li_2O$	-143
$2Li + O_2$	⟶	Li_2O_2	-152
$6Li + N_2$	⟶	$2Li_3N$	-48
$2Li + 2H_2O$	⟶	$2LiOH + H_2$	-49
$2Li + H_2$	⟶	$2LiH$	-21.6
$2Li + LiOH$	⟶	$2LiO_2 + H_2$	
$4Li + 3CO_2$	⟶	$2Li_2CO_3 + C$	-148.6
$2Li + 2C$	⟶	Li_2C_2	-14.2
$2Li + 3H_2 + 2O_2$	⟶	$LiOH \cdot H_2O$	-189
With Concretes:			
$8Li + Fe_3O_4$	⟶	$3Fe + 4Li_2O$	-151.3 (magnetite)
$4Li + SiO_2$	⟶	$Si + 2Li_2O$	(basalt)
$2Li + H_2$	⟶	$2LiH$	-21.6
Others:			
$nLi + mPb$	⟶	$Li_n Pb_m$	$-13n$ for $\frac{n}{m} < 1$

Note: Li_2O_2 is unstable above 250 °C.

1.2 Scope of Present Work

This study involves two main areas: one is experimental determination of the reaction kinetics of liquid lithium with nitrogen and oxygen, and the other is modification of the code LITFIRE. The first major effort is placed on obtaining experimental data on the reaction kinetics of liquid lithium with the mixed gas. This includes: 1) upgrading the previous experimental apparatus in order to improve accuracy and consistency of experimental data; 2) spot checking and verifying Ijams's lithium-nitrogen reaction rate; 3) measuring the reaction rate of lithium under nitrogen-oxygen atmosphere while observing the nitrogen and oxygen reaction rate inhibition factors; and 4) observing the lithium-oxygen reaction rate in few experiments.

The second major task of this study involves the following modifications of LITFIRE. First, applying Ijams's lithium-nitrogen reaction rate in the code, HEDL's LA-5 experiment is re-simulated. And then, the "new" LITFIRE (MOD4) is compared with the "old" LITFIRE (MOD3). In addition, a parametric study on the sensitivity of the nitrogen and oxygen inhibition factors is performed, and the result is applied to the LA-5 test simulation. Second, using the LITFIRE-MOD4, a case study of a postulated large lithium spill accident for prototypical fusion reactor conditions under both air and nitrogen atmospheres is performed. And third, a lithium-carbon dioxide reaction model is added to the code allowing pure carbon dioxide environment in which the lithium-CO_2 reaction can take place, and normal air environment in which lithium-CO_2 reaction is allowed as part of the multiple-reactions. Then, the modified version of LITFIRE is checked against HEDL's experiment, LC-2, the sole lithium ignited experiment which has been performed in this area. The CO_2 capability enables the code to assess the hazards of Li spills if the building gas atmosphere was CO_2.

CHAPTER II Review of Previous Investigations

2.1 History of Lithium Air Reaction Kinetics Experiments

2.1.1 Earlier Reaction Kinetics Experiments

Before mentioning the recent history of lithium-air reaction kinetics experiments, it is important to realize that in 1970 there was a serious lack of data on physical and chemical properties of lithium including chemical reactions lithium may undergo with various materials. The validity and applicability of the past small scale experiments for large scale, high temperature accident conditions had to be verified by actual experimentation. During the past decade, the state of knowledge concerning lithium and the effects of spills has been significantly improved due to the considerable effort spent on this area. Reference [3] is an excellent source for reviewing lithium's properties and chemical interactions.

i) Reactions with Nitrogen

First noticeable experiment on the nitridation of lithium was performed by E.F. McFarlane and F.C. Tompkins [4]. They attempted to find how the low temperature lithium-nitrogen reaction rate changes with time. The lithium pool temperature in this experiment was 345.5 °C. From their experiments, they concluded that the reaction rate depends on the rate of diffusion of the lithium gas through the intervening nitride layer. They accepted this mechanism because, first, it was not dependent on the gas pressure, and, second, because it required the nitrogen consumption to follow a parabolic law. A parabolic law governs reactions in which the rate controlling mechanism is the diffusion of one of the reactants through a surface film.

In order to determine the effect of the nitrogen layer on the lithium-nitrogen reaction kinetics, C.C. Addison and B.M. Davies performed a series

of experiments in 1969. While running their experiment at a temperature of 400 °C, they spun a magnet under a lithium pool at 3000 rpm, which induced currents in the lithium and caused the metal to rotate rapidly [5]. By placing a metal baffle at the surface of the spinning pool, they were able to break up the forming nitride and maintain a clean lithium surface for some time. Thus, by running some unstirred tests, a comparison between the nitridation reaction of a clean lithium surface and the reaction of a nitride coated lithium surface could be made.

From their experiments, they once again verified that the nitrogen consumption depends on a parabolic law for the unstirred case. However, in the early stages, the reaction seemed to pass from a linear stage to a logarithmic transition stage to the dominating parabolic stage. This indicated that in the early stage of the reaction, cracks in the nitride layer allowed for an unhindered lithium nitrogen reaction for as long as they existed in large numbers. Then, as the cracks were completely sealed, the reaction followed a parabolic path. Therefore, although the parabolic law prevails in the unstirred reaction as McFarlane and Tompkins indicated, when there is no established nitride layer, a different mechanism must be postulated. However, Addison and Davies could not conclude what this new mechanism was. They postulated two possible mechanisms. One is that the lithium nitrogen reaction could take place at the metal surface, a process involving chemisorption of the lithium, followed by electron transfer. The other one is that the nitrogen might first dissolve in the liquid lithium, as lithium has a high nitrogen solubility.

In addition, Addison and Davies observed that liquid lithium has an unusual property of spreading and covering the entire inner surface of its container. As the reaction rate is a function of the lithium surface area, this mechanism may greatly affect accuracy of reaction rate measurements; particularly if the container is relatively small.

ii) Reactions with Oxygen

Solid lithium is highly resistant to oxidation even at elevated temperatures in pure oxygen or even in dry air atmospheres [3]. The rate of oxidation of lithium is low all the way to the ignition temperature cited to be as high as 630 °C [3]. No reaction of lithium in dry oxygen occurs below 250 °C. With moist oxygen, the reaction proceeds exothermally. As observed in lithium-nitrogen surface reaction, the oxide coating that forms on the surface of solid lithium at low temperature may effectively prevent further reaction of lithium with oxygen. These reports are based on early experimentation. There has been no recent large-scale experiment. Due to its high heat of formation (about three and half larger than Li_3N formation) and vigorous reaction at high temperatures, a high temperature experiment is expected to be very difficult to perform.

iii) Reactions with Air

Solid lithium reacts slowly in dry air. In moist air, it oxidizes more rapidly... Solid lithium becomes coated with lithium nitride, lithium hydroxide, lithium monohydrate, lithium carbonate, lithium carbide, and lithium oxide. Earlier experiments show that actual reaction rates, products, and temperatures are contradictory. Values between 180 °C and 640 °C have been reported for the ignition temperatures of lithium in air [3]. Many small as well as quite large (100 Kg of lithium) experiments were conducted at HEDL which show more consistent and reliable data. The HEDL's experiments will be explained in detail in a later section.

iv) Reactions with CO_2

According to reference [6], dry carbon dioxide will not react with lithium at temperatures up to 300 °C. Lithium carbonate, the reaction product from lithium-carbon dioxide interaction, is comparatively insoluble in water in contrast to corresponding alkali salts. It has been observed that formation of the protec-

tive carbonate coating slows the reaction significantly. However, the HEDL's experiments indicate that the lithium- carbon dioxide reaction is very vigorous at high temperatures and the carbonate layer inhibition effect is negligible.

2.1.2 Ijams's Experiements on Lithium-Nitrogen Reaction Kinetics

In 1984, W. Ijams at MIT ran a series of experiments in order to characterize lithium pool temperature dependent lithium-nitrogen reaction kinetics under forced convection [7]. From these experiments, he was able to obtain a lithium-nitrogen reaction rate curve as a function of lithium pool temperature. Figure 2.1 shows the entire apparatus involved in his experiment while Figure 2.2 shows the lithium pool container in detail.

The basic approach in his experiment was to measure the pressure decrease due to the combustion of lithium reacting with nitrogen. Prepurified nitrogen gas, taken from a highly pressurized tank, passed through a Linde Molecular Sieve, Grade 4A, to remove water, and then flowed into the tank 1 where it was stored. During a run, the pure nitrogen flew from tank 1 to the preheated reaction site and the preheated lithium pool, while constant flow rate was maintained. At the reaction site, some gas reacted with pure liquid lithium at a known temperature, and the unreacted gas and generated aerosols passed through the heat exchanger and the filter, and were eventually stored in tank 2. Pressure gauges on tank 1 and 2 recorded the respective losses and gains of pressure. Using thermocouples to record gas temperatures, the respective losses and gains of gas (in units of moles) can be deduced using the ideal gas law.

The difference between the amount of gas accumulated in tank 2 and the amount lost from tank 1 is equal to the amount of gas lost to the lithium-nitrogen reaction. Using internal clock in a data acquisition system, the reaction rate was deduced.

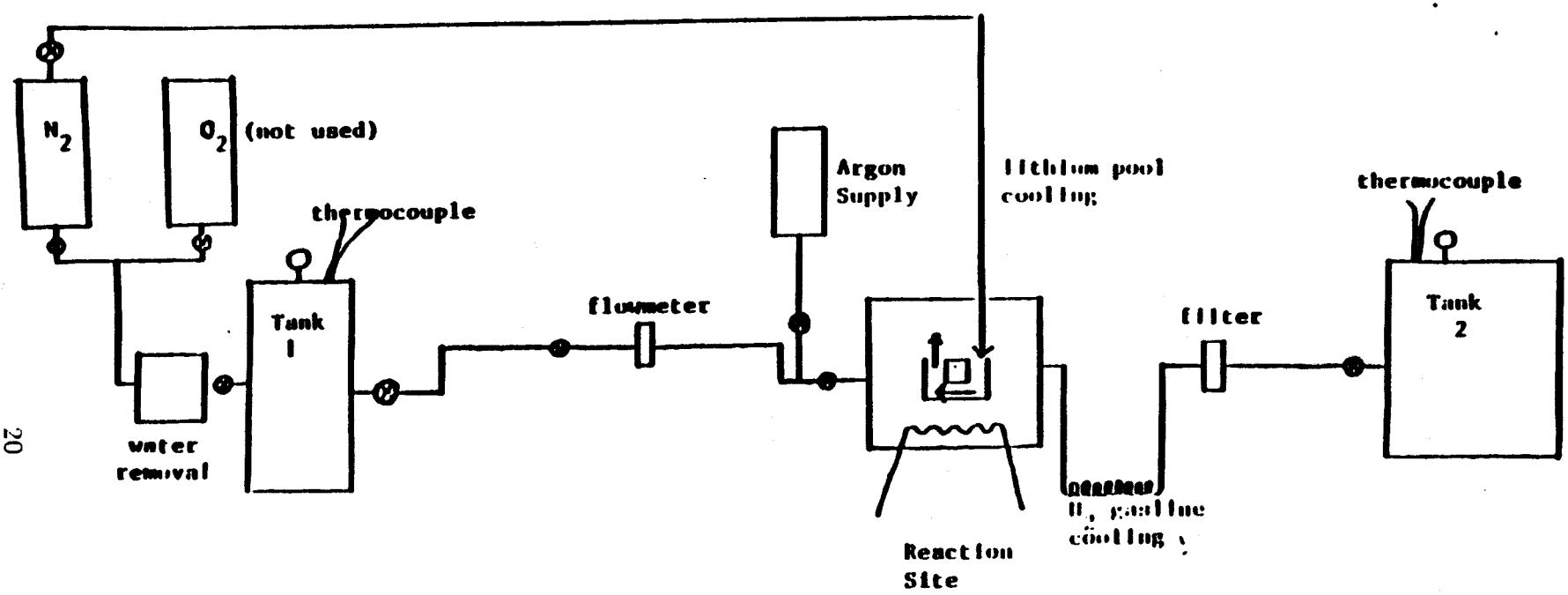

Fig. 2.1 Experimental appatus of Ijams

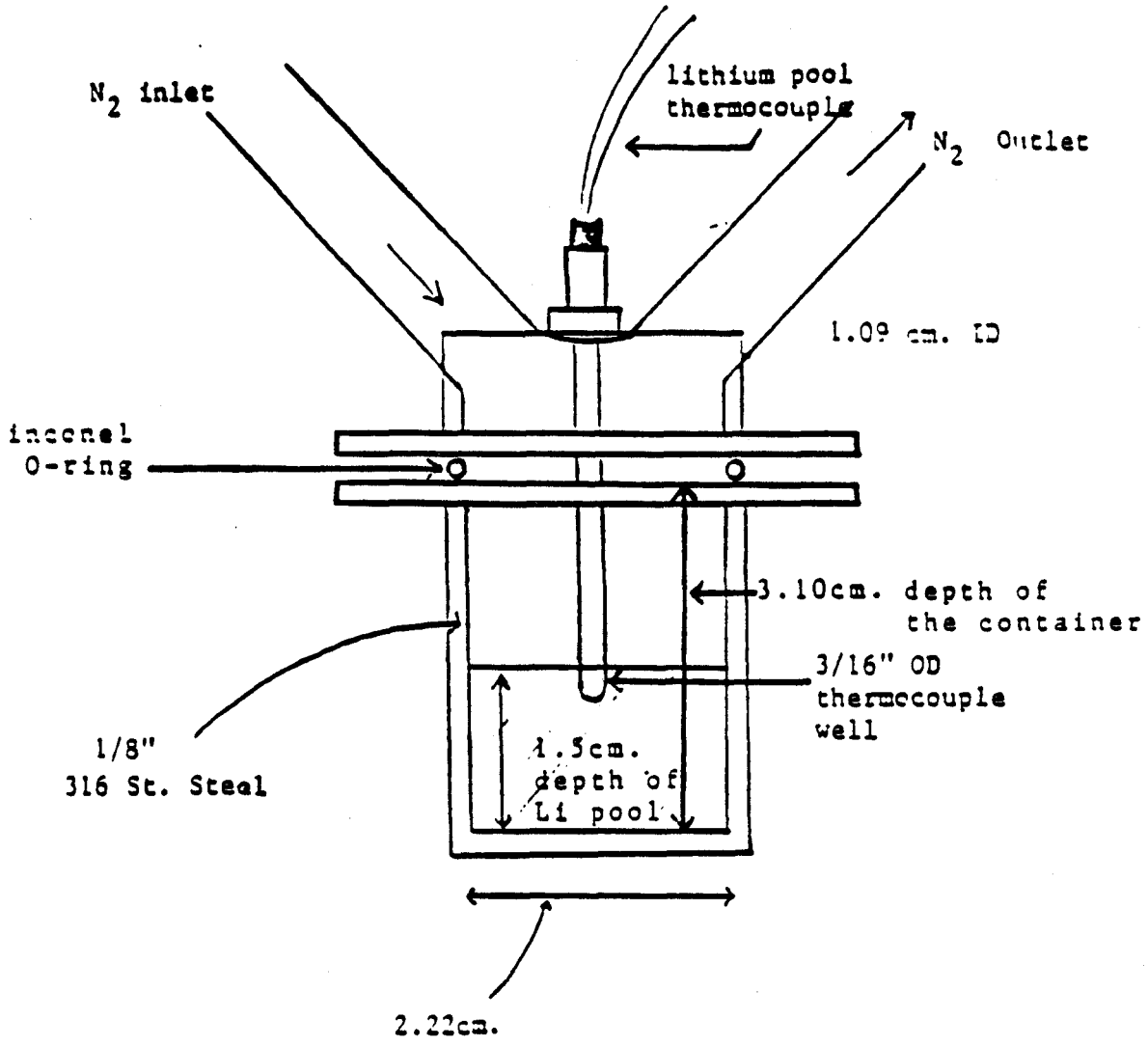

Fig. 2.2 lithium pool container

From his experiments, he obtained a relation between lithium-nitrogen reaction rate and the lithium pool temperature which is shown in Figure 2.3. Ijams explained possible experimental uncertainties associated with lithium-nitrogen reaction kinetics experiments. The first identified source of uncertainty is the formation of a nitride layer which caused subsequent slowing of the reaction rate. However, this is a fundamental phenomenon of the lithium-nitrogen reaction; this effect should be included in the analysis of lithium spills in fusion reactors.

The second source of uncertainty was caused by an increase in the lithium pool surface area, which in turn was caused by two things: first, the molten lithium climbed along the walls and roof of the container, as Addison and Davies indicated this unusual property of spreading. Second, the contours of the cooled nitride surface were often quite irregular, implying that the lithium surface was not flat during the reaction. An increase in the lithium pool surface area means an increase in the reaction rate. Ijams attempted to eliminate the spreading effect by measuring the reaction rate few seconds after the gas started to flow into the reaction site to allow for burning thin lithium films along the walls and roof of the container. This may have introduced some error since nitrogen reacted with the lithium at the pool surface forming a nitride layer.

Third, impurities in the lithium and in the nitrogen affected the reaction rate. Fourth, uncertainties in meter readings, and gas volume measurements, and the effects of the gasline friction pressure drop added to a significant uncertainty. Fifth, at high temperatures, insufficient gas flow led to gas flow controlled reaction rates while the goal of the experiment was to measure reaction rates independent of the gas flow. In addition, one important source of uncertainty came from the drastic changes in the lithium pool temperature due to the vigorous reaction at high temperatures in spite of much efforts to control it. The error bars due to the combined uncertainties are shown in Fig. 2.3.

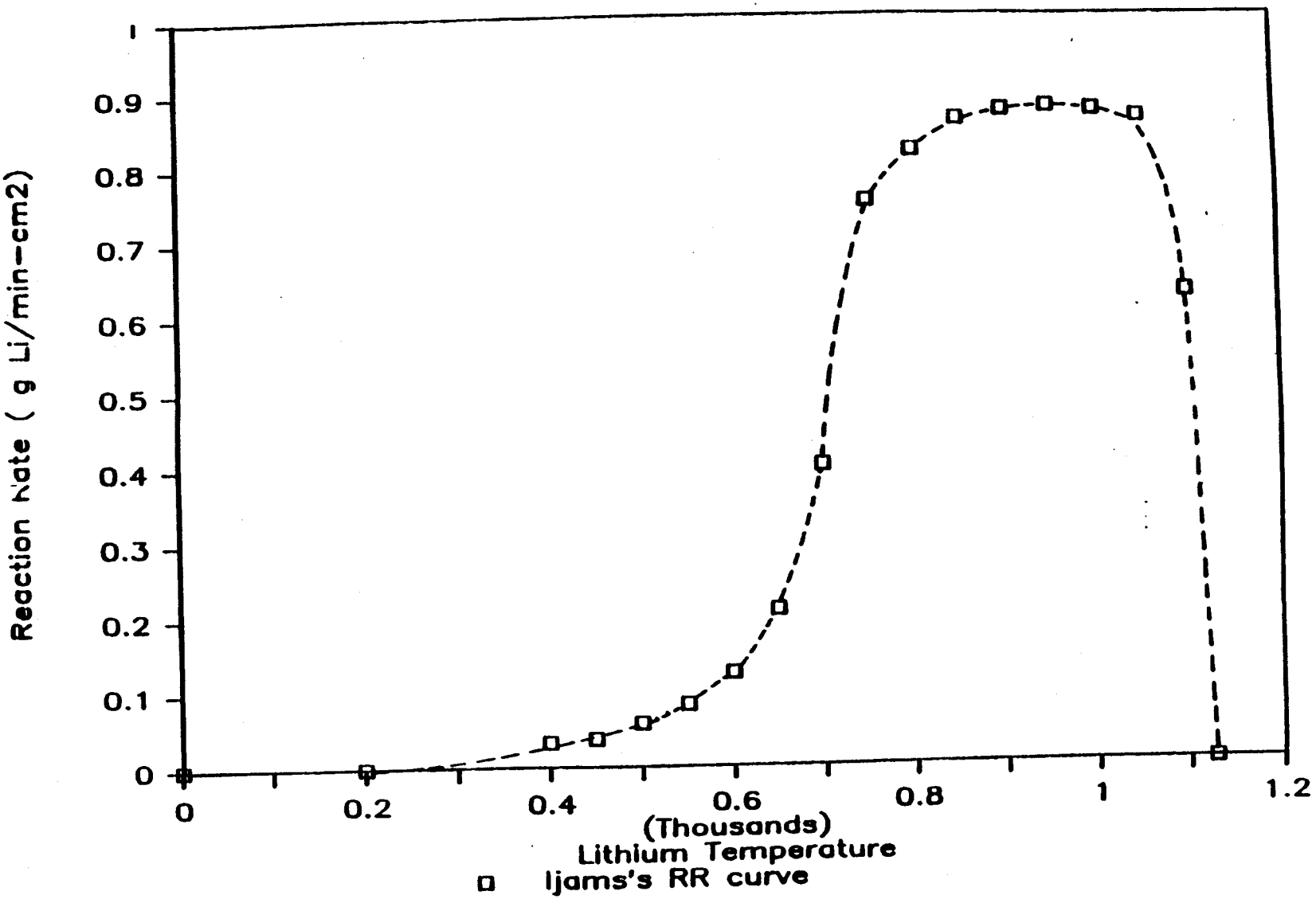

Fig. 2.3 Ijams's Lithium-Nitrogen reaction rate curve in a function of lithium pool temperature.

2.2 HEDL's Experiments

Since 1978, Hanford Eningeering Development Laboratory (HEDL) has been performing a series of experiments in order to scope the effects of lithium reactions with various materials which may be present in future fusion reactors [8,9,10]. The objectives of HEDL's tests were to provide data to: 1) substantiate the safety analysis of fusion facilities under both normal operating and postulated accident situations; 2) assist in making design decisions for both power plants and support facilities; and 3) document experience in handling large quantities of liquid lithium under normal operating and minor accident conditions. Table 2.1 shows a summary of the HEDL's experiments which are of interest in this study. They included the experiments in the following areas: 1) lithium-air reaction, 2) lithium-nitrogen reaction, 3) lithium-moist air reaction, and 4) lithium-carbon dioxide reaction. In addition, HEDL ran a series of experiments involving lithium interaction with water and various types of concretes.

The basic geometry of the test facility to be described below is shown in Figure 2.4 and 2.5. All of the experiments described have been performed at HEDL's Large Sodium Fire Facility (LSFF). For small scale experiments, the Small Fires Room was used while larger scale ones were performed at the Air Cleaning Room. Figure 2.4 shows the Small Fires Room and Figure 2.5 shows the reaction pan of small-scale experiments in detail. The lithium pool-air (LA-4 and LA-5) reaction tests were performed in a carbon steel containment vessel measuring 20.4 meters in height and 7.6 meters in diameter with standard dished top and bottom heads. This containment formed the primary pressure and aerosol boundary within which each test was carried out. Inner surfaces were coated with a modified phenolic paint and the interior of the vessel was essentially void. However, the platform and structural supports provided a 50 percent increase in horizontal surface area for aerosol particle settling.

TABLE 2.1

Summary of HEDL's Experiments on Lithium-Gas Reactions [8,9,11]

Test	Li-Air					Li-Moist Air		Li-Nitrogen			Li-CO2	
Test Number	LA-1	LA-2	LA-3	LA-4	LA-5	LAM-1	LAM-2	LN-1	LN-2	LN-3	LC-1	LC-2
Amount of Li. (Kg)	10	10	45.4	26.7	100	10	10	10	10	10	10	10
Lithium pool surface area (m2)	0.2	0.2	0.555	0.124	2.0	0.2	0.2	0.2	0.2	0.2	0.2	0.2
Initial Li. temperature (C)	243	510	232	600	500	248	539	222	532	840	238	540
Peak Lithium temp. (C)	1038*	950	1040	-	1147	1060	1100	224	542	960	238	1350
Containment vessel temp. (C)	28	45	-	31	32	24	68	37	37	46	47	52
Peak containment vessel temp. (C)	102	118	-	68	83	113	165	37	49	82	47	100**
Vessel wall temp. (C)	28	45	-	-	31	18	46	30	29	38	40	31
Peak vessel wall temp. (C)	68	75	-	-	50	60	100	30	41	66	42	50**
Flame temperature (C)	1260	1110	-	-	-	1150	890	-	-	-	-	>1400
Aerosol generated (% Li)	-	-	7.3	-	-	6.1	7.3	-	-	-	-	3
Max. 1/2 hour burning rate (Kg Li/m2)	-	-	21	-	-	27	12.6	-	0.44***	5.67***	-	6.9***

* surface reaction temperature.

** Around 3 min. after the initiation of reaction, the pan was corroded. All the temperatures reported here are at 3 min. after the reaction is initiated.

*** In Kg Li/m2-min

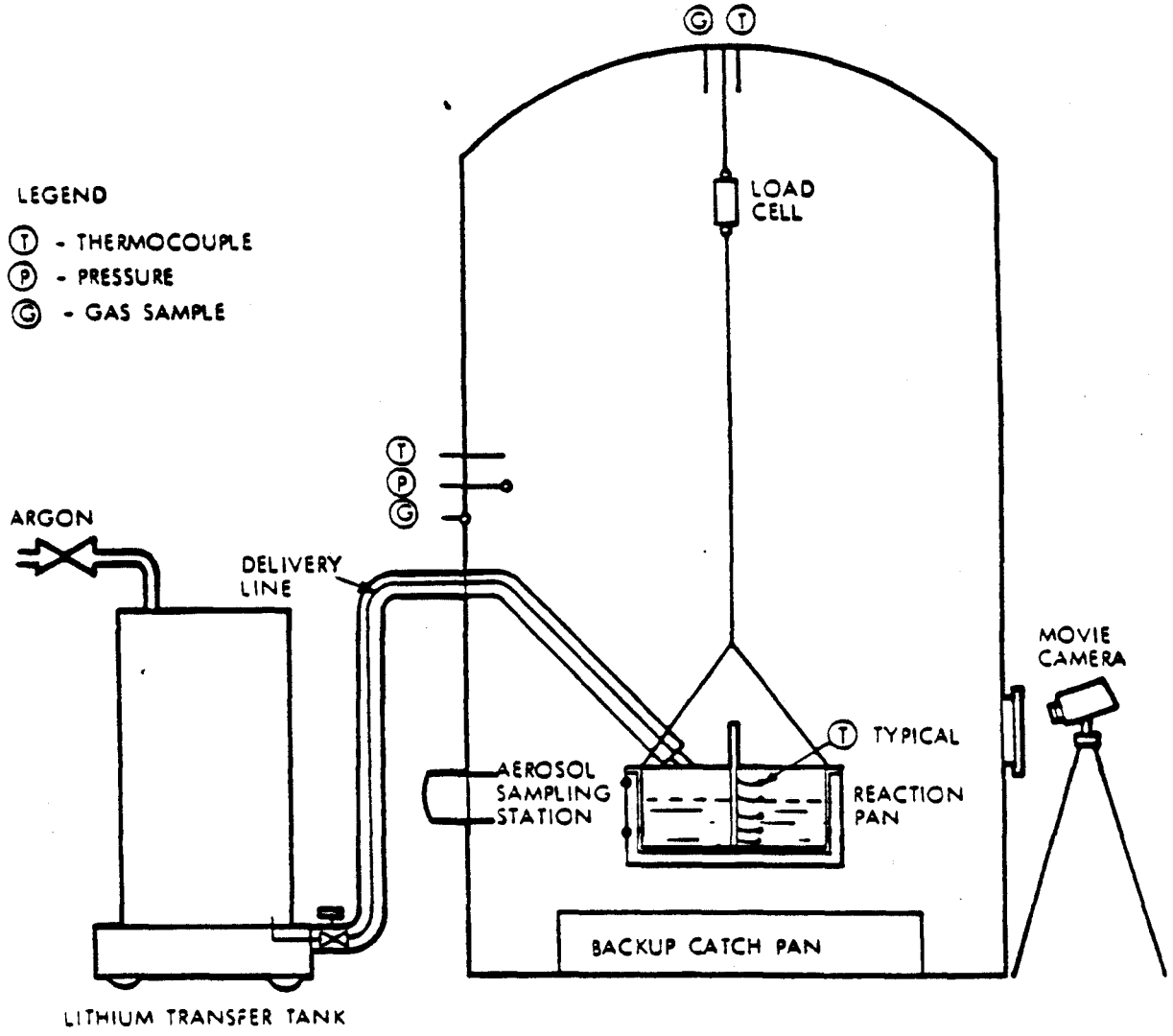

Fig. 2.4 Schematic of Lithium-Atmosphere Reaction Test Equipment Arrangement.

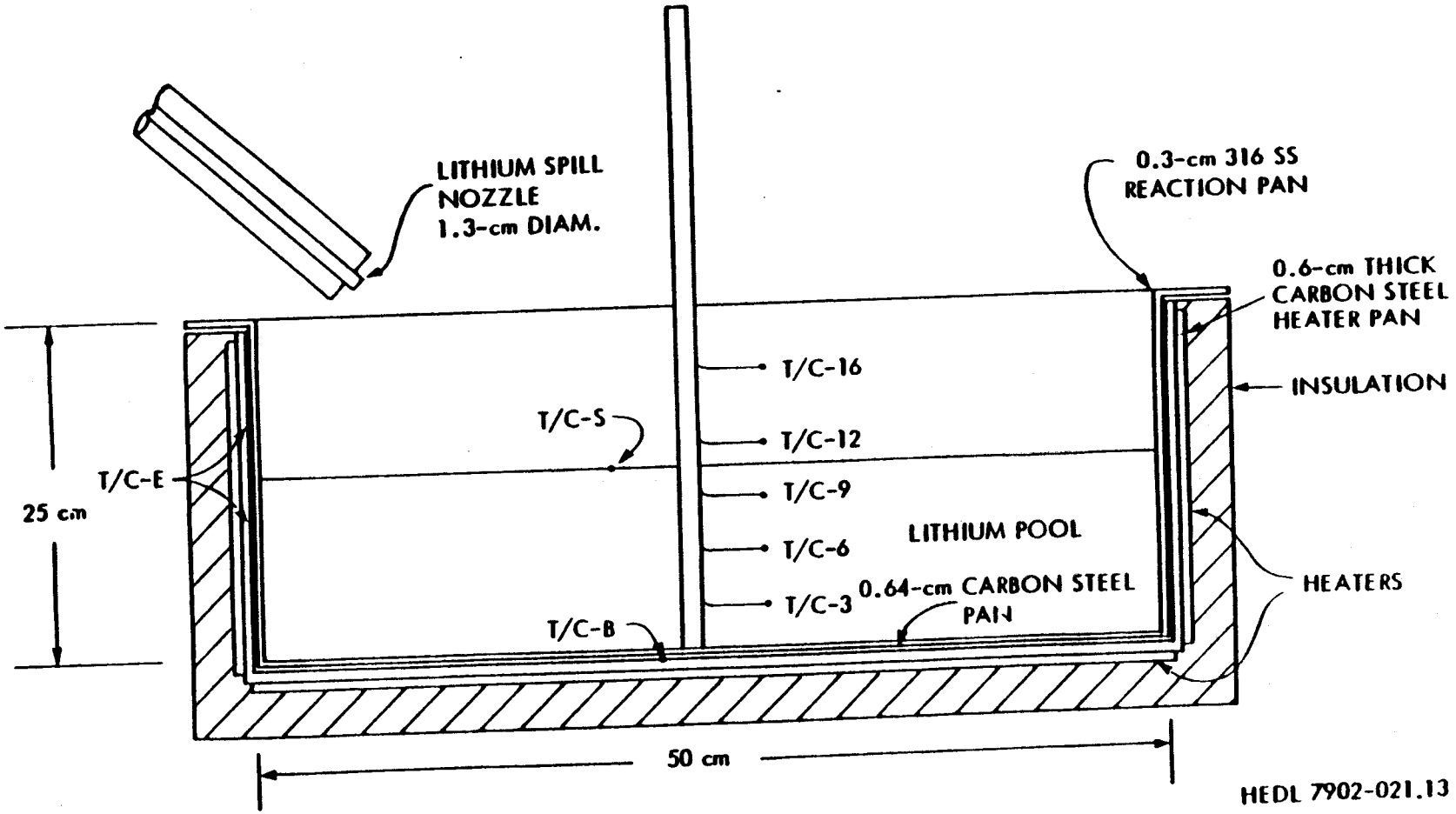

Fig. 2.5 Schematic of Lithium-Atmosphere Reaction and Heater Pans.

Results from the lithium-air tests indicate that the initial lithium temperatures had little effect upon the maximum pool and flame temperatures produced when reacted with a limited quantity of normal humidity air. LA-3 was the lithium/unlimited air reaction test which also produced about the same maximum lithium pool and peak temperatures. The rate of reaction was very similar in LA-1 and LA-2 tests; the pool temperatures reached 1000 °C within 18 minutes during Test LA-1 and 14.4 minutes during Test LA-2. This initial time difference essentially equals the time required to heat the LA-1 pool to the starting temperature of the LA-2 pool by heat of reaction with air.

Both LA-1 and LA-2 tests produced similarly composed final reaction products and aerosol concentration. However, Test LA-3 showed significantly different aerosol and final solid reaction product compositions; 29.4 percent of lithium carbonate aerosol and 94 percent solid lithium oxide were found. (see Table 2.2) Tests LA-1 and LA-2 showed that half of lithium reacted with nitrogen and the other half reacted with oxygen. In addition, Li_2O dominated over other aerosol compositions. Here, one should notice that the LA-3 test was a lithium/unlimited air reaction test and much larger scale experiment. In the LA-3 test, 22.7 Kg of lithium were transferred to the unheated reaction pan in 6.5 minutes and also few grams of powered test metals were added to the lithium pool and the lithium was stirred to mix the metals. The lithium spontaneously ignited and burned in the normal humidity atmosphere to generate aerosol. Air was allowed to enter the room to maintain atmospheric pressure in the room. 1.4 Kg of lithium was added at 111 minutes, 2.3 Kg were added at 127 minutes and 19 Kg were added at 140 minutes from the start of first lithium transfer. This particular result suggests that lithium aerosol is more stable as lithium carbonate than as lithium oxide or lithium hydroxide. Furthermore, here one can see nitrogen reaction rate inhibition effect. At high temperatures and high availbility of oxygen, lithium-nitrogen reaction is hindered by the preferred lithium-oxygen reaction.

TABLE 2.2

Solid and Aerosol Reaction Products of Selected HEDL's Experiments

(% total lithium)*

Test	Li-Air				Li-Moist Air		$Li-CO_2$
Test Number	LA-1	LA-2	LA-3	LA-5	LAM-1	LAM-2	LC-2
Solid Products							
Li_3N	44	47	5	25**	2.7	41	0
Li_2O	45	49	94	75**	82	56	83 (91.3)***
LiOH	9	0.2	1	-	13	2	0
Li_2CO_3	<1	0.3	0	-	2.4	0	1 (5.7)***
Li_2C_2	0	0	0	0	0	0	1 (3.0)***
Metallic Li	-	-	0	-	0	0	2
Aerosol Products							
Li_2O	-	76	55	-	0	5	1
Li_2CO_3	-	2	29.4	-	0.1	10	90
LiOH	-	1	2	-	90	40	0
$LiOH-H_2O$	-	-	0	-	0	40	0
Li_2C_2	-	-	0	-	0	0	<0.05

* Note: % of total Li, note weight % of reaction products. Total lithium includes lithium on structure and metallic surfaces as not appearing as aerosol.

** See reference [12].

*** converted to weight % of reaction products (not including metallic lithium).

The same effect can be seen in Test LA-5. Although there was about 4 times as much nitrogen present in the containment, the dominating reaction was lithium-oxygen reaction. In cases of limited quantity of normal humidity air reacting with lithium, the pronounced effect of "preferred" reaction of lithium-oxygen was signicantly reduced due to the decrease in availability of oxygen. However, as seen from LA-1 and LA-2 tests, the inhibiting effect was still considerable.

During the first 27 minutes in Test LAM-1, the lithium did not ignite nor did it react with oxygen, but the water vapor in the vessel atmosphere slowly reacted with the lithium. It appeared that if the reaction were left, it would continue to cool down with only a surface reaction. However, the lithium was then ignited by spraying some water droplets onto the lithium pool surface. The reaction then proceeded much like the normal humidity air tests. In the LAM-2 test, the lithium was ignited shortly after the start of lithium addition to the reaction pan. It burned with a yellow-red flame. Tests LAM-1 and LAM-2 were basically under the same physical conditions; the only major difference was that some water droplets were sprayed on the surface of the lithium pool in Test LAM-1. This explains the reason for such difference between Test LAM-1 and LAM-2 aerosol and solid reaction products. For the lithium-moist air tests, it is important to recognize the significant contribution of the lithium-water vapor reaction, forming lithium hydroxide.

As seen in Table 2.1, three lithium-nitrogen tests indicate that the lithium-nitrogen reaction is not as vigorous as lithium-air reaction. Some of the reasons for this are: 1) the heat of reaction is much lower; 2) a single nitrogen atom reacts with three lithium atoms (consumes lithium much faster); and 3) the nitride buildup effect reduces the reaction rate significantly. While in the lithium-air tests, the peak lithium temperatures were about the same regardless of the initial lithium temperature, the peak temperatures in the lithium-nitrogen tests were heavily dependent upon the initial lithium temperature.

In the LC-1 lithium-carbon dioxide reaction test, only the surface reaction was observed and the lithium temperature decreased slowly. This result implies that the ignition temperature of lithium-carbon dioxide is above 238 °C. One report indicated that the carbonate buildup effect could effectively stop lithium-CO_2 reaction below the lithium temperature of 300 °C [3]. On the contrary, in Test LC-2, the reaction was very vigorous, which resulted in a peak lithium temperature of 1350 °C, reaching its boiling temperature. The flame temperature exceeded the rated thermocouple reading temperature which was about 1400 °C. A bright intense flame was observed during the ignition of lithium. After about 3 minutes from the beginning of the reaction, the reaction pan failed and the lithium fell to the catch pan, where it reacted with an exposed surface area of 1.14 m^2. This caused a huge pressure and temperature peak in the containment vessel atmosphere. In addition, as obseved in the LA-3 test, the dominating aerosol was lithium carbonate which seemed to be more stable than lithium oxide. Furthermore, the test indicates that the perferred reaction was lithium-oxygen reaction rather than lithium-CO_2, which was different from the expectation.

CHAPTER III LITFIRE History and Model Description

3.1 LITFIRE History and Development

LITFIRE, a computer code, is an analytic tool devolped at MIT in order to simulate consequences of lithium fires in various containment schemes. LITFIRE started as a modified version of SPOOL-FIRE [13] which modeled liquid-metal sodium fires in containments. In the process of adopting SPOOL-FIRE to LITFIRE, many changes were incorporated [1,14]. The changes include allowance for nitrogen and water vapor reactions in addition to oxygen reactions as well as changing sodium properties implicit in the code to lithium properties. In addition, the effect of aerosols in the containment on radiative heat transfer was included. By far the most important change to the modeling was the incorporation of a "combustion zone" above the lithium pool. It is in this zone that lithium combustion takes place, according to mass and heat transfer mechanisms described by Dube [14].

With these changes in effect, LITFIRE was used to predict the consequences of a postulated lithium fire in a prototype fusion reactor geometry. A sensitivity analysis was perfomed on many of the important parameters in LITFIRE and best estimates for these parameters were adopted. An analysis of strategies for mitigating the consequences of lithium fires was perfomed and found to have significant effects.

After the original study was completed, lithium combustion experiments were conducted at HEDL. The geometry of these experiments differed significantly from the capabilities of LITFIRE and useful comparisons were not readily attainable. So several changes were made to LITFIRE to model the experimental setup and the predictions of LITFIRE were then compared to the experimental data. The new modifications brought the temperature field predictions to within 30 percent of the HEDL's experimental results for a variety of lithium reactions

[1]. Other unverified extensions of the code were also devolped at that time which include the capacity for lithium-concrete reactions and a two compartment containment scheme with combustion in one cell and mass and heat transfer between the two cells.

The inclusion of LiPb-air reactions was next incorporated into LITFIRE-MOD3. This task as well as effort to upgrade the original LITFIRE was preformed by Gilberti [15]. Major changes were performed to the LITFIRE-MOD2 single-cell model. This included improvements of many parameters, particularly of radiative heat transfer parameters such as gas emissivity, combustion zone emissivity and transmissivity. An optional mechanism for the removal of aerosols from the primary cell gas has been included. Performing careful parametric studies, the accuracy of LITFIRE in predicting thermal and pressure responses of containment atmosphere and structures was tested against large scale (100 Kg. Li) spills performed at HEDL. The agreement between experiment and LITFIRE prediction was within 10 percent. Additionally, an optional two cell containment scheme in LITFIRE was allowed. This change brought more flexiblity for geometry, and made the available options more compatible with one another. Third, the option to account for lithium-lead alloy reaction in air was used in a study that indicated that lithium-alloys are less reactive than pure lithium and generate maximum cell gas temperatures that are nearly a factor of two lower than those resulting from pure lithium fires, for the same volume of liquid metal spilled.

MOD #	PRINCIPAL FEATURES	YEAR	REFERENCE
1	Single Cell Building Pool on Floor Li-Air Reaction Model Inert Gas Injection Convective and Radiative Heat Transfer from Pool	1978	Dube [14]
2	Added: Pool in Pan Geometry N_2Li Reactor Kinetics Aerosol Suspension Effects Improved: Radiative Properties of Combustion Zone and Containment Gas	1980	Tillack [1]
3	Added: Two Cell Building Li-Pb Pool Model Improved: Code Structure	1983	Gilberti [15]
4	Add: Li-CO_2 Reaction Model Improved: Li-N_2 Reaction Model Li-Air Reaction Model	1986	Gil

Figure 3.1: History of LITFIRE Development

3.2 LITFIRE Model Description

LITFIRE generates the temperature and pressure profiles in an idealized geometry with a single heat source and many heat sinks. The heat source term represents the combustion of lithium with various gases. When the combustion process is ceased, the hottest structural component or the lithium pool itself will act as a decaying heat source until equilibrium containment temperature is reached. The heat flow between nodes is one-dimensional and allows for convective, conductive, and radiative transfer.

Correlations for the heat transfer are fairly simple and the combustion source term is highly idealized in order to: 1) permit greater flexibility for users; 2) base the calculations on available data, and; 3) to reduce computation time and costs. For a given geometry, many user defined coefficients and parameters enable accurate modeling of the principal heat transfer mechanisms. But the combustion zone model is fairly inflexible and is also the most simplified part of the LITFIRE model. The effects of surface layer formation, wicking, product buildup in the pool, and multiple species reactant competition are ignored or very crudely modeled. Furthermore, the lithium-nitrogen reaction rate dependence on lithium temperature was guessed as seen in Figure 3.2. HEDL's experiments generated only few data points of the lithium-nitrogen reaction. Due to the scaricity of data, Tillack [1] was forced to guess the reaction rate curve. Gilberti [15] did not make any attempt to modify the reaction rate curve due to the scaricity of experimental data even though the predicted lithium-nitrogen reaction was much lower than HEDL's experimental value in TEST LA-5.

From the results of Gilberti's work, LITFIRE overpredicted the reaction rate for multiple species combustion. As Gilberti mentioned, the overprediction may be due to approximations in modeling of a combination of the following: mass diffusion rate of gases to the combustion zone by convection; the transport rate of lithium to the combustion zone by vapor diffusion; effect of product

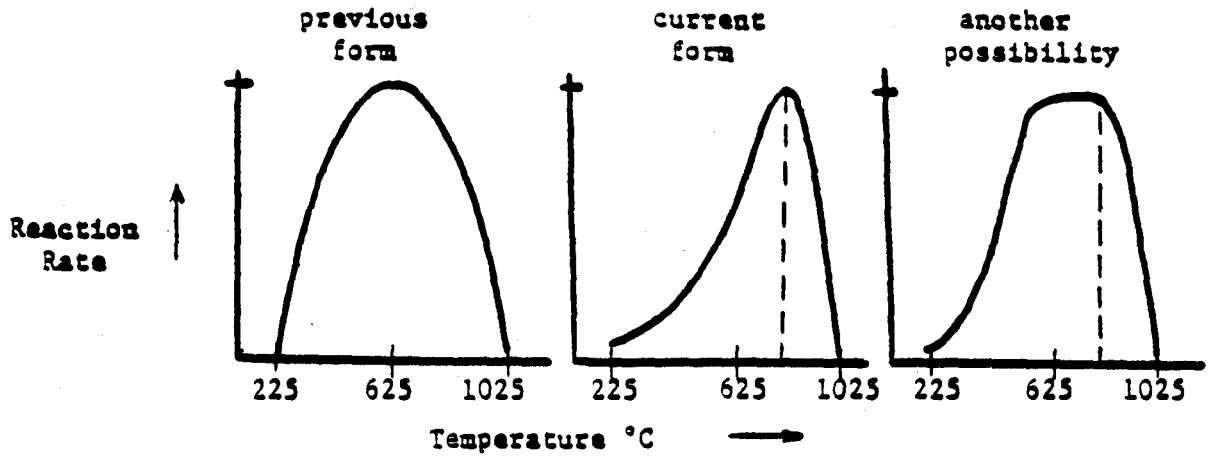

Figure 3.2 Tillack's guessed lithium-nitrogen reaction rate curve in a function of the lithium pool temp.

accumulation on either of the above; and the nitrogen hindrance factors for a given temperature and oxygen concentration. Accurate measurement of the gas consumption rates, temperatures, and oxygen concentration near the flames of the lithium fires would indicate which of the above effects are causing the discrepancy [15].

The idealized energy flows in LITFIRE (one and two cell versions) are shown in Figures 3.3 and 3.4. Each node has a heat capacity approximating that of its counterpart (average specific heat of the material times the total mass of the node) and a single, bulk averaged temperature. Heat transfer between two nodes is a function of temperature difference and the equivalent thermal resistance (for each heat transfer mechanism) of that specific pair of nodes.

Mass flows in LITFIRE are also lumped and are principally between the two cell gas nodes, the combustion zone and lithium pool, and the combustion zone and primary cell gas. Figure 3.5 shows this schematically. Structural materials are excluded in the mass exchange or flow and are assumed to be stable at any temperature. Thus, LITFIRE does not yet account for the effects of volatilization or melting of structural components.

A set of simultaneous coupled differential equations are solved at each appropriate time step in order to follow up the thermal and pressure history as well as mass accumulation and depletions. For each thermal element in the model, the temperature history is calculated by a set of numerical integration subroutines in which the method of finite differences in the spatial regime (either Simpson's rule or a fourth-order Runge-Kutta method) was used. For an example of the temperature history, the actual integration equation would be:

$$T(t) = T(t_0) + \int_{t_0}^{t} dt' \frac{dT}{dt'},$$

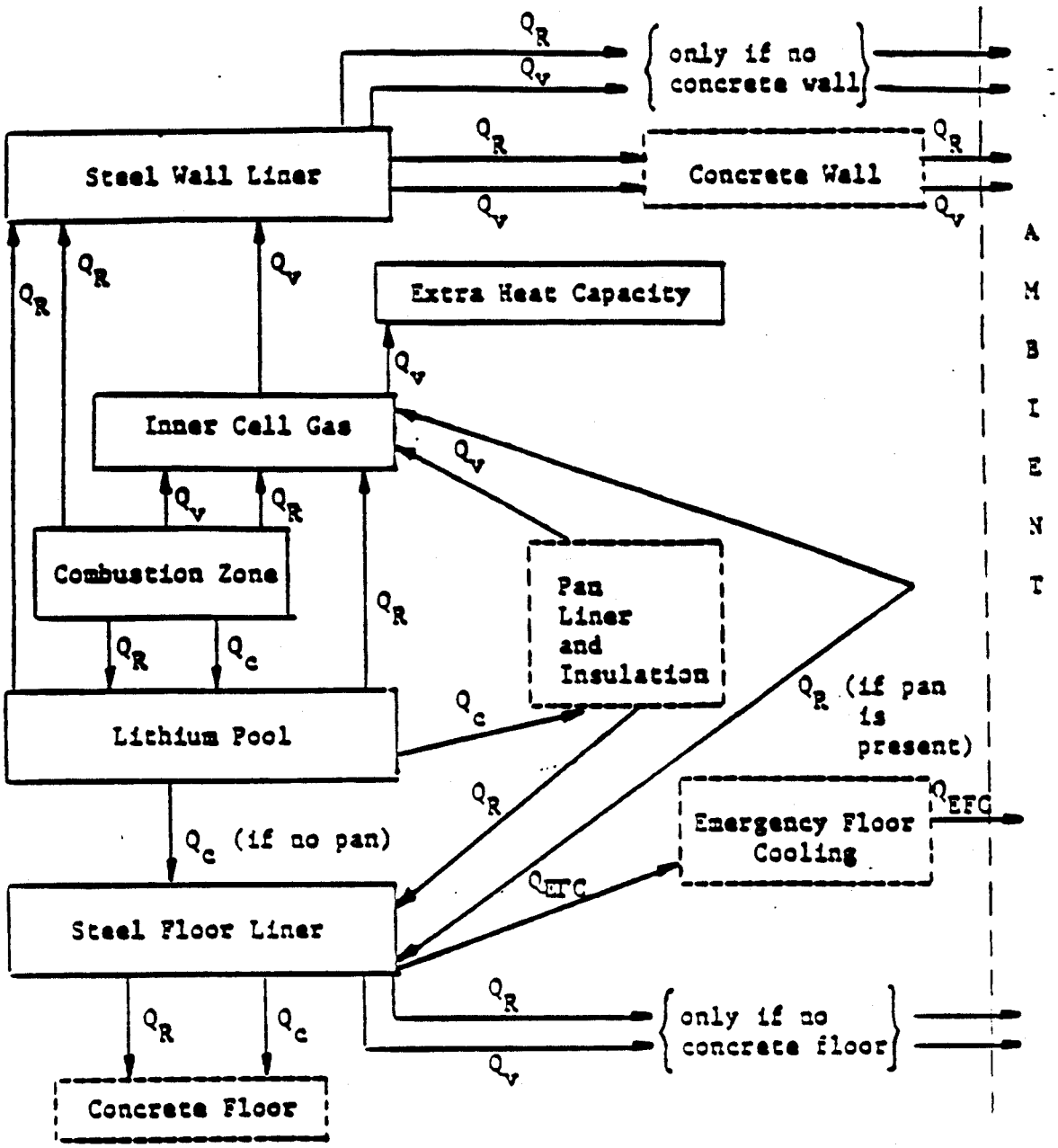

Figure 3.3 Energy flow in single cell LITFIRE

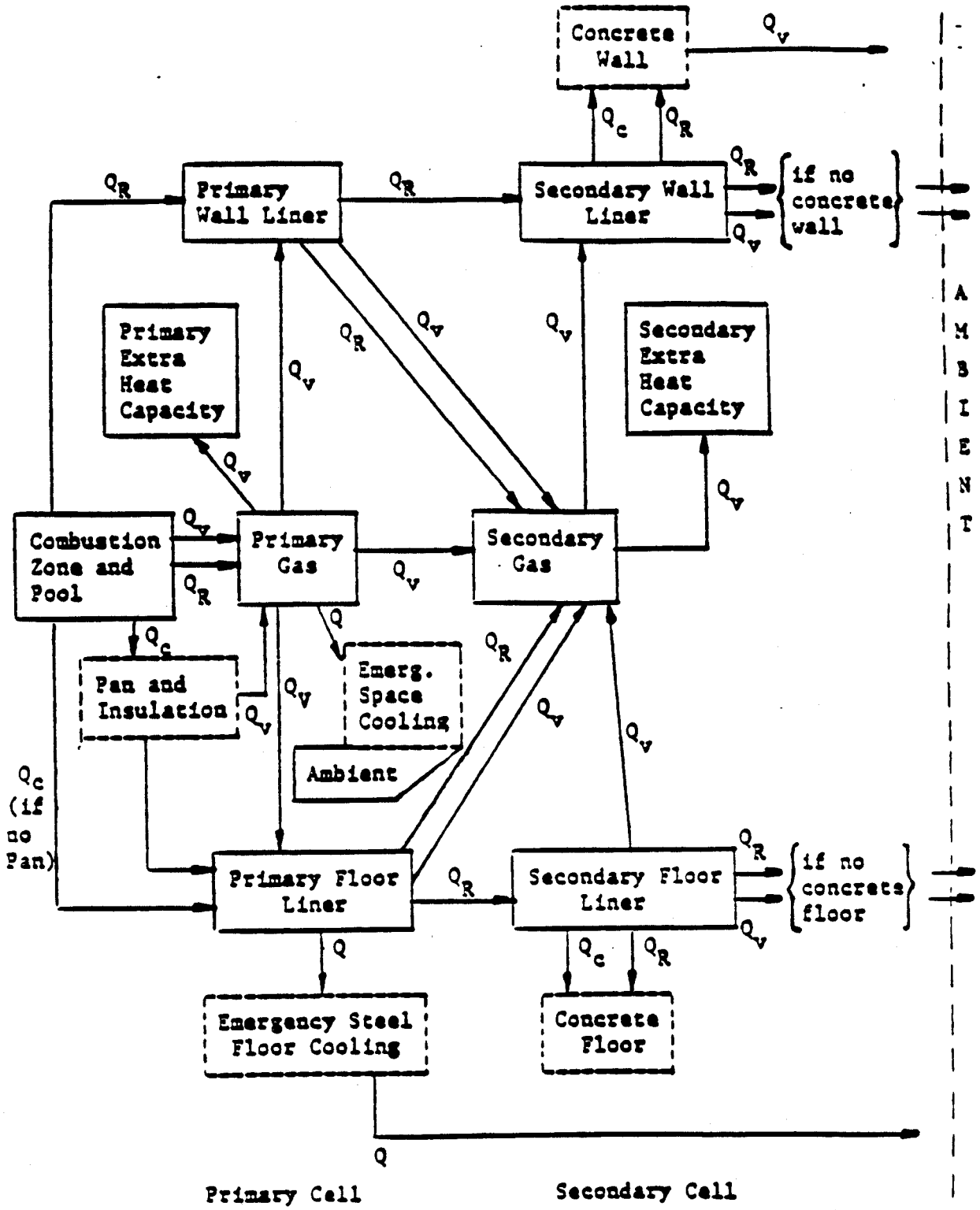

Figure 3.4 Energy flow in two-cell LITFIRE

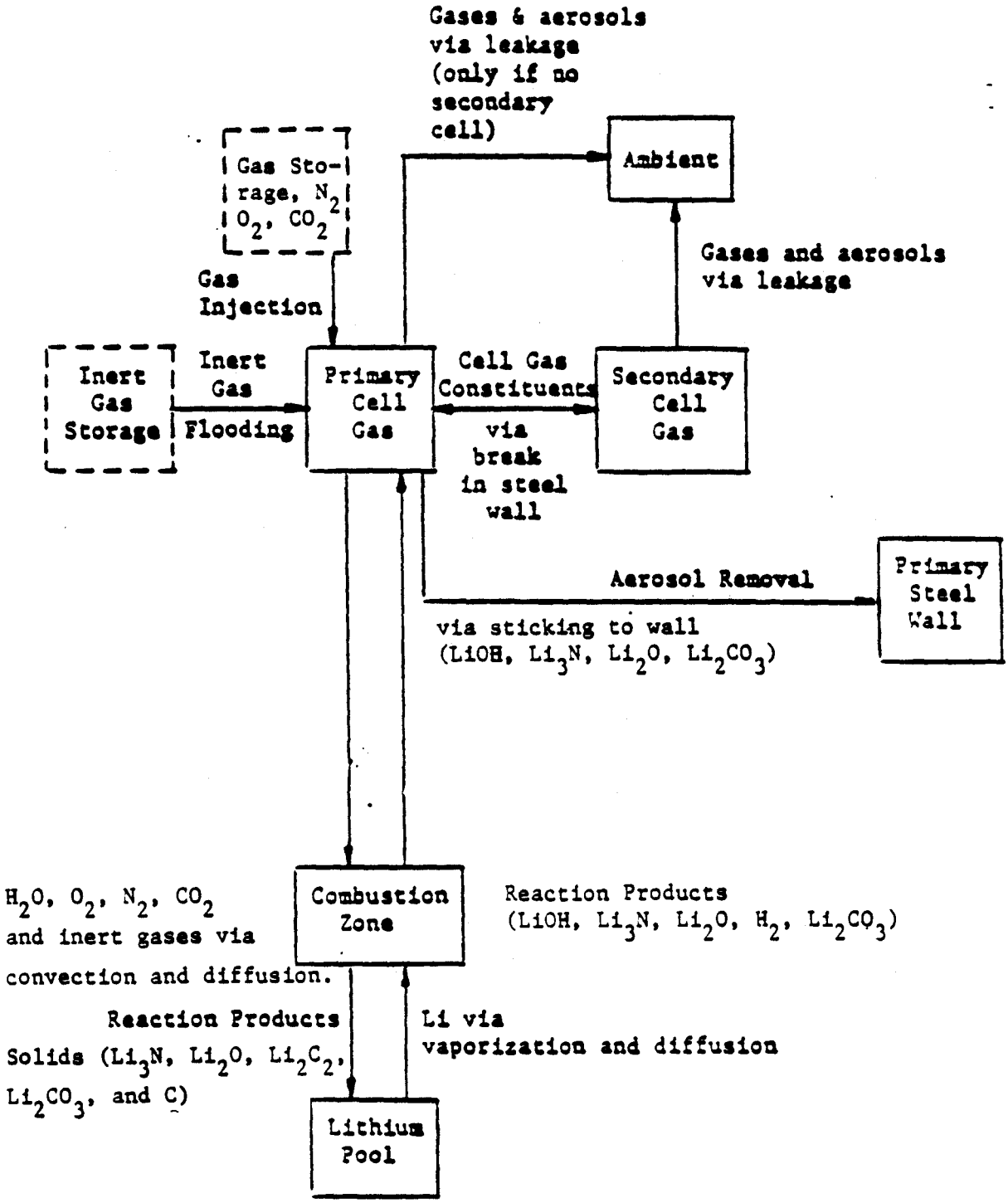

Figure 3.5 Mass flows in LITFIRE

where the time rates of temperature change (dT/dt') are calculated in the main LITFIRE program for each node by finite differencing. The numerical stability is monitored during each time step and the fractional temperature change at certain nodes during a single time step is limited in order to ensure stability. LITFIRE uses the most sensitive nodes to determine the stability criteria, but it is still possible that under certain regimes, the code may produce nonphysical results due to numerical divergence. These results are usually observed when a node is specified as too thin or having too high a conductivity. Recommended values are shown in the user's guide [16]. All the modifications involved in this study will be explained in detail in other sections.

CHAPTER IV Description of Experimental Apparatus and Procedures

4.1 Introduction

Approximately forty experiments were conducted in order to characterize the lithium reaction kinetics with nitrogen and oxygen. Several runs were performed in order to verify Ijams's lithium-nitrogen reaction rate as a function of the lithium pool temperature, while approximately ten runs were conducted to observe the lithium-oxygen reaction kinetics [17]. The majority of the experimental runs were dedicated to characterize the lithium-nitrogen and oxygen reaction kinetics (mixed gases in different compositions) in order to simulate lithium-air reaction kinetics without water vapor (humidity). Knowing the lithium-mixed nitrogen and oxygen reaction kinetics, one can later deduce the effect of the water vapor as a catalyst of the reaction rate, when the water vapor is introduced to the mixed nitrogen and oxygen atmosphere. Then, one can basically characterize the lithium-air reaction kinetics without considering the small contribution of other lithium reactions such as lithium-carbon dioxide.

These experiments are part of a continuing effort to characterize the lithium reaction kinetics with various gases and materials. The basic parts of the experimental apparatus including the reaction chamber, furnace, and piping system were retained from Ijams's lithium-nitrogen reaction kinetics experiment [7]. Many new features were added to the previous system in order to improve the accuracy of the system and to monitor the compositions of nitrogen-oxygen mixtures and purity of gases. The experimental apparatus is described in detail in Section 4.2.

The experimental runs were conducted within a lithium pool temperature range between 350°C and 1100°C for the lithium-mixed nitrogen and oxygen reactions and a temperature range of 450°C and 700°C for the lithium-nitrogen reactions. In these experiments, pure oxygen, nitrogen, or mixed nitrogen and

oxygen gas flowed at a fixed rate across the face of a small liquid lithium pool.

The flow rate was kept approximately the same as in the previous experiments conducted by Ijams for the runs with temperatures below 900°C; from 2.0 to 3.5 liters/min were used since the lithium- mixed gas reaction rate were not significantly higher than the lithium-nitrogen reaction rate. In order to obtain reaction rate measurements independent of gas flow, for some of the runs with pool temperatures greater than 900°C, about 5.5 liters/min flow rate was used. The lithium pool surface was 3.88 cm^2 and was kept small in order to limit the total amount of energy that could be released in an accidental fire. Every 3 seconds, the pressures and temperatures were monitored while previous experiments were monitored every 7 to 10 seconds.

4.2 Description on the Experimental Apparatus

The basic experimental appratus is shown in Figure 4.1 and the detailed diagram of the lithium pool chamber is shown in Figure 4.2. Several parts of the appratus have been replaced or have been added to the previous experimental apparatus which was originally constructed by Ijams [7] (see Figure 2.1 and 2.2 in Chapter Two). The volume of tank 1 was 0.00416 m^3 and the volume of tank 2 was 0.01402 m^3; so that 3 psi drop in tank 1 pressure approximately corresponded to 1 psi increase in tank 2 when there was no leak in the piping system. For the lithium-nitrogen and lithium-mixed nitrogen and oxygen runs, the dimensions of the tanks were fairly appropriate. Particularly, since the new data acquisition system read all the inputs every 3 seconds (although it could read much faster), the incremental pressure increase in tank 2 and the decrease in tank 1 were much smaller than the previous experiments. Therefore, sizing the tanks corresponding to the appropriate reaction rate posed a lesser problem. For the lithium-oxygen reaction runs with high initial lithium tempratures, about 4 times larger tank 2 was constructed.

The lithium container was made of 316 stainless steel. The inner diameter was 2.22 cm, with wall thickness of 0.32cm. The area of the container cross section was 3.88 cm^2. The depth of the container was about 3.1 cm. The thermocouple well made by Omega Engineering, Inc. of Stamford, CT was also made of 316 stainless steel. A K-type thermocouple was used to measure lithium pool temperature while E-type thermocouples were used to measure the gas temperatures of tank 1, tank 2, and the heat exchanger. The rated maximum temperature reading of a K-type thermocouple was 1375°C. The K-type thermocouple was protected from high temperatures by a ceramic insulator which could withstand 1100°C for continuous use. All the thermocouples were made by Omega Engineering, Inc., too.

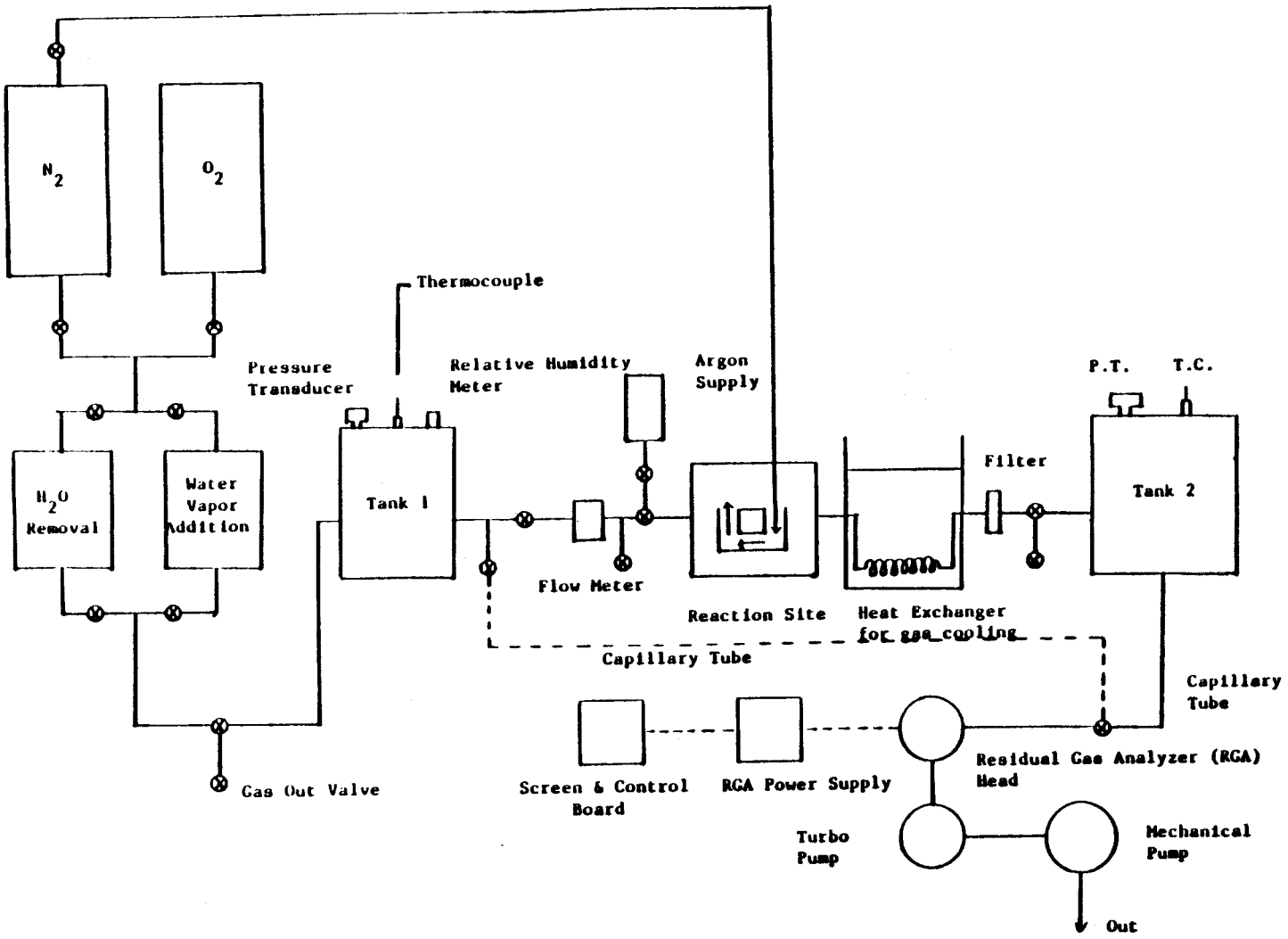

Figure 4.1 Experimental Setup Diagram

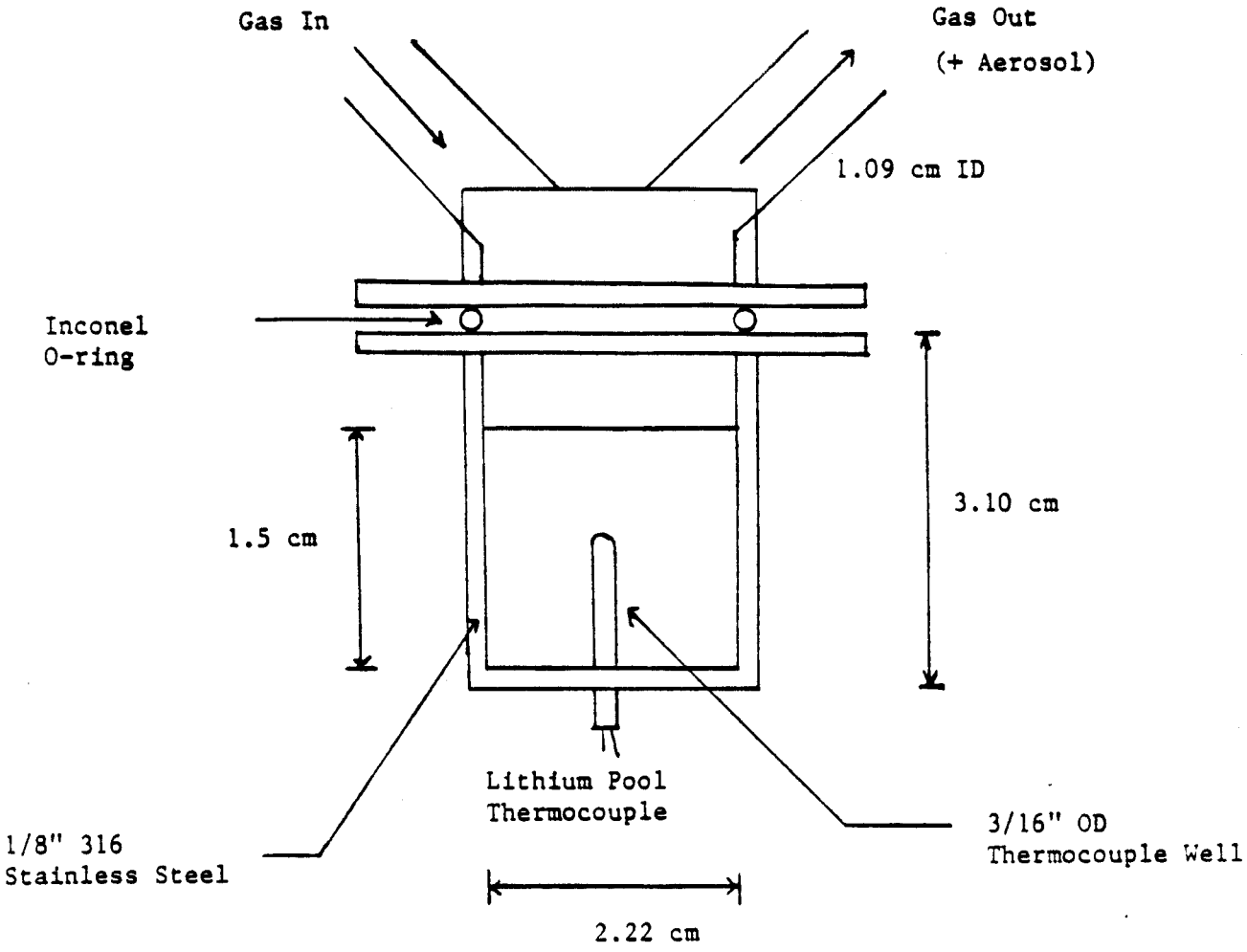

Figure 4.2 LITHIUM POOL and CONTAINER

The well was mounted through a hole in the bottom of the reaction chamber and was welded. Previously, the well was mounted through a hole in the pool cap and then welded to the cap. In the lithium-oxygen reaction runs, the well melted due to a high lithium fire flame temperature, exceeding its melting temperature of about 1500°C. Then, it was observed that inserting the well from the top has few drawbacks. First, at high temperature and vigorous reaction conditions, the well could melt at the vicinity of the lithium pool surface, the hottest area due to the lithium fires. By inserting the well from the bottom, the problem of melting can be virtually eliminated since the lithium pool temperature would seldom increase above 1500°C. Secondly, in many runs, the bottom part of the well was not completely covered by liquid lithium, in return, the flame temperature was measured instead of the lithium pool temperature.

Initially, lithium pellets purchased from Aldrich Chemical Co. of Milwaukee, Wi. was used. The lithium was delivered in 25 gram samples in bottles under argon. However, the pellets were not always shiny in their bottle, but rather were discolored, mostly a dark grey color, and occasionally white or specked with red. This discoloring indicated the presence of nitride, oxide, or hydroxide on the lithium. A personal conversation with an engineer at Aldrich Chemical Co., indicated that the lithium which was previously used had 0.5 to 1 percent sodium impurity in addition to surface contaminations.

In consequence, new lithium of 99.9 percent purity was purchased from the same company. The lithium was in ribbon form with .38 mm thickness and 23 mm width. Most of the lithium was in its silver shiny color indicating that the lithium was quite pure. However, most of the time, some black colored surface reaction product layers were still observed. The discolored portion of lithium was cut off and only the shiny part of lithium was used. Doing so, the lithium completely melted even below 400°C. For the runs with temperatures below 500°C, one of major sources of error came from the impurity of lithium. All the lithium was handled under argon atmosphere.

The flow meter initially used was rated from 0 to 3.5 liters/min of air at STP. Ijams indicated that at high temperature and vigorous reaction conditions, the reaction rate measured was gas dependent. This dependency was often observed when the lithium temperature exceeded 900°C. A new flow meter made by Fischer and Porter was used for the runs involving lithium temperatures greater than 900°C. This flow meter was rated from 0 to 7.7 liters/min of air at STP when used with a black glass float and 0 to 14 liters/min of air at STP when used with a stainless steel float. For most of the high temperature runs, 5.5 liters/min flow rate was used.

Two pressure transducers and their digital indicators with a power supply made by Setra Systems Inc. of Acton, Ma. replaced the previously used conventional pressure gauges. Anolog outputs from the transducers were directly connected to a data acquisition system. In Ijams's experiments, the major source of error of the experiment came from the pressure gauge reading. His experiment required two persons; first person to control the flow rate and read the first tank pressure and a second person to read the second tank pressure and control the data logger at the same time. The first person gave a signal to the second person when the pressure of the first tank decreased to a certain amount, then the second person read the second tank pressure and pressed the data logger to print the temperatures. When the pressure was changing quickly, it was very difficult to read the gauges with bare eyes.

This procedure lead to some experimental error as Ijams indicated. The new data acquisition system made by Cyborg Corp. of Newton Ma. virtually eliminated the error related to the pressure reading. The response time of the transducers and the data acquisition system to quick pressure changes was very small (less than 10 milliseconds). In the transducers, two capacitors were used. As pressure went up, a small and very thin capacitor was instantaneously pushed upward due the pressure increase, thus the pressure change can be deduced from the decrease in the gap between the capacitors, which resulted in an increase in

its capacitance.

The data aquisition system was connected to an IBM AT microcomputer in which acquired data were stored. Some software was developed in order to acquire raw data from E-type and K-type thermocouples and transducers, to control the time interval of acquisition, and to convert the raw values in terms of engineering units. In order to increase accuracy of thermocouple readings, the software developed by Cyborg Corp. was not used. Instead, 9th order polynomial fitting equations were used. The acquisition system has 16 bit analog to digital converter which was more accurate than the "old" 12 bit A/D converter. The rated channels/second reading for the system was 500 channels/second. However, due to the large computation time required by the program, the fastest reading was about 40 channels/second.

In all the runs performed, the 9 recoding channels (two from the transducers, two readings for each of tank 1 and 2 temperatures, one for the lithium pool temperature, one for the cold junction temperature compensation, and one for the heat exchanger) were read every 3 seconds. For high temperature runs with the lithium temperature exeeeding 900°C, the maximum temprature increase was about 20°C during each time interval. This virtually eliminated the error associated with temperature reading. Previously, the temperature increase in the high temperature runs during the time was as high as 50°C and the average value of the temperature was used. Since the lithium-nitrogen and oxygen reaction was not significantly more rapid than the lithium-nitrogen reaction, a data acquisition interval of 3 seconds was ideal. For the lithium-oxygen reaction runs, it would be necessary to reduce the time interval of data acquisition since the reaction is expected to be much more vigorous and the temperature increase due the reaction and the consumption of oxygen would be significantly faster than the lithium-nitrogen or the lithium-nitrogen and oxygen runs.

All the lithium-nitrogen and lithium-oxygen reaction runs were done

with the old Kaye system, which Ijams had used. But the lithium-mixed nitrogen and oxygen runs were conducted with the new data acquisition system. While the data acquisition system was reading the anolog inputs, all the data were transferred to the hard disk of the IBM AT. Then, the data were again transferred to LOTUS 1-2-3, a software with an electronic worksheet in which data were analyzed and proper calculations to obtain the reaction rate were performed.

In order to measure the gas composition of nitrogen and oxygen mixture runs, a residual gas analyzer (RGA) was purchased from Dycor Electronics Inc. of Glenshaw, Pa. It consisted of a control unit, power supply, analyzer head, electrometer, and graphics printer. A very thin silica tube of an inside diameter of 50 micrometer was connected from tank 1 to the RGA and from tank 2 to the RGA in order to measure the gas composition before and after the reaction has taken place.

The basic theory involved in obtaining gas mass spectroscopy is as follows. Electrons emitted from a hot filament collide with gas molecules in the ionizer region of the analyzer head producing ions of the parent molecules and ion fragments also. These ions are directed toward the mass filter by the electric fields produced by a focus electrode. The mass filter rejects the passage of all ions except those with a specific mass-to-charge ratio. The ions that make it through the mass filter strike a cup-shaped element and produce an electric current that is proportional to the pressure of those ions at the source, then producing gas mass spectroscopy in terms of partial pressures. The rated pressure reading was from 10^{-3} to 10^{-12} torrs. It also had a background subtraction option in which a background spectrum can be effectively subtracted in order to measure partial pressures of newly introduced gases to the RGA. Since the system can only be operated under 10^{-3} torr, a convectron vacuum gauge made by Granville-Phillips of Boulder, Co. was used in order to ensure pressure less than 10^{-3} torr, before the RGA was turned on.

In order to use the RGA, it was necessary to vacuum the analyzer head. The first vacuum pump used was a diffusion pump in conjuction of a roughing pump. This system did not have a cryo-trap. It was necessary to have a cryo-trap in which liquid nitrogen cools the vaporized silicon oil used by the diffusion pump, preventing a backstream of the oil to the analyzer head. For several months, the RGA and vacuum system had been working properly. However, due to the accumulated silicon oil in the ionizer and the filament effectively blocked most of the ions generated. Due to this serious oil contamination in the analyzer head, the head had to be serviced three times.

Therefore, obtaining a new vacuum system became mandatory. The choice made was a turbomolecular pump made by Balzers. A turbomolecular pump was the most appropriate vacuum system for the RGA. It did not require oil, unlike a diffusion pump, and also required a very short time to vacuum the analyzer head free of contamination. Two additional features were added to the vacuum system to provide precautionary measures. One was an emergency vent valve and the other was a coaxial trap. An emergency vent opens its valve to return to normal atmospheric pressure when there is a power failure, preventing any backstream of the roughing pump oil to the analyzer head. A coaxial trap made by MDC Vacuum Products Corp. of Haywood, Ca had a similar function Under normal operating conditions and power failure conditions, when there is a backstream of the roughing pump oil to the head, the trap effectively traps most of the vaporized pump oil eliminating most of the backstream of the oil. Using the described vacuum system, under normal conditions, the vacuum pressure reached about 10^{-8} torr, low enough to obtain precise partial pressure readings of oxygen and nitrogen.

4.3 Experimental Procedures

4.3.1 Introduction

The experimental procedures are somewhat similar to the procedures Ijams used. However, since many parts of the apparatus were either added or replaced, some procedures had to be changed. In particular, the new data acquisition system, vacuum system, and the RGA usage required more complex procedures. In addition, several previous procedures were modified in order to reduce the number of discarded runs and to produce more consistent and accurate data. In the begining, each run took approximately 5 to 6 hours, while the time of the actual reaction was about 1 minute. The shortest time spent for one experimental run was about three hours. Of course, in addition of the experimental runs, a considerable amount of time was spent on maintaining proper conditions of the apparatus. In particular, the thermocouple attached to the bottom of the lithium container fell out numerous times. In other words, the preparation for each experiment was very time consuming. However, since all the data acquisition was done electronically, only one person was needed to conduct experiments, while the previous experiments required two persons.

4.3.2 Preparations before the Actual Run

i) Filling Tanks with Gases

The first step was to fill appropriate gases in tank 1 and tank 2 before the experiment. In the case of the lithium-nitrogen or lithium-oxygen reaction run, pure nitrogen or oxygen gas filled tank 1 and it did not matter to fill the second tank with pure argon gas. However, in the case of the lithium-mixed nitrogen and oxygen run, it was necessary to fill the second tank with pure argon gas because composition of the gas after the reaction had taken place was to be measured. Here, the description of the lithium-nitrogen or lithium-oxygen reaction runs will not be presented (see reference [7]), but only the lithium-mixed

gas run will be described in detail.

Before the tanks were filled with appropriate gases, the vacuum system was turned on. It usually took about half an hour before the pressure of the analyzer head went down to a 10^{-8} torr range. During that time, pure nitrogen and argon were slowly bled into tank 1 and tank 2 respectively. All the gases used here came from pre-pressurized tanks and were Grade 5, which means 99.9995 percent purity of gases. When tank 1 and tank 2 were filled to 60 psig and 10 psig respectively, nitrogen in tank 1 and argon in tank 2 were released to the atmosphere after giving enough time for the gases to become well mixed in their respective tanks. This process was repeated several times in order to purge out all the impure gases. It was important to ensure the purity of gas since impure gases could react with the lithium. In particular, the content of water vapor was carefully monitored since it can catalyze the reaction.

By that time, the pressure in the head fell low enough so that the RGA could be turned on. Then, using the capillary tube, nitrogen in tank 1 was bled into the head. From the controlling board of the RGA, appropriate parameters were set in order to perform the background spectrum subtraction and to set an appropriate pressure level reading. On the screen, partial pressures of each gas composition were shown. Until all the impure gases were purged out to atmosphere, the procedure of purging was repeated. At each time, gas purity of 99.9 percent or higher was obtained and then the spectrum was printed for a record. This same procedure was performed for the second tank. Figures 4.3 and 4.4 show the spectrum of pure nitrogen and argon atmospheres respectively. The total pressures shown in the figures are much higher than the pressure described earlier. It is because as the gas was continously bled into the head, the pressure increased significantly although the vacuum system was continously pumping the gas out of the head.

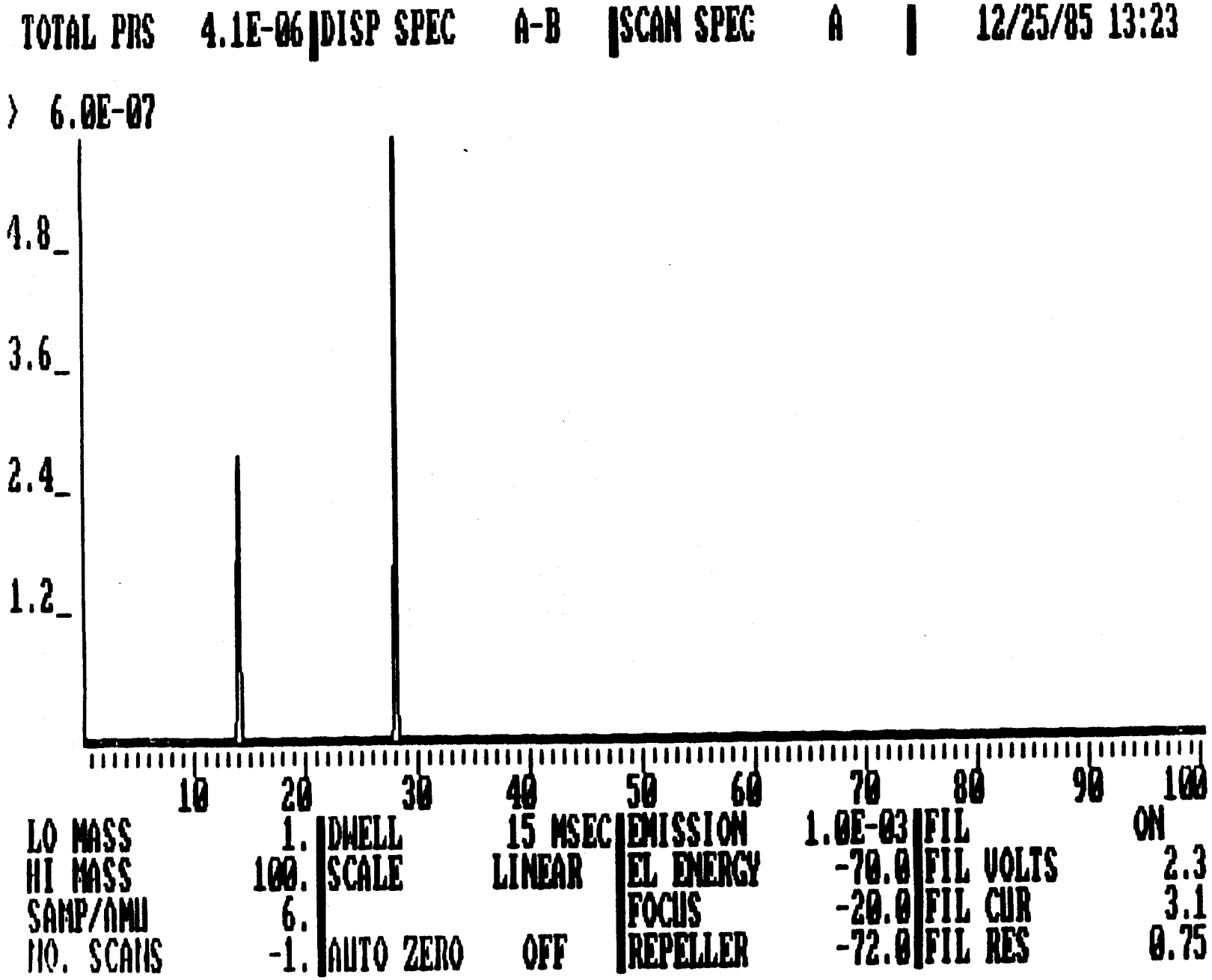

Figure 4.3 A spectrum of pure nitrogen atmosphere at tank 1

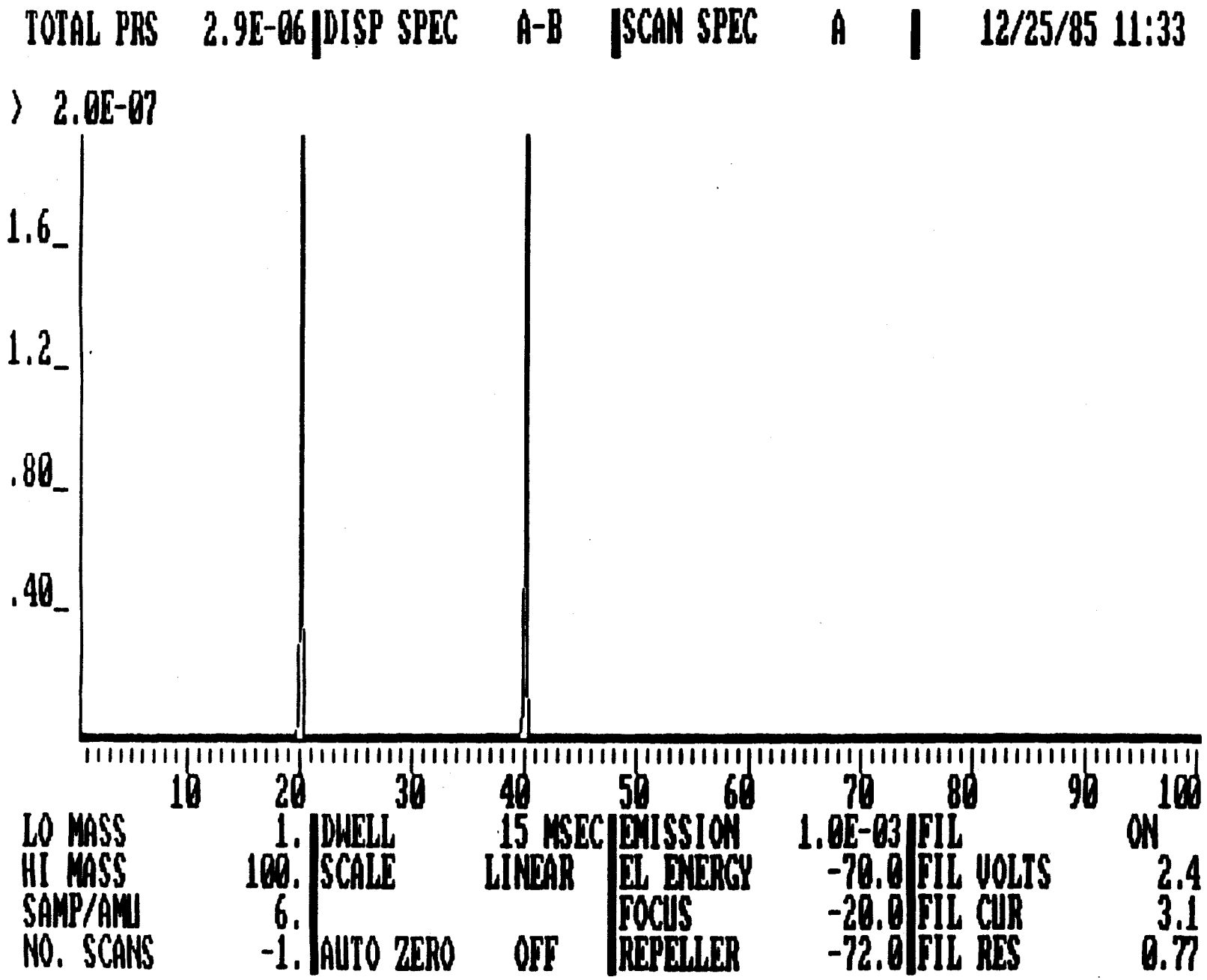

Figure 4.4 A spectrum of pure argon atmosphere at tank 2.

Both nitrogen and oxygen gases in the pre-pressurized tanks existed in mono-atmomic (O and N) and di-atomic forms (O_2 and N_2). There was a tendency that those mono-atomic gases combined themselves to become di-atomic gases if enough time were given. One major handicap of using a turbomolecular pump was that heavier gases were pumped out of the head faster than lighter gases. Therefore, the pressure measurements were taken as soon as the gases were introduced into the head. However, the error resulting from this particular characteristic of a turbomolecular pump was insignificant. In particular, the mass differences between the mono-atomic and di-atomic gases were ralatively small. In Figure 4.3, the spectrum shows both mono-atomic and di-atomic nitrogen gas. Also, in Fig. 4.4, the peak at the mass number 20 was an escape peak of argon. Due to unavoidable leaks in the piping system, it was not ideal to bleed oxygen into the first tank at this time in order to obtain an appropriate gas composition. Since it took a long time to heat the reaction chamber and also the first tank was highly pressurized, even a small leak could lead to a considerable pressure decrease. If oxygen were bled into tank 1 at this time with a proper nitrogen and oxygen composition, by the time the actual run takes place, the pressure level would be too low so that additional oxygen and nitrogen must be added to the first tank, resulting in more time and effort to obtain the right composition of gases. Using a partial pressure gas law, an exact gas composition can be obtained and then can be verified by the RGA. On the contrary, the second tank was very much leak tight since the pressure was much lower.

In these experiments, nitrogen gas fractions were varied from 80 to 95 percent; in other words, oxygen gas compositions were varied from 20 to 5 percent. Oxygen gas was bled into the first tank during the time when the reaction chamber was heated up to a desirable liquid lithium temperature. After the purity of gases were obtained, all the valves were closed at the pressure level described earlier. So it was impossible for gases in atmosphere to diffuse through the tanks.

ii) Loading Lithium into the Container

As mentioned earlier, the lithium used in this experiment was 99.9 percent pure and was in a thin ribbon form. In order to load the lithium into the container, the container and its associated piping had to be removed from the rest of the piping system, which was done by unscrewing the stainless steel union joints. Before the lithium was transferred to the container, the nickel coated inconel X-750 o-ring was inserted into the gap between the cap and the container. The o-ring was thinnly coated with a silver goop in order to seal any gap between the o-ring and the container and cap. As the temperature of the container went up, the cap and container expanded pressing the o-ring from the bottom and the top. And any possible gap between the o-ring and the cap and the container was further sealed by a silver goop. This prevented any possible leaks around the o-ring.

In a tightly sealed large clean bag, the lithium was handled. Before transferring the lithium into the bag, the bag was filled with pure argon by purging the other gases out. Then, a stream of pure argon was continously introduced from a pre-pressurized tank to the bag. Since argon is much heavier gas than air, argon was likely to settle down to the lower part of the bag. So all the handling were done in the lower part of the bag. As a result, the lithium was almost completely separated from air atmosphere.

Under the bag, the lithium ribbons were inspected for purity by the color of the lithium, and then the discolored portion of the lithium was cut and discarded. The shiny part of the ribbons was rolled into a small cylinder shape, sized appropriate enough to be inserted into the chamber. Approximately 2 to 3 grams of lithium were transferred to the container. After the ribbon was rolled into a cylinder shape, the bag was temporarily sealed and the argon gas line was removed. Then, the argon gas line was inserted into one side of the pipe which was connected to the container cap. Unused portion of the lithium was putted

into a bottle filled with argon. And the bottle was placed in a large sealed plastic bag filled with argon in order to ensure the purity of the lithium for a later use.

While argon was flowing in the pipe, lithium was transferred to the container and the container cap was sealed by 6 stainless steel bolts, which were coated with a ceramic material that prevented the nuts and bolts from seizing at high temperatures. At this time, the container was completely filled with argon. During the whole process, the time in which the lithium was exposed to air was less than 10 seconds. This procedure ensured the purity of the lithium to a good degree.

After the container was sealed, the entire piece, consisting of container, cap and piping, was put back into the original location. Since any leak around the o-ring and the joints between pipes was detrimental to the experiment, the cap and the container were tightly sealed with 6 bolts and nuts with even forces. In addition, the threaded parts of the joints were taped with a teflon tape and at each run, old teflon tape was replaced with new teflon tape. These consistent efforts to prevent any leak resulted in only a single run out of approximately forty runs, which leaked around the o-ring.

After the entire piece was put back, the argon gas line was connected to the pipe located just before the reaction chamber, after tank 2 was depressurized and the valve just before the second tank was open (see Fig. 4.1). So a continous stream of argon flowed through the reaction chamber. Previously, argon was supplied to the reaction chamber in same manner as described. However, the gas line was pressurized to 3-4 psig and all the valves were closed. The reason for the continous stream of argon was that by pressurizing the gas line too early could lead to a relatively large leak between the o-ring and the container if there was even a tiny leak. It was better to pressurize the gas line when the container temperature reached 300 to 400°C. By that time, due to the expansion of metal, the gap between the o-ring and the container would be completely sealed. And

at that temperature, the gas line was pressurized to about 1 psig and all the valves were closed except the valve between the second tank and the chamber. Monitoring the pressure of the second tank (the chamber and the second tank were connected at this point), one could ensure whether there is a leak or not.

As Ijams noticed, for runs at high and intermediate temperatures (600-1100°C), the lithium impurity almost certainly had little effect on the reaction rate, because once the lithium had melted, the reaction products would diffused into the lithium and, because they have greater density than the lithium, they would more likely have sunk to the bottom of the container. Also, reaction rates at these temperatures were quite vigorous so that one or two seconds of reaction would produce enough reaction products to make the initial deposits of impurities very negligible.

Ijams indicated that for low temperature runs (500°C and lower), the impurities seemed to hinder the smooth melting of the lithium and to increase the melting temperature of the lithium. Taking an advice from Ijams's previous experience, for the low temperature runs, the lithium was heated up to about 600°C to ensure melting of the lithium. Then, the lithium temperature was brought down to the desirable temperature. So in most cases, melting of lithium was observed in the low temperature runs. After ensuring the purity of the lithium, observation of the reaction products after the runs at low lithium temperature (below 400°C) indicates that the reaction products formed at the surface of the lithium can effectively prevent any further reaction of the lithium with gases. In addition, the inconsistent reaction rate Ijams observed may be due to the different surface area of the lithium; since the previous experiment had used lithium pellets, the surface area could have been very irregular. However, there is no doubt that the impurity can affect the consistency of the reaction rate in these low temperature runs since the impurity causes higher melting temperature of lithium.

iii) Heating lithium Pool

Heatup of the lithium pool began once argon was continously flowing over the chamber. Heatup time varied depending on the initial liquid lithium temperature desired. For the high temperature runs (greater 1000°C), the heatup time took as long as one hour. During the heatup period, several tasks were performed. First, the data acquisition system was turned on at the same time when the IBM AT was turned on. Several programs were developed for the data acquisition purpose; depending on the time interval of the acquisition and an option to store data on the hard disk or just to print out on the screen, an appropriate program was used. At this time, a program which prints all the data at the screen at every second without storing in the hard disk was used in order to monitor temperatures and pressures continously.

While the pool was heating up, the first tank pressure was set at a desirable pressure (in this case, 40 psig). At this time, the first tank was still filled with pure nitrogen. Adding pure oxygen of 14 psi (since there was about 55 psia of nitrogen in the tank), the composition of nitrogen and oxygen were 80 and 20 percent respectively in moles. So the total pressure was 54 psig; 4 psi were accounted for the leak while the temperature reached and settled down to a desirable point. For the runs that required other compositions, appropriate pressures were added. It was necessary to give few minutes for nitrogen and oxygen to mix together. After few minutes, the mixed gas was bled to the RGA in which the exact gas composition was obtained. The spectrum was then printed out for a record. Then, the capillary tube connecting from the first tank to the RGA was removed and the tube connecting from the second tank to the RGA was inserted to the RGA.

In the mean time, the lithium temperature was continously increasing. When the lithium pool temperature reached around 300 to 400°C, the gas line was pressurized to about one psig and all the valves were closed except

the valve between the second tank and the chamber. Then, the second tank pressure was monitored for any possible leaks. For most cases, no leak was observed. When there was a leak, the joints between pipes were checked and were re-tightened. This virtually eliminated most leaks. For the low temperature runs (below 600°C), in order to ensure complete melting of the lithium, the heating process continued until the temperature reached above 600°C. Then, the heaters were turned off and lithium was allowed to cool until a desirable lithium temperature was obtained. This process often took 10 to 20 minutes. During that time, there was enough time for the lithium to melt completely.

For the runs with initial lithium temperature greater than 600°C, the heating process continued until a desirable lithium temperature was obtained and then the heaters were turned off. However, due to the thermal inertia, the temperature continued to increase usually about 50°C higher than the desirable temperature. Then, the temperature went down slowly reaching the desirable temperature. Before the temperature reached the desirable point, the heaters were momentarily turned on to establish a stable lithium pool temperature at a desirable point. This process took long enough for all the lithium in the container to melt completely. At this time, everything was finally ready to conduct the lithium mixed gas reaction run.

4.3.3 Taking the Measurements

When the lithium temperature was stable, a new computer program, which prints data on the screen as well as stores data in the hard disk, was loaded. Opening and closing appropriate valves for the gas line were done so that the gases at tank 1 would flow through the reaction chamber to the second tank. As soon as the program was executed, the flow from tank 1 to the chamber was established. In the initial one to two second period, a valve was controlled to let small flow of gas to go through the chamber, burning out thin films of the lithium along the wall and ensuring the pool surface to be flat. Then, a predetermined full flow rate was established and the reaction process continued.

In the runs with the temperature greater 600° C, as soon as the reaction proceeded, the lithium pool temperature went up due to the heat generated from the reaction. Waiting until at least 5 data points were obtained, the valve of the flow meter was closed. And at the same time, the valve between the chamber and the second tank was also closed, retaining the gas which just went through the reaction chamber. This process ensured that the gas reaching the second tank was the part of the original gas which was not reacted with the lithium. Stopping the gas flow to the second tank at an appropriate time enabled one to find the gas composition after the reaction has taken place. From this final gas composition, how much oxygen and nitrogen were reacted with the lithium could be deduced. Furthermore, the lithium-nitrogen reaction rate inhibition factor due to the presence of oxygen could be deduced, too. Then, the gas in the second tank was bled to the RGA where the composition of the gas after the reaction was found. Then, argon was introduced to the chamber to terminate the reaction completely. From the hard disk of the IBM AT, the stored data were tansferred to a floppy disk and later were again transferred to LOTUS 1-2-3 software.

4.3.4 Post-Experiment Procedure

Once the experiment was complete, the chamber was allowed to cool down. When the lithium pool temperature reached below 30° C, the container was opened and the reaction products were inspected. The colors of reaction products were black and white. The black reaction product was lithium nitride, while the white reaction product was lithium oxide. Depending on the peak lithium temperature, the intensities of the colors were slightly different. Also, the effect of the lithium spreading was observed in order to check the constant lithium pool surface. At very high temperatures (greater than 800° C), the lithium usually did not spread too much, as Ijams also observed.

The reaction container was cleaned by soaking the container in water, under a hood. Lithium nitride, lithium oxide, and some of unreacted lithium reacted violently with water to form lithium hydroxide, ammonia, and hydrogen. After the container is completely cleaned by water, the container was allowed to dry. When the container was completely dried, the container was thoroughly cleaned with sandpapers. The top surface of the container and the bottom surface of the cap were resurfaced with sandpapers, leaving shiny stainless steel surfaces. The insides of the pipes connected to the container cap were thoroughly cleaned too, since the aerosol generated was often deposited inside.

After the cleaning process was done, the container was placed in the furnace in order to check the thermocouple. The container was heated and its temperature was checked by using a thermometer. The reason for this check was due to the location of the thermocouple. Since the thermocouple well was mounted from the bottom of the container, it was also soaked in the water during the cleaing process. Due to the harsh chemical environment in the contaminated water, the thermocouple placed in the well was often loose and came out of the well although the thermocouple was securely placed and bonded with a ceramic material between the thermocouple and the well. This check gave an additional

assurance of adequate performance of the thermocouple.

4.3.5 Difficulties

Some of the difficulties faced during the experiments were: 1) the effects of the liquid lithium spreading along the walls of the container; 2) the irregular lithium pool surface formation in the low to intermediate lithium pool temperatures (350 to 700°C); 3) the air filter between the heat exchanger and the second tank clogging; 4) obtaining the right composition of nitrogen and oxygen; 5) melting of the reaction chamber and the thermocouple well due to high lithium flame temperatures during the lithium-oxygen reaction runs; 6) impurity of the lithium causing only partial melting of the lithium in the low temperature runs with the temperature less than 400°C; 7) the corrosion of the stainless steel thermocouple well by the molten lithium and reaction products; and, 8) frequent failure of the thermocouple during the cleaning process of the container after the experiments.

Most of the items described above were previously mentioned. Some items will be explained further in detail in later sections. Several runs were discarded due to the impurity of the lithium which caused only partial melting of the lithium. For low temperature runs (the lithium tempearture less than 500°C), obtaining an accurate measurement was very difficult; first, because the reaction rate was very small, and second, because only surface reaction was observed. This surface reaction occurred during a short period of time so that only few data points were obtained while in the high temperature runs (greater than 600°C), at least 5 good data points were obtained. However, for a small scale experiment with a very small lithium pool surface area, the surface reaction effectively prevented any further reaction in the low temperature runs.

One of the runs of the lithium-mixed nitrogen and oxygen reaction was discarded due to clogging of the air filter. After performing many high temperature runs (greater than 900°C), the aerosol formation was clearly observed. The air filter was cloaked due to excessive aerosols created during the high tempera-

ture runs. Even though the heat exchanger cooled most of the generated aerosols before they reached the filter, still a large amount of the aerosols went through the heat exchanger without being condensed. This aerosol formation was particularly seen in the mixed gas kinetics runs while an insignificant amount of aerosols was observed in the lithium-nitrogen reaction runs.

Lithium flowing along the walls and roof of the lithium pool container increased the overall reaction area, therefore increasing the measured reaction rate. In addition, the irregular pool surface formation during the reaction in the low to intermediate temperature runs (350 to 700°C) indicated that the actual reaction area was larger than the cross-section area of the container, in turn, also increasing the measured reaction rate. However, the irregularity of the surface was not too large, which gave some assurance that the error in the reaction rate due to the irregularity of the surface was not significant. In Ijams's experiments, the lithium pellets were used. Since each pellet had its own surface area, when the pellets were not completely melted, the reaction surface would have been much larger than the cross-sectional area. This would have greatly impaired the accuracy of the reaction rate.

One of the difficulties faced was getting the right composition of nitrogen and oxygen for the mixed gas reaction kinetics runs. Due to small leaks developed in tank 1, by the time the lithium pool temperature was stablized so that the actual run could be initiated, the pressure of tank 1 had already dropped significantly. Then, from the screen of the RGA, one could calculate the approximate composition from the partial pressure peaks. Reading an exact value of the pressure peaks from the screen was not easy. This led to some variations in the composition of nitrogen and oxygen. However, in most cases, the percent of nitrogen or oxygen varied about 1 to 2 percent from the desired gas composition.

During the lithium-oxygen reaction runs, many difficulties were confronted. First, since impure lithium pellets were used, the lithium partially

melted even at the temperature of 500°C. Obtaining the lithium in a ribbon form with 99.9 percent purity, the lithium melted at temperature lower than 500°C. Two additional runs were conducted with the new lithium. Around a lithium pool temperature of 600°C, the lithium was ignited and the upper surface (flame) temperature melted the 316 stainless steel well and the temperature went beyond the rated temperature value of K-type thermocouple which was about 1375°C. So the thermocouple well was mounted from the bottom of the container and was covered by the lithium. The second run with the new lithium resulted in melting of the 316 stainless steel reaction chamber (0.32 cm thick) in the vicinity of the surface of the pool. And the lithium pool temperature increased beyond the rated value of the thermocouple, but the well did not melt, indicating that the lithium pool temperature was below the melting temperature of the 316 stainless steel. At this point, it was realized that a new design with different materials for the reaction chamber and thermocouple well would be necessary to conduct the lithium-oxygen reaction experiments.

CHAPTER V Experimental Results and Analysis of Data

5.1 Results and Observations

5.1.1 Lithium-Nitrogen Reaction

Five lithium-nitrogen reaction runs were made in order to verify Ijams's experimental results. Ijams indicated that the reaction rates obtained at lithium pool temperatures ranging from 500°C to 800 °C had the largest error (20 - 30%). Therefore, five runs were made in this temperature range in order to check reproducibility of the experimental data. As seen in Figure 5.1, the previous results by Ijams were found very reasonable.

For these runs, the previous apparatus was used except for the addition of two transducers and digital readouts. According to Ijams, the two largest sources of error came from pressure gauge reading and a large lithium temperature increase in the short recording period. With improved pressure reading, no noticeable difference between the previous data and "new" data was seen.

However, even at the lithium pool temperature of 500°C, the lithium pool temperature increased about 40°C during a 7.5 second period. Ijams had observed that the temperature increased rapidly in the runs with pool temperature ranging from 500 to 800°C. However, the lithium temperature increase observed in lithium-mixed nitrogen and oxygen runs at the peak reaction temperature (about 950°C) was about 50 to 60°C during a 7.5 second period. In these lithium-mixed gas runs, the heat generated from the reaction was much larger since the lithium-oxygen reaction has about three and half times larger heat of reaction. This indicated that the large increase in the lithium pool temperature may have resulted from measuring the flame pool temperature or the effect of radiative heat generated from the surface reaction. Therefore, if the measurement were made at the beginning of the reaction after "full" flow rate has been established, the pool temperature measured would be relatively accurate.

However, if the measurement were made in the middle of the reaction process, the temperature measured may be the temperature of the lithium fire flame. Due to this reason, all the data plotted in Figure 5.1 were the first measurement point as soon as "full" flow was established. It usually took about 5 to 6 seconds before full flow rate was established.

This reasoning was once again proven to be correct in lithium-oxygen reaction runs. When the thermocouple well was inserted from the top of the container cap, the well melted due to the high flame temperature. However when the well was inserted from the bottom of the container and was completely covered by liquid lithium, the thermocouple well did not melt.

As seen in Ijams's experiments, one of the sources of error was impurities in the lithium. In some cases, lithium did not melt even at a measured temperature of 500°C. In all five runs made, the lithium pellets instead of high purity lithium ribbon were still used. Impurites present in the lithium can either act as a catalyst for the lithium-nitrogen reaction, or they can interfere somehow with the reaction mechanism and slow it down. There were mainly two types of impurities; one was sodium impurity (0.5 to 1 percent in lithium pellets) and the other was surface reaction products consisting of lithium nitride, lithium oxide, and lithium hydride. These impurities may have hindered complete melting of lithium. This led to a new experimental procedure in which the lithium pool temperature was intentionallly increased to above 600°C to ensure complete melting and was then brought down to the desirable lithium pool temperature.

The nitrogen gas used in these runs was Grade 5, which meant 99.9995 percent purity. Therefore, nitrogen gas impurity effect on the reaction may be assumed negligible. In particular, the gas impurities were so small that even the RGA could not detect any impurities.

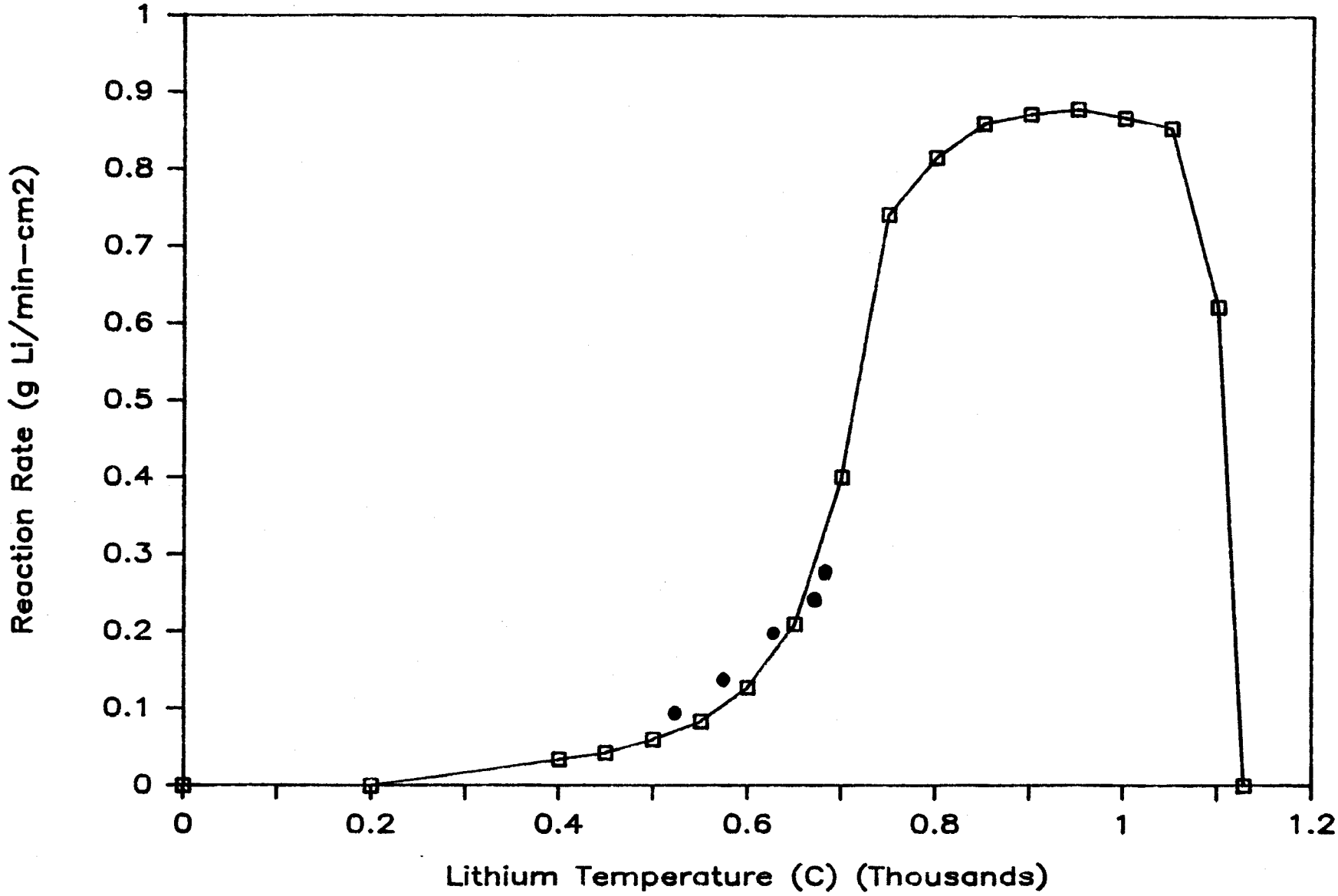

Figure 5.1 Ijam's reaction rate curve and verified reaction rates (black dots).

As Ijams observed, the lithium nitride reaction product was a jet black ceramic material, varying in strength according to its density. In addition, a red reaction product was occasionally found in a very small amount on the surface of the pool. Ijams indicated that the red reaction product was the amorphous nitride.

5.1.2 Lithium-Oxygen Reaction

Several attempts were made in order to measure lithium-oxygen reaction rates at different lithium pool temperatures [17]. In the beginning, many problems were confronted. The major problem was impurities of the lithium pellets. Even at 600°C, the lithium partially melted and the reaction rate measured was very inconsistent. Due to this problem, new "freshly" ordered lithium pellets were used. However, the same problem persisted. So, the new lithium in a ribbon form with 99.9 percent purity was obtained.

With the "new" lithium, two additional runs were conducted at the initial lithium temperature of 600°C. The results were quite surprising. In the first run, the lithium was ignited and the flame temperature was high enough to melt the thermocouple well made of 316 stainless steel, welded into the container from its cap. The bottom part of the well was found underneath of the lithium pool. The shape of the melted well indicated that it melted due to the high flame temperature, not by corrosion. Melting of the well indicated that the flame temperature exceeded 1400°C, the approximate melting temperature of stainless steel 316. The thermocouple rated temperature of 1375°C was also exceeded. The melted portion of the well was in the vicinity of the surface of the lithium pool. In addition, all the lithium had reacted with oxygen, creating white fluffy, but relatively hard lithium oxide.

Therefore, it was necessary to mount the well from the bottom of the container so that the well would be completely covered by liquid lithium. After inserting the well in the new location, the second run with the new lithium resulted in melting of the 316 stainless steel reaction chamber (0.32 cm thickness) in the vicinity of the surface of the pool. And the lithium pool temperature increased beyond the rated value of the thermocouple within about 30 seconds after the initial reaction, but the well did not melt, indicating that the lithium pool temperature was below the melting temperature of the 316 stainless steel.

All the lithium was consumed by lithium-oxygen reaction.

These results demonstrated that in order to conduct lithium-oxygen reaction runs, a new design with different materials for the reaction chamber and thermocouple well would be needed. A new material should have a very high melting point, preferably greater than 2000°C and should be oxidation resistent. Also, R or S-type thermocouples would be recommended. In a high temperature and corrosive environment, there is only limited number of materials which can be used. Tungsten, silicon carbide or tantalum may be suitable for the container and well materials.

5.1.3 Lithium-Mixed Gas Reaction

Twenty six experimental runs were conducted in order to characterize the lithium-mixed gas reaction kinetics. Three gas compositions were used: 1) 80 percent nitrogen and 20 percent oxygen; 2) 90 percent nitrogen and 10 percent oxygen; and 3) 95 percent nitrogen and 5 percent oxygen. Fourteen runs of the "80-20" percent composition, seven runs of the "90-10" percent composition, and five runs of the "95-5"percent composition were conducted. One of the major reasons for varying the composition was to observe the lithium reaction rate with each of the gases as the fraction of oxygen in the mixed gas decreases. When oxygen is present with nitrogen in a gas mixture, each tends to stifle the reaction rate with the other gas. Out of 26 runs, four runs were discarded. Three of those four runs were discarded due to the impurity problem in the low temperature region (less than 500°C). One run was discarded due to clogging of the air filter. Air filter clogging occured due to an excessive amount of aerosols generated from the high temperature runs. Most of the aerosols generated were lithium oxide. There was only a trace of lithium nitride aerosol found in the filter. Appendix 1 provides a summary of the all the runs made.

Calculation of the reaction rate of lithium-nitrogen and oxygen is shown below:

$$\Delta P_{initial} - \Delta P_{unreacted} = \Delta P_{reacted} \tag{5.1}$$

$$\Delta P_{initial} * F_{O_2,i} = \Delta P_{O_2,i} \tag{5.2}$$

$$\Delta P_{initial} * F_{N_2,i} = \Delta P_{N_2,i} \tag{5.3}$$

$$\Delta P_{unreacted} * F_{O_2,f} = \Delta P_{O_2,f} \tag{5.4}$$

$$\Delta P_{unreacted} * F_{N_2,f} = \Delta P_{N_2,f} \tag{5.5}$$

where $\Delta P_{initial}$ is the pressure increment in tank 2 in the absence of any reaction, $\Delta P_{unreacted}$ is the observed pressure increment in tank 2 with the reactions,

$F_{O_2,i}$, $F_{N_2,i}$, $F_{O_2,f}$, and $F_{N_2,f}$ are initial and final fractional composition of oxygen and nitrogen in moles respectively, and $\Delta P_{O_2,i}$, $\Delta P_{N_2,i}$, $\Delta P_{O_2,f}$, and $\Delta P_{N_2,f}$ are the initial increment of oxygen and nitrogen pressure before the reaction and the observed increment of oxygen and nitrogen pressure after the reaction.

From Eq. 5.1 through 5.5, the decrease in the nitrogen and oxygen pressure increment in tank 2 due to lithium reactions can be deduced as follows:

$$\Delta P_{reacted,N_2} = \Delta P_{N_2,i} - \Delta P_{N_2,f} \tag{5.6}$$

$$\Delta P_{reacted,O_2} = \Delta P_{O_2,i} - \Delta P_{O_2,f} \tag{5.7}$$

From Eq. 5.6 and 5.7, using the ideal gas law, one can calculate the number of moles of N_2 and O_2 consumed by the reaction:

$$N_{N_2} = \frac{\Delta P_{reacted,N_2} * V_2}{R * T} \tag{5.8}$$

$$N_{O_2} = \frac{\Delta P_{reacted,O_2} * V_2}{R * T} \tag{5.9}$$

$$RR_{N_2} = \frac{N_{N_2}}{t} \tag{5.10}$$

$$RR_{O_2} = \frac{N_{O_2}}{t} \tag{5.11}$$

where N_{N_2} and N_{O_2} are the number of moles of nitrogen and oxygen consumed by the reaction respectively, RR_{N_2} and RR_{O_2} are the lithium-nitrogen and lithium-oxygen reaction rates in moles per second respectively, T is the temperature of the gas in tank 2 in degrees Kelvin, V_2 is the volume of tank 2 in m^3, R is 8.314 joules/gmole °K, and t is the time interval (3 seconds in this case).

The above equations basically state that knowing the amount of nitrogen and oxygen available for the reaction and the final amount of nitrogen and

oxygen left in Tank 2 after the reaction, the amount of nitrogen and oxygen consumed by the reaction could be calculated. From Eq. 5.10 and 5.11, one can further deduce the reaction rate of lithium-nitrogen and lithium-oxygen in terms of gram of lithium consumed per unit time and unit area. Figures 5.2, 5.3, and 5.4 show the results of lithium mixed gas reaction experiments in varying gas compositions.

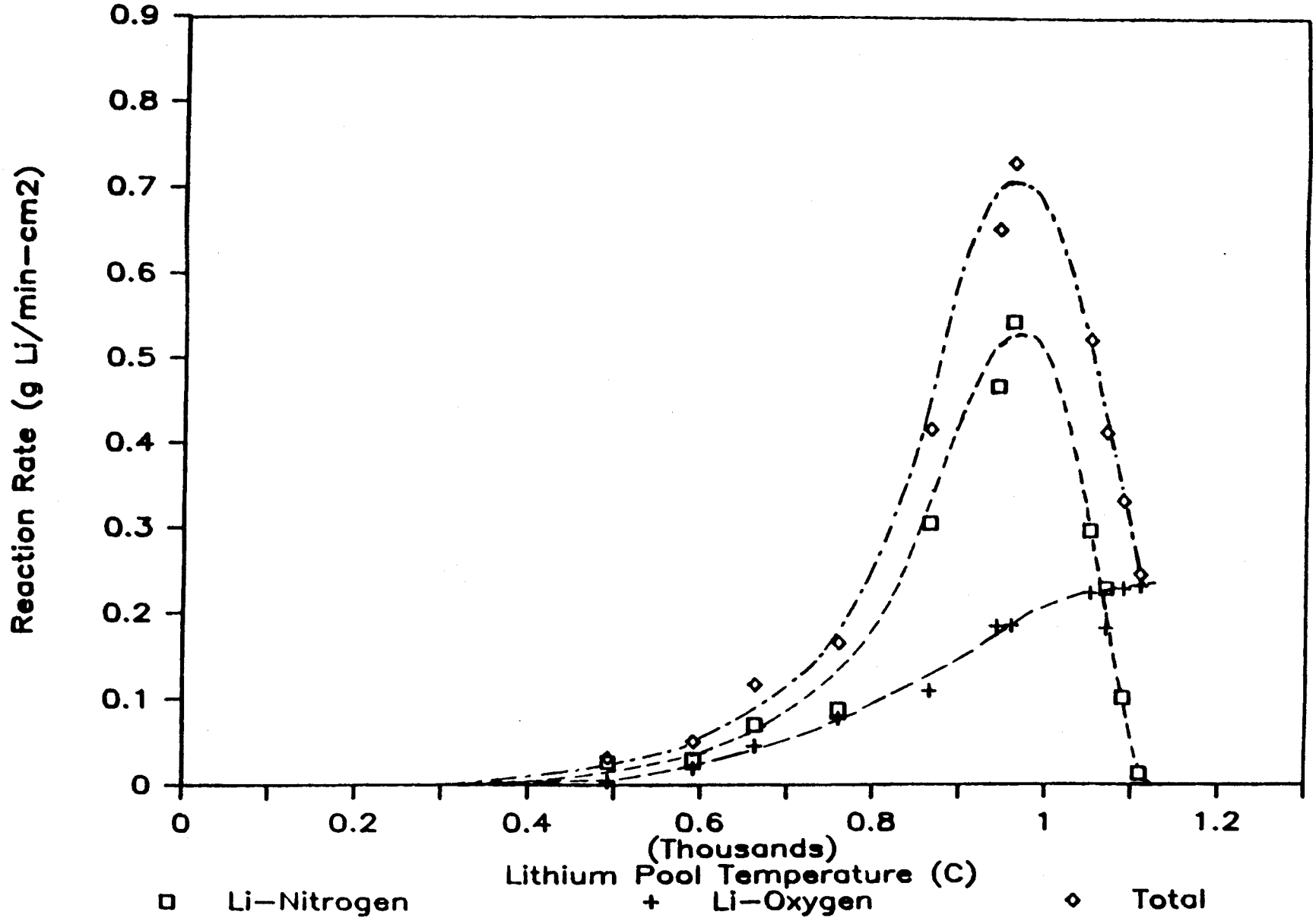

Figure 5.2 Lithium-mixed gas reaction rate with 80% nitrogen and 20% oxygen.

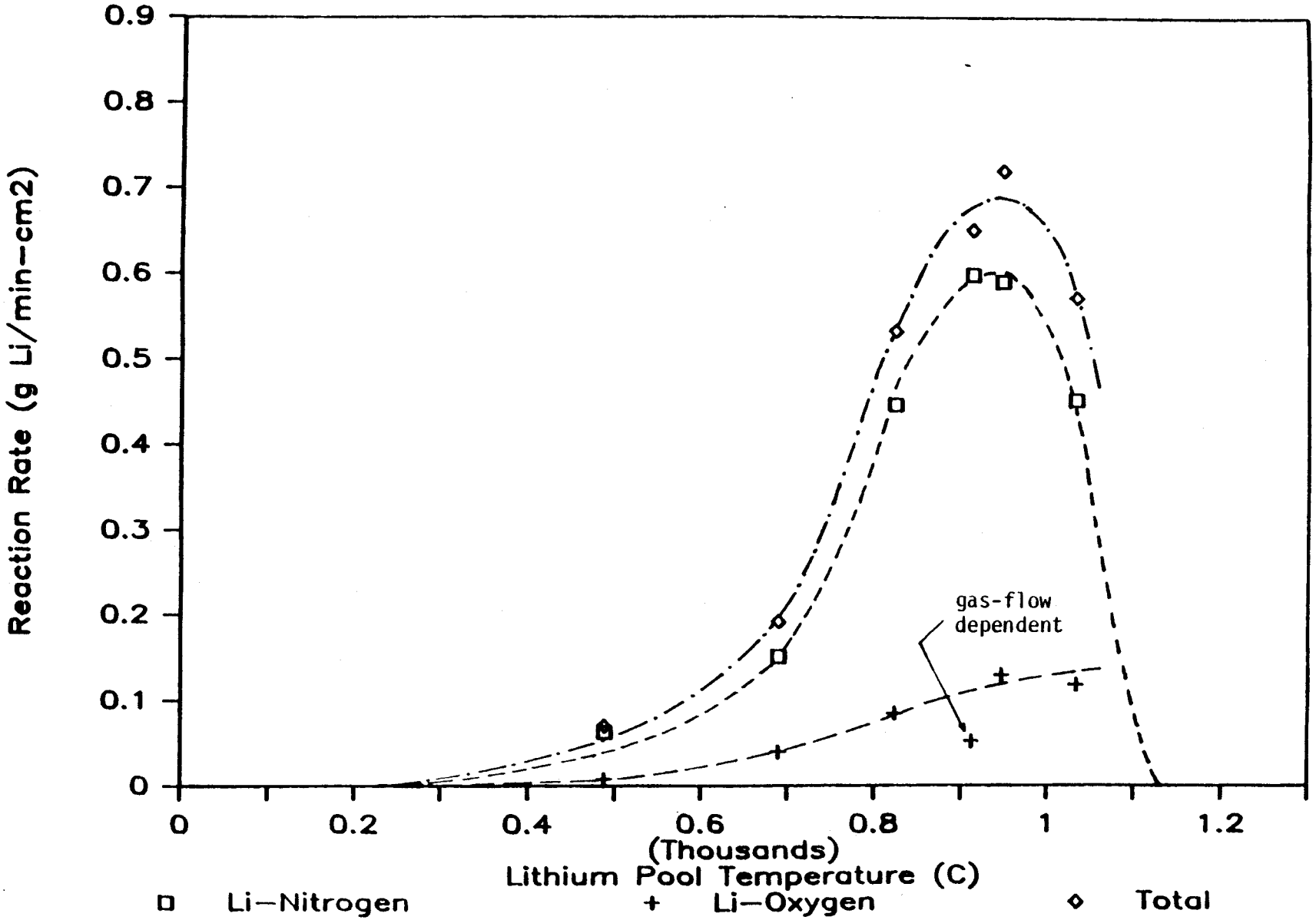

Figure 5.10 Lithium-mixed gas reaction rate with 90% nitrogen and 10% oxygen.

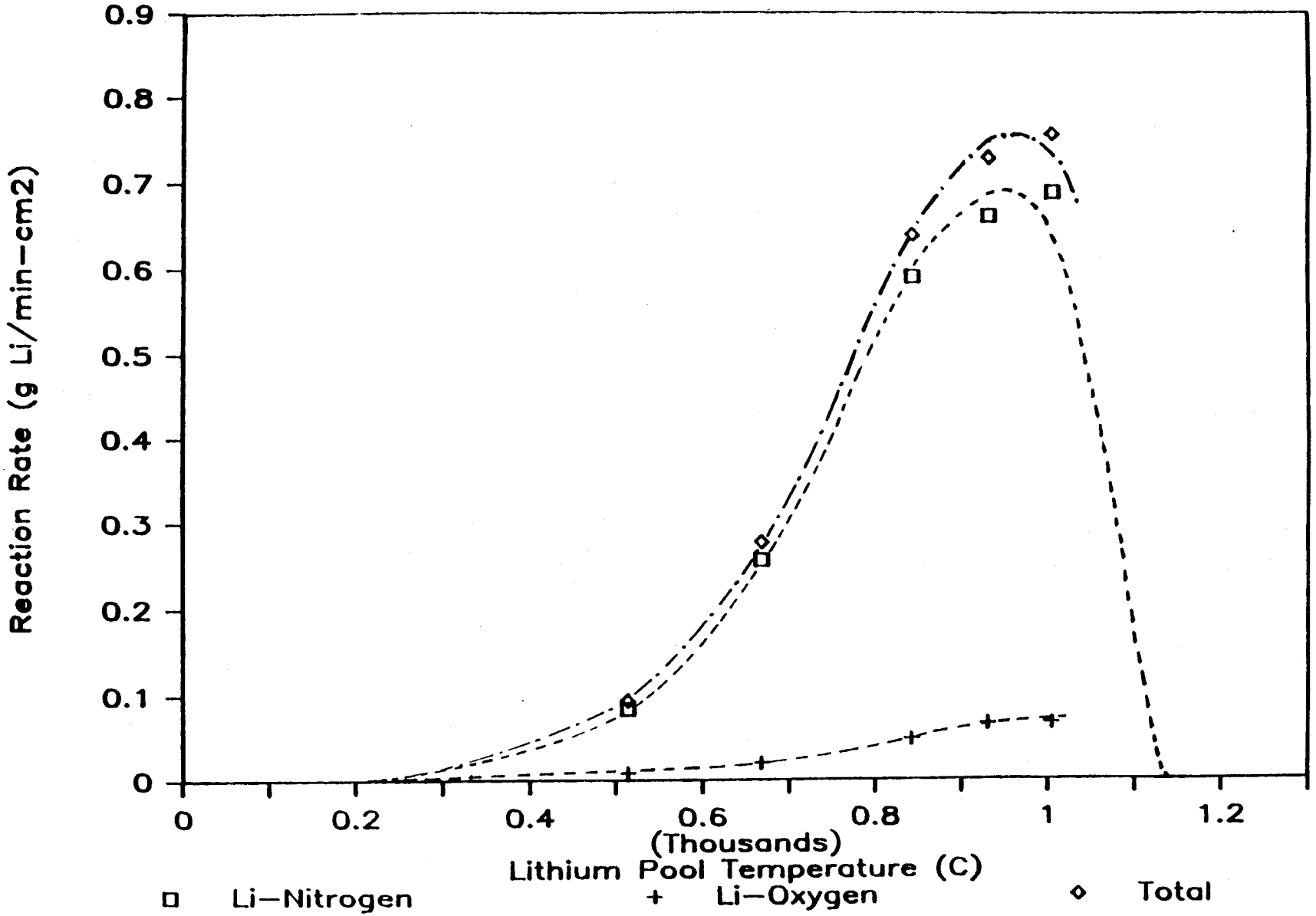

Figure 5.4 Lithium-mixed gas reaction rate with 95% nitrogen and 5% oxygen.

5.1.4 Discussion of Experimental Accuracy

The largest relative errors in the data occured at the low end of the pool temperature spectrum. Error at the low end of the scale was probably due to the lithium impurities. Since lithium was 99.9 percent pure, the sodium impurity effect was very negligible. However, the reaction products formed at the surface of the ribbon may contribute a large error in the data. Even though the lithium completely melted near 400°C and a large amount of the contaminated ribbons was cut away, the melting temperature of the lithium was still considerably higher than the reported value of 185°C. However, there was a certain increase in the thermocouple temperature at 250°C. This indicated that some portions of the lithium was beginning to melt at this temperature, increasing the heat conduction. But due to the impurity, complete melting of the lithium occured much later at near 400°C.

The second source of error was the lithium pool "creep" and surface irrgularities. As seen in the lithium-nitrogen reaction runs, the tendency of spreading was frequently observed in the temperature range of 600 to 800°C. In one of the runs, the effect of spreading was quite significant. The thickness of the reaction products along the wall was larger than the other runs. In particular, on top of the lithium nitride layer, a fine layer of lithium oxide covered the wall. This was one of the "95-5" runs. During the first 12 seconds after the initial reaction, due to the increase in the reaction surface area, the total reaction rate was considerably higher than the other runs of the about same lithium pool tmperature with the different compositions.

However, the reaction rate quickly dropped and somewhat stablized. This indicated that the thin film of the lithium along the wall has burned out in about 12 seconds. The estimated surface area at the beginning of this run was about 8 cm^2 which was about two times larger than the cross-sectional area of the pool. This indicated that the spreading effect may introduce a significant

error if the measurements obtained in the first 12 seconds were used. Therefore, at the beginning of the run, a small of amount of gas was introduced to burn off the thin films of the lithium along the wall and also to prevent a rush of gas flowing through the chamber which may cause a shift in the leveled surface of the liquid lithium. Usually, the desired "full" flow rate was obtained after a 6 second period.

Irregularities of the surface were frequently observed in the temperature range from 400 to 700°C. In particular, the irregularities were significant in the temperature range from approximately 600 to 700°C. The major form of the irregularities was dome-shaped contours covering some portion of the surface. On top of these small domes, some smaller domes were also observed. These irregularities certainly increased the reaction rates to a degree (later estimated not to exceed 20 percent). However, it is difficult to approximate the degree of the effect caused by the presence of the irregular surface.

The third source of error came from the inconsistent nitrogen and oxygen compositions. Since the available nitrogen was at least three times larger than the consumed nitrogen, a small decrease or increase in the amount of the available nitrogen would not create any substential error. However, the differences in the oxygen fraction of the gas might have created a large source of error. The maximum difference in oxygen fraction of the mixed gas was about 20 percent. In most cases, the difference in oxygen fraction was less than 10 percent. In the "80-20" percent runs, the maximum difference was about 15 percent while the average difference was about 7 percent. In other words, the fluctuation on the oxygen composition of the gas mixture was much higher in the "90-10" and "95-5" runs because of their smaller oxygen content.

In addition, the calculated reaction rates were based on the assumption that during the reaction process, the same fraction of oxygen or nitrogen was consumed. However, since the reaction rate was time-dependent, this assump-

tion may not be valid. In order to avoid the error related to this assumption, in most cases, as soon as about 5 data points were obtained, the valve located just before the second tank was closed in order to store only the gas which had just passed through the container. Furthermore, in runs with pool temperature greater 900°C, most of the oxygen was consumed. Knowing the amount of nitrogen gas available for the reaction, and that gas left in tank 2 was mostly nitrogen, the reaction rate can be calculated. Therefore, the error based on this assumption may have been quite negligible.

The fourth source of error was due to the reaction product layer formation. Most of the reaction product formed on the surface of the pool was lithium nitride. In most cases, lithium oxide was found as aerosols and only very thin layer of powder-like lithium oxide was oberved. It was easy to scrape off the lithium oxide layer while the lithium nitride layer was not easily scraped off. This indicated that the lithium oxide layer does not affect the reaction rates considerably. However, the lithium nitride layer seemed to reduce the reaction rate considerably. Therefore, the reaction rate was time-dependent since the thickness of the lithium nitride layer increased with time. The reaction rates shown in Figure 5.2, 5.3 and 5.4 were the average reaction rate over 6 to 9 seconds in most of the cases. Since the previous experiments used 7 to 10 second time interval, in order to make an adequate comparison between the previous results and the new results, it was necessary to average the reaction rates. Averaging the reaction rates often resulted in quite a decrease in the reaction rate compared to the peak reaction rate. In low temperature runs with the lithium temperatures below 500°C, only few data points were obtained since the reaction product formed seemed to prevent the reaction rather quickly. In most of these runs, only surface reaction was observed and only one or two data points were avaialble for averaging.

The fifth source of error came from the high temperature runs in which the reaction rate was gas-flow dependent. In most of the runs, less than one

third of the available gas was consumed. In addition, for runs with the temperature greater than 900°C, 5.5 liters/min flow rate was used as opposed to the 3.5 liter/min. This effort seemed to eliminate the problem of gas-flow dependent reaction rates. However, the lithium-oxygen reaction rates were gas-flow dependent. In Figure 5.3, the effect of the gas-flow dependency can be observed. Although there was an excessive amount of nitrogen gas available so that the lithium-nitrogen reaction rate was gas independent, there was still a shortage of oxygen to react with liquid lithium. In fact, the reaction rate in the high temperature region seemed to approach a finite value which was the maximum supply of oxygen. However, the lithium-oxygen reaction rates measured at temperatures below 700°C are gas flow independent, since at least half of the oxygen supplied did not react.

The error contributed by the lithium temperature increase due to the reactions is insignificant. The maximum temperature increase during a 3 second interval in the high temperature runs was about 20°C. And the response time of the thermocouples was quite negligible. According to the specification provided by Omega Engineering, Inc., the response time of the thermocouple was about 1.5 to 2 seconds when the thermocouple was exposed to fast hot flowing air. In our case, the thermocouple well was submerged in the lithium pool. The time response of the metal to the liquid metal would be considerably faster. Even if the response time was 2 second, 20°C difference in the temperature would not contribute a significant source of error.

The effects of the lithium nitride layer on the reaction rates and the lithium-nitrogen reaction rate inhibition due to the presence of oxygen will be further discussed in the following sections.

5.1.5 Estimate of Experimental Errors

In order to determine the accuracy of the data, it is important to estimate the maximum deviation of the data. The error contributed from the impurity of the lithium is difficult to quantify and the reaction product layer effect is part of a natural process which can hardly be called an error. Therefore, only errors generated from the enlargement of the surface area, the inconsistent oxygen fraction of the mixed gas, and the lithium pool temperature creep will be considered in the error analysis.

However, it is important to realize that the relative error contributed from the impurity of the lithium in the tempeature range below 500°C is quite significant. Also, in most cases, the reaction rate as a function of the lithium pool temperature is the average value of 2 to 3 data points. In addition, most of the lithium-nitrogen reaction rates plotted were gas flow independent by assuring that the amount of gas consumed was less than one-third of the available gas. However, the lithium-oxygen reaction rates for temperatures greater than 900°C were definitely gas-flow dependent.

In order to perform an error propagation calculation, a reasonable value of each error must be obtained. The maximum error caused by the enlargement of the pool surface was assumed to be about 20 percent. The low (below 500°C) and high temperature (above 800°C) cases, the error is lower. The 20 percent error basically came from a rough calculation of the surface irregularities, assuming there were one hundred dome shaped contours, and the total surface area of one dome is one-third of a hemisphere, and about one-half of the surface was covered by these domes.

The error generated from the inconsistent fraction of oxygen in the gas was about 20 percent since the maximum difference in the oxygen composition was 20 percent. The error due to the temperature increase from the vigorous reaction was about 2 percent since at about 1000°C, there was about 20°C in-

crease.

The maximum value obtained from the error propagation was about 28 percent. In reality, some of the reaction rates measured may have had a much lower value of error. It is difficult to quantify the more dominating factors. The effect of the enlargement of the surface area may have been larger than the inconsistency of the fraction of oxygen gas mixture. This is because there was an excess amount of nitrogen gas available and the amount of oxygen increase or decrease relative to the amount of the total available gas was very small.

5.1.6 Characterisitcs of the Reaction Product

The characteristics of lithium nitride formed in the mixed gas runs were essentially the same as the product observed in the lithium-pure nitrogen runs. Lithium nitride was a jet black ceramic material, varying in strength to its density. Also, a small amount of red reaction product which is believed to be lithium nitride in an amorphous form was frequently observed in the runs with temperature greater than 800°C. No significant amount of the lithium nitride aerosol was generated. From the RGA, no aerosols generated from the reactions were seen. The aerosols were effectively stopped by the heat exchanger or the air filter before they reached the second tank.

In most cases, lithium nitride was formed on the surface of the lithium pool and lithium oxide was formed on top of the lithium nitride layer. While lithium nitride was a very hard substance, lithium oxide was a powder-like substance which could be easily scraped off from the surface. Lithium oxide was a white substance, also varying in strength according to its density. In the high temperature runs with temperatures greater than 900°C, a little amount of lithium oxide was observed on the surface of the pool. However, in the piping system between the chamber and the second tank, a significant amount of the settled lithium oxide aerosols was seen. It seems that at high temperatures, lithium oxide is likely to be formed as aerosols.

5.2 Anaysis of Data

5.2.1 Introduction

In the previous section, several experimental errors were discussed, and from the overall error estimate calculation, the maximum error was about 28 percent. In this section, two very significant phenomena seen in the lithium-mixed gas experiment will be discussed. One is the lithium-nitrogen reaction rate inhibition effect due to the presence of varying amounts of oxygen in the gas mixture. And the other is the lithium nitride layer effect on the reaction rates. Note that the inhibition effect of the nitrogen on the oxygen reaction rate will not be quantified here.

5.2.2 Lithium-Nitrogen Reaction Rate Inhibition Effect

The decrease in the lithium-nitrogen reaction rates due to the presence of oxygen is clearly seen in Figure 5.5. In Fig. 5.5, the three lithium-nitrogen reaction rate curves obtained from the lithium-mixed gas runs are plotted against the lithium-nitrogen reaction rate without the presence of oxygen. The lithium-nitrogen reaction rate inhibition effect increases as the fraction of oxygen present in the gas increases. In the low lithium temperature region, the inhibition effect is not significant. One of the possible explanations of such tendency is that the lithium-oxygen reaction rate was relatively small in the low lithium temperature region. The lithium-oxygen reaction rate was also temperature dependent as the lithium-nitrogen reaction rate was. In the high temperature region between 800 and 1100°C, the inhibition effect is not as large as the temperature region between 500 and 750°C. This effect is clearly seen in Figure 5.6.

In Figure 5.6, the lithium-nitrogen reaction rate inhibition factor is plotted as a function of the lithium pool temperature. The inhibition factor is defined as:

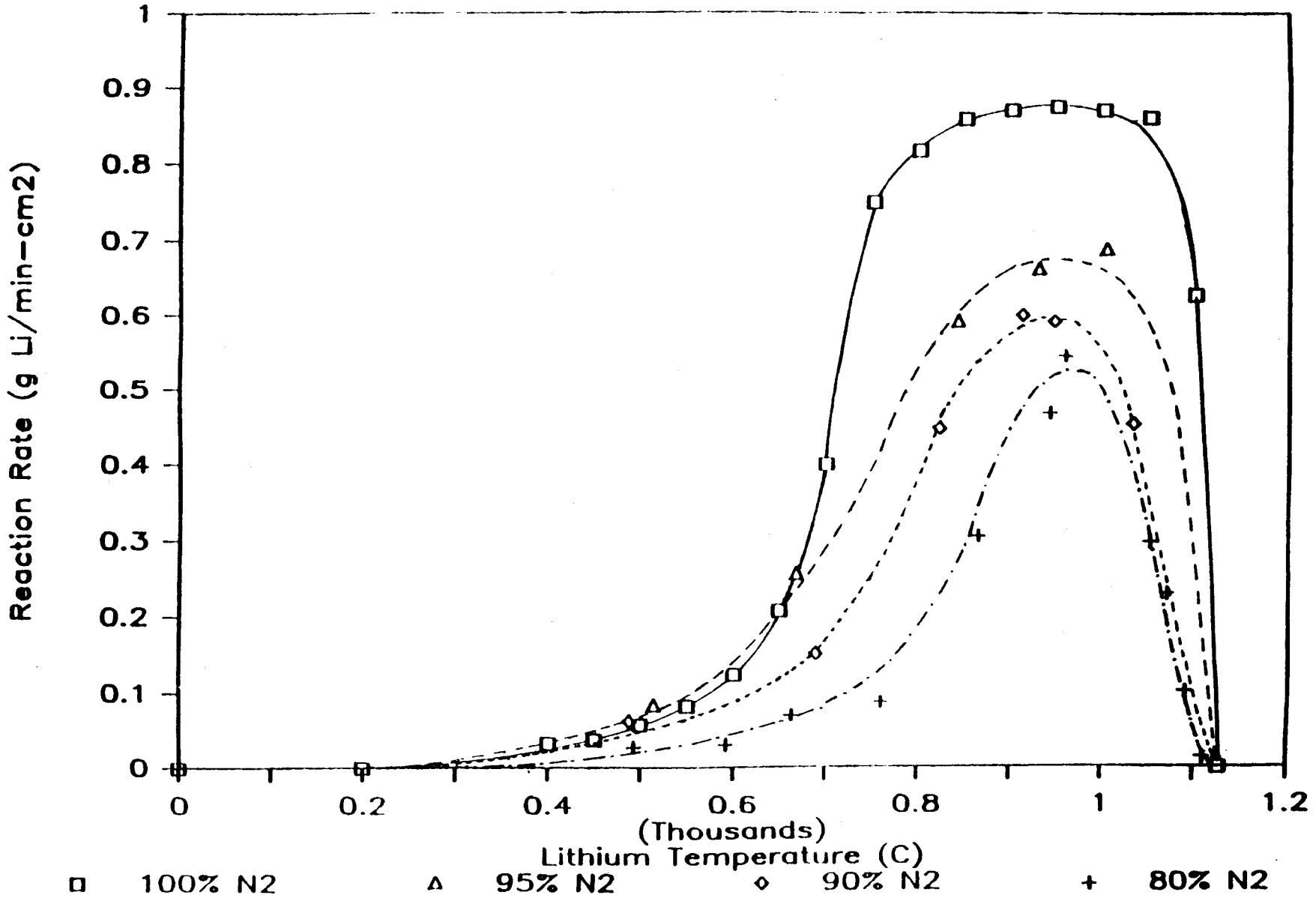

Figure 5.5 Lithium-nitrogen reaction rates with various fractions of oxygen present.

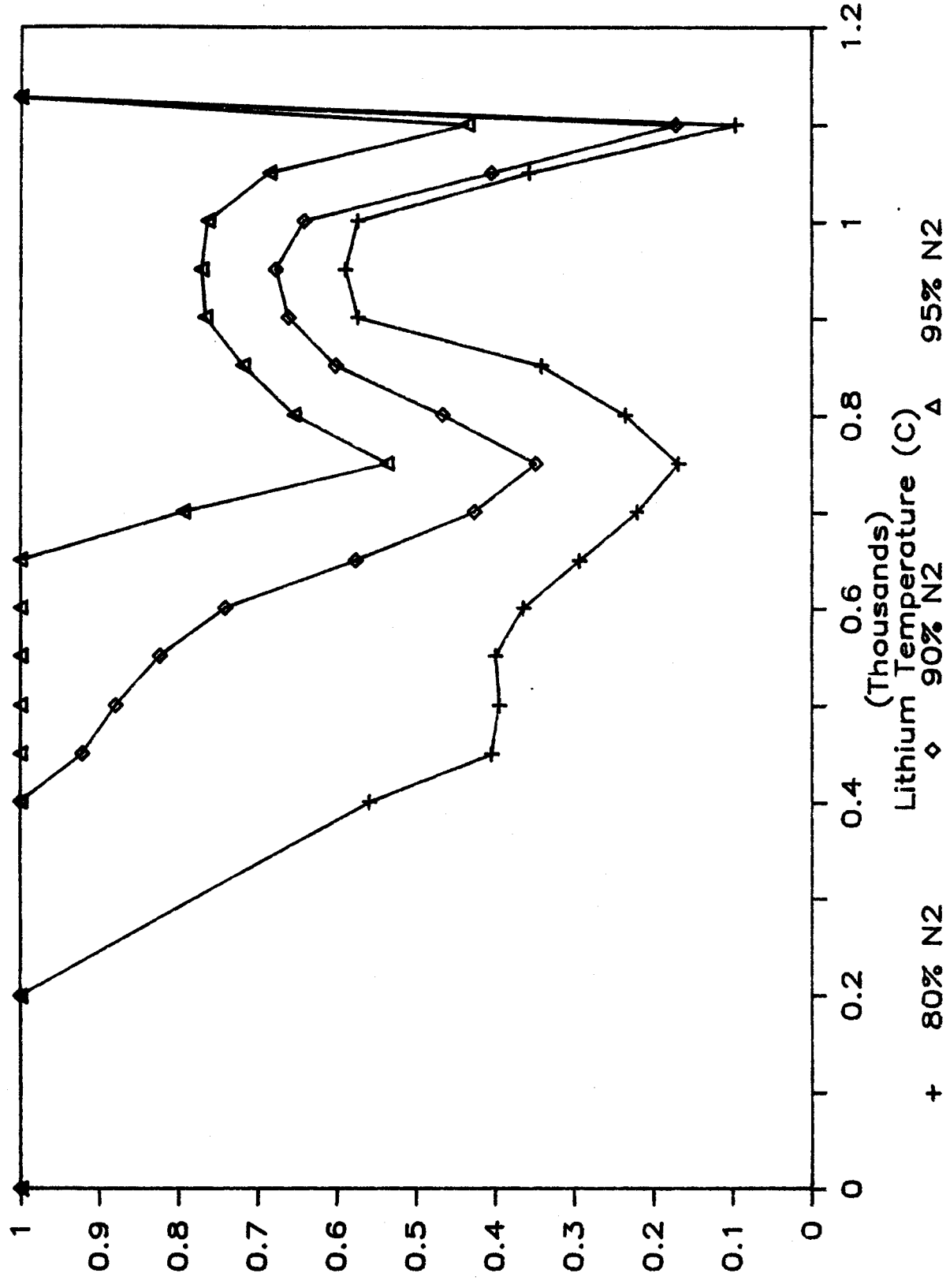

Figure 5.6 Lithium-nitrogen reaction rate inhibition factor in terms of lithium temperature and the fraction oxygen.

$$R_{N_2} = \frac{RR'_{N_2}}{RR_{N_2}} \tag{5.12}$$

where RR'_{N_2} is the lithium-nitrogen reaction rate with the presence of oxygen, and RR_{N_2} is the lithium-nitrogen reaction rate without the oxygen presence. Fitting these three curves with a 3^{rd} order polynomial results in the following equations:

$$R_{N_2,1} = 11.751 - 41.255(\frac{T}{750}) + 53.002(\frac{T}{750})^2 - 22.962(\frac{T}{750})^3,$$

$$500 \leq T < 750^\circ C \tag{5.13}$$

$$R_{N_2,1} = 13.173 - 55.058(\frac{T}{750}) + 77.625(\frac{T}{750})^2 - 35.276(\frac{T}{750})^3,$$

$$750 \leq T \leq 1100^\circ C \tag{5.14}$$

$$R_{N_2,2} = -0.176 + 5.295(\frac{T}{750}) - 6.998(\frac{T}{750})^2 + 2.218(\frac{T}{750})^3,$$

$$350 \leq T < 750^\circ C \tag{5.15}$$

$$R_{N_2,2} = 16.936 - 73.32(\frac{T}{750}) + 104.629(\frac{T}{750})^2 - 48.067(\frac{T}{750})^3,$$

$$750 \leq T \leq 1100^\circ C \tag{5.16}$$

$$R_{N_2,3} = 0.391 + 4.128(\frac{T}{750}) - 8.161(\frac{T}{750})^2 + 3.8(\frac{T}{750})^3,$$

$$200 \leq T < 750^\circ C \tag{5.17}$$

$$R_{N_2,3} = 26.456 - 109.284(\frac{T}{750}) + 148.31(\frac{T}{750})^2 - 65.412(\frac{T}{750})^3,$$

$$750 \leq T \leq 1100^\circ C \tag{5.18}$$

where T is the lithium pool tmeperature in Celcius and $R_{N_2,1}$, $R_{N_2,2}$, and $R_{N_2,3}$ are the inhibition factors of 5, 10, and 20 percent oxygen present in the mixed gas environment. The equations predict the inhibition factor within 10 percent deviation.

As seen in Fig. 5.6, the dependence of the inhibition factor on the lithium pool temperature was quite significant. Therefore, it becomes important that the inhibition factor is expressed in terms of both lithium pool temperature and fraction of oxygen present in the gas mixture. One interesting phenomenon seen in the figure is that the inhibition factor seemed to increase in the temperature range from 800 to 1000°C. This indicates that in this temperature range, the lithium-nitrogen reaction was so vigorous that nitrogen actually competed with oxygen to react with the liquid lithium. The lithium-nitrogen reaction rate seemed to peak at the temperature of 950°C.

In Figure 5.7, the three lithium-oxygen reaction rates are plotted as functions of the lithium pool temperature. In high temperature runs ($T > 950°C$) of the lithium-mixed gas reaction, most of the oxygen was consumed by the reaction. The reaction rate seemed to approach a finite value which corresponded to the maximum supply of oxygen. This indicated that the measured lithium-oxygen reaction rates were gas-flow dependent. So, if the supply of oxygen was higher, the reaction rates would have been larger. Therefore, in the condition in which the lithium-oxygen reaction is gas-flow independent, the inhibition effect would be surely somewhat larger. At low temperature runs of temperature less than 600°C, the inhibition effect seen in the figure would not be any larger since more than half of the oxygen did not react with the lithium. However, at temperatures greater than 800°C, as the lithium-nitrogen reaction was very vigorous, this may have considerably offset the inhibition effect.

In addition, the lithium-oxygen reaction rate was lithium pool temperature dependent. It may be important to measure the lithium-oxygen reaction rate at different lithium pool temperatures since it would once more verify that the reaction rate measured was gas-flow dependent. While the lithium-nitrogen reaction rate approaches zero at 1127°C, the lithium-oxygen reaction rate would still increase as the temperature increases until it reaches the dissociation temperature of lithium oxide.

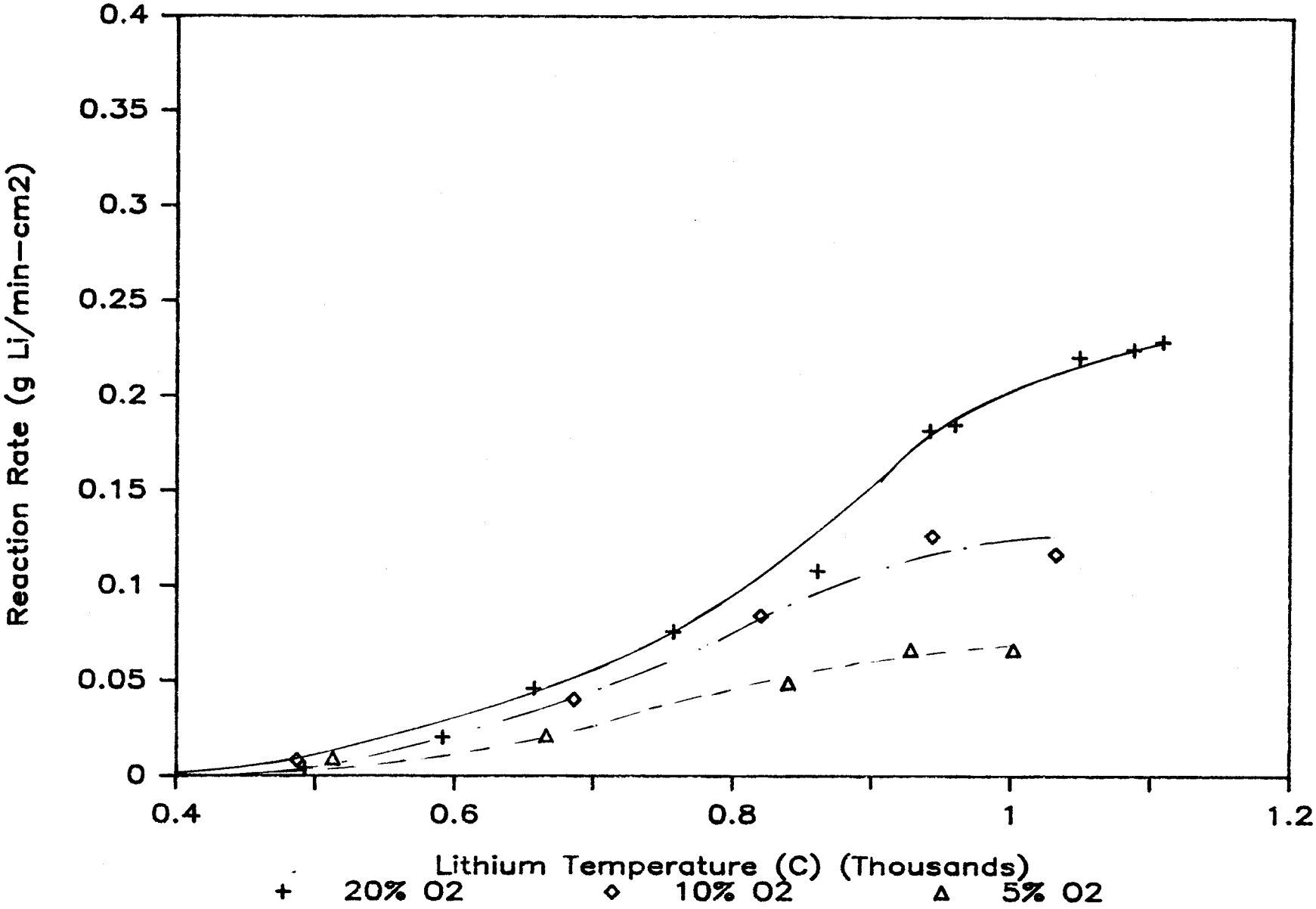

Figure 5.7 Lithium-oxygen reaction rates with varying fractions of oxygen.

5.2.3 Reaction Product Effect on the Reaction Rate

When the liquid lithium reacts with the mixed gas, lithium nitride and lithium oxide are formed on the surface of the pool. In the temperature region from 400 to 800°C, both lithium nitride and oxide were seen on the surface of the pool; usually, the oxide was formed on top of the nitride. In the temperature region of 800°C or greater, most of the layer was lithium nitride and most of the oxide was formed as aerosols. As Addison and Davies', and McFarlane's experiments indicated, the reaction rate as a function of the reaction time seemed to follow a parabolic law [4,5]. In Addison and Davies' experiment, in the early stage of the reaction, the reaction seemed to pass from a linear stage (constant reaction rate) to a logarithmic transition stage to the dominating parabolic stage. As explained earlier, a parabolic law governs reactions where the rate controlling mechanism is the diffusion of one of the reactants through a surface film. The surface film in this case is the reaction product, lithium nitride and oxide.

Figures 5.8 through 5.14 show the inhibition effect of the nitride. The figures are plotted in either the reaction rate (gram Li/min-cm^2) or the square of the lithium consumed, w^2 in g^2 Li. As explained earlier, the effect of the lithium oxide layer on the reaction rate seemed to be very negligible since most of it was generated as aerosols and the lithium oxide was a powder-like substance. Therefore, all the reaction layer effects discussed here pertain to the lithium nitride layer.

In Figure 5.8, w^2 plotted against the reaction time shows that in the early stage of the reaction, the reaction seemed to pass from a linear stage to a logarithmic transistion stage to the parabolic stage. In Figure 5.8, Run 14 with lithium temperature of 690°C and 10 percent oxygen was plotted while in Figure 5.9, Run 9 with lithium temperature of 960°C and 20 percent oxygen was plotted. From these figure, several observations can be made. Firstly, the parabolic law seemed to be dominating the reaction.

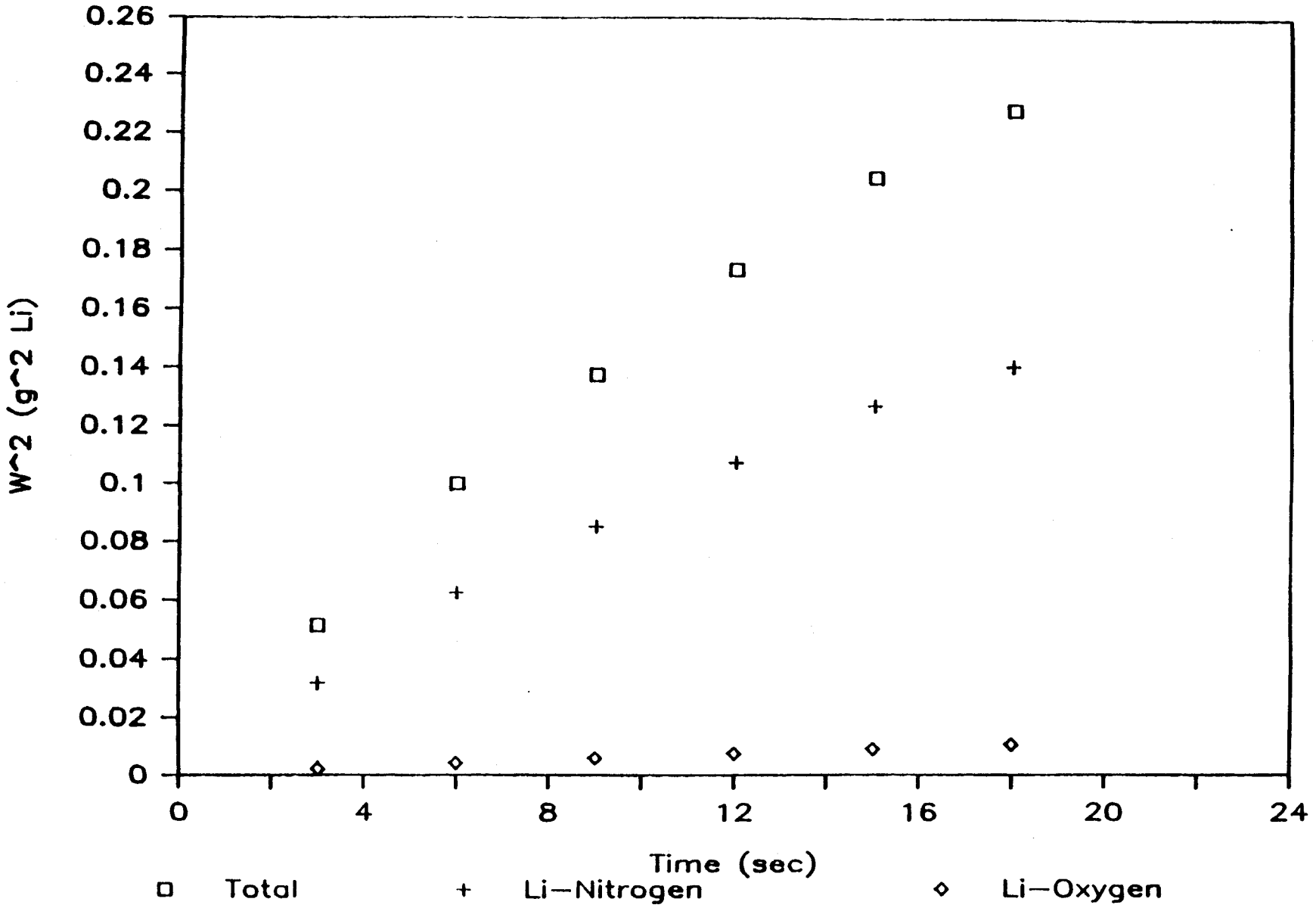

Figure 5.8 Nitride effect on reaction rate (Run No. 14); T_{Li} = 690 C and "90-10" composition.

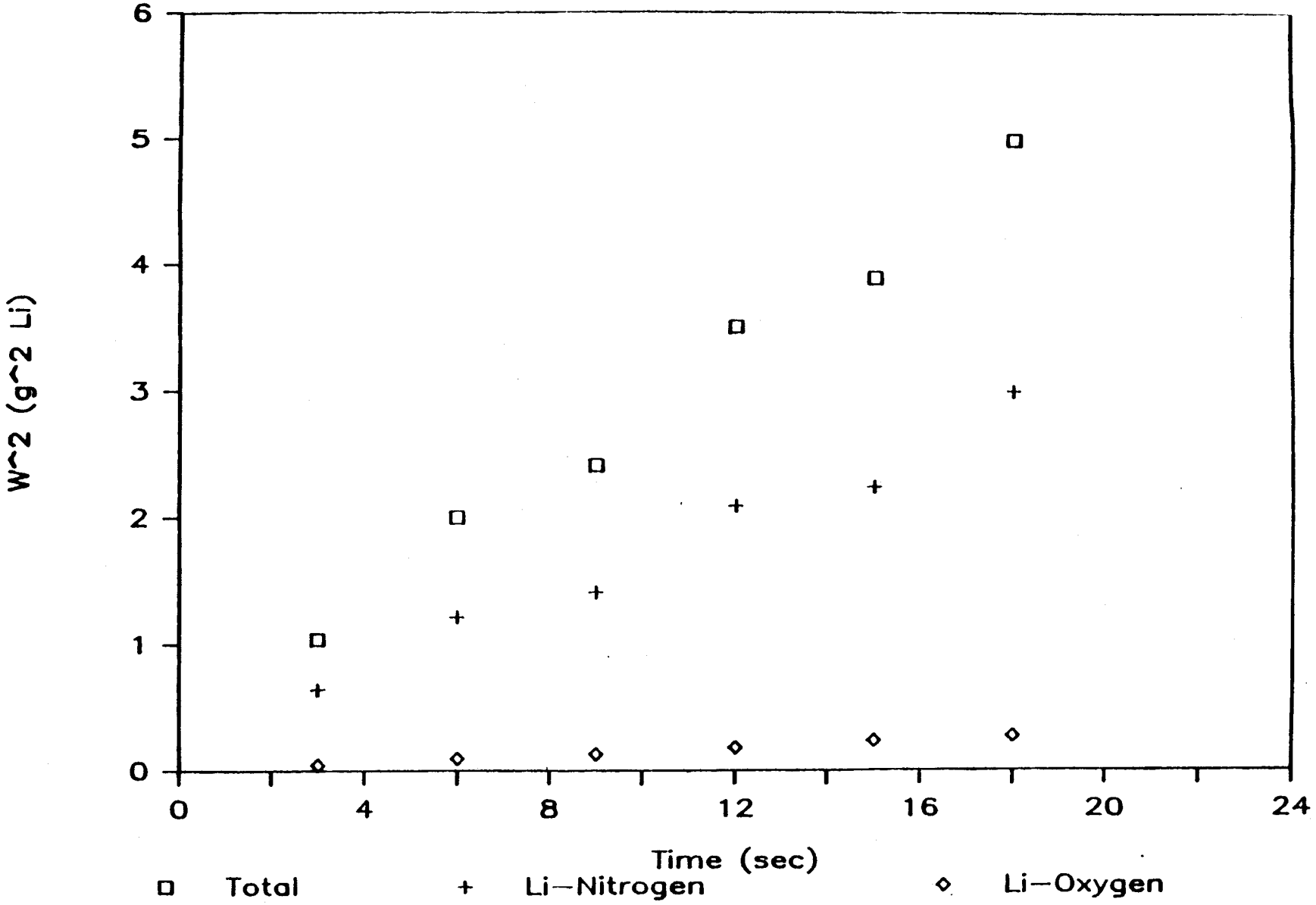

Figure 5.9 Nitride effect on reaction rate (Run No. 9); T_{Li} = 960 C and "80-20" composition.

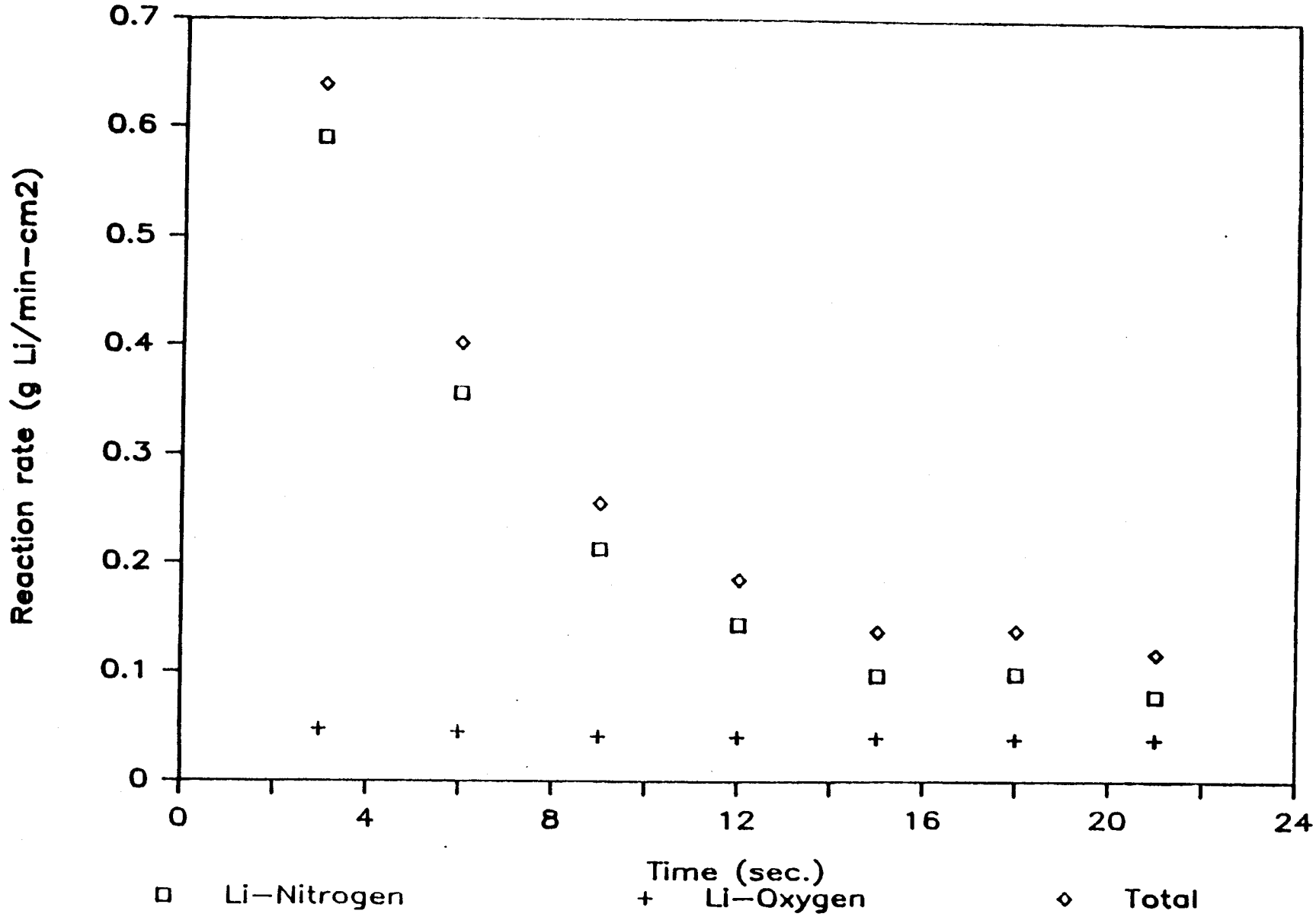

Figure 5.10 Nitride effect on reaction rate (Run No. 52); T_{Li} = 852 C and "95-5" composition.

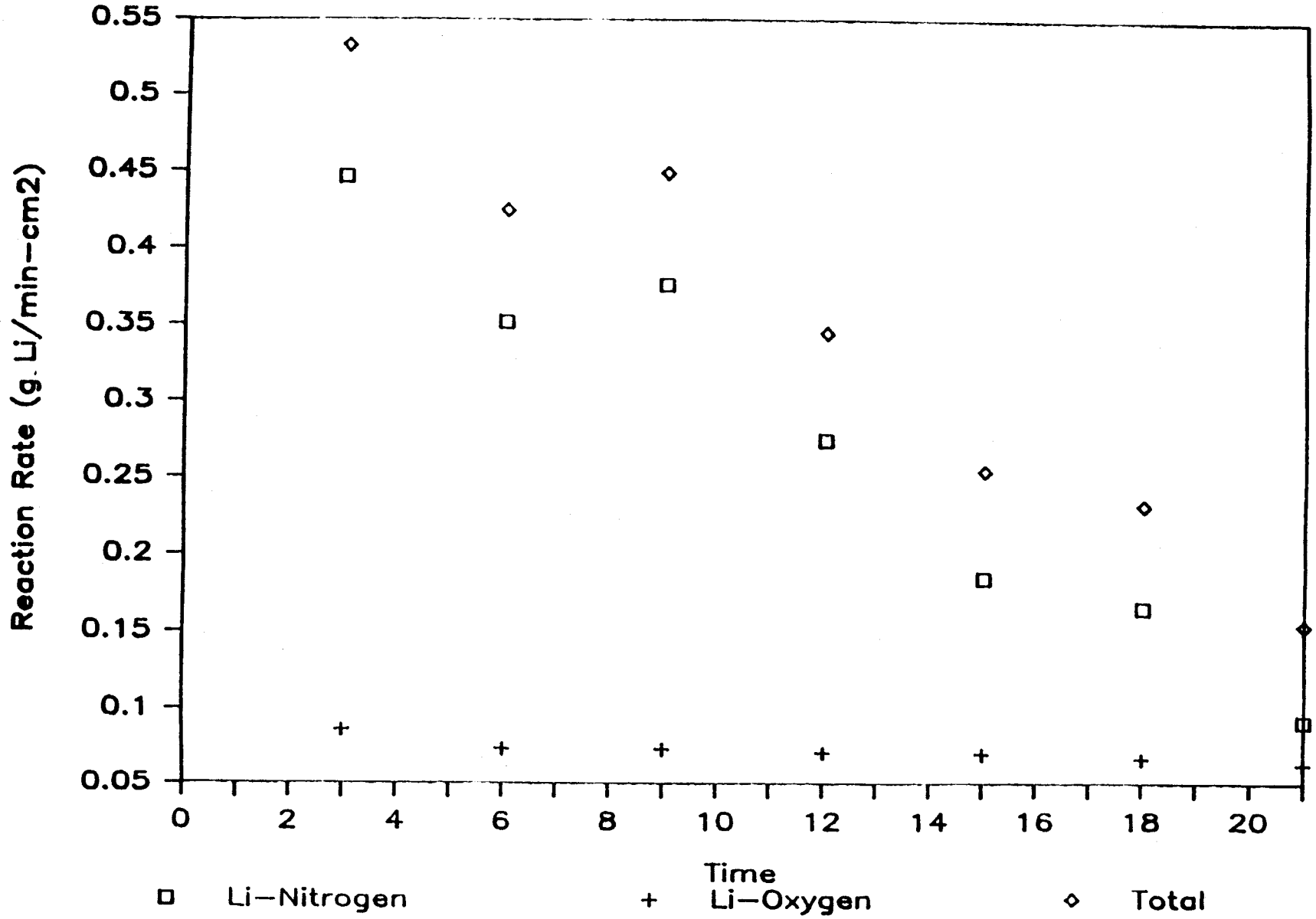

Figure 5.11 Nitride effect on reaction rate (Run No. 19); T_{Li}=823 C and "90-10" composition.

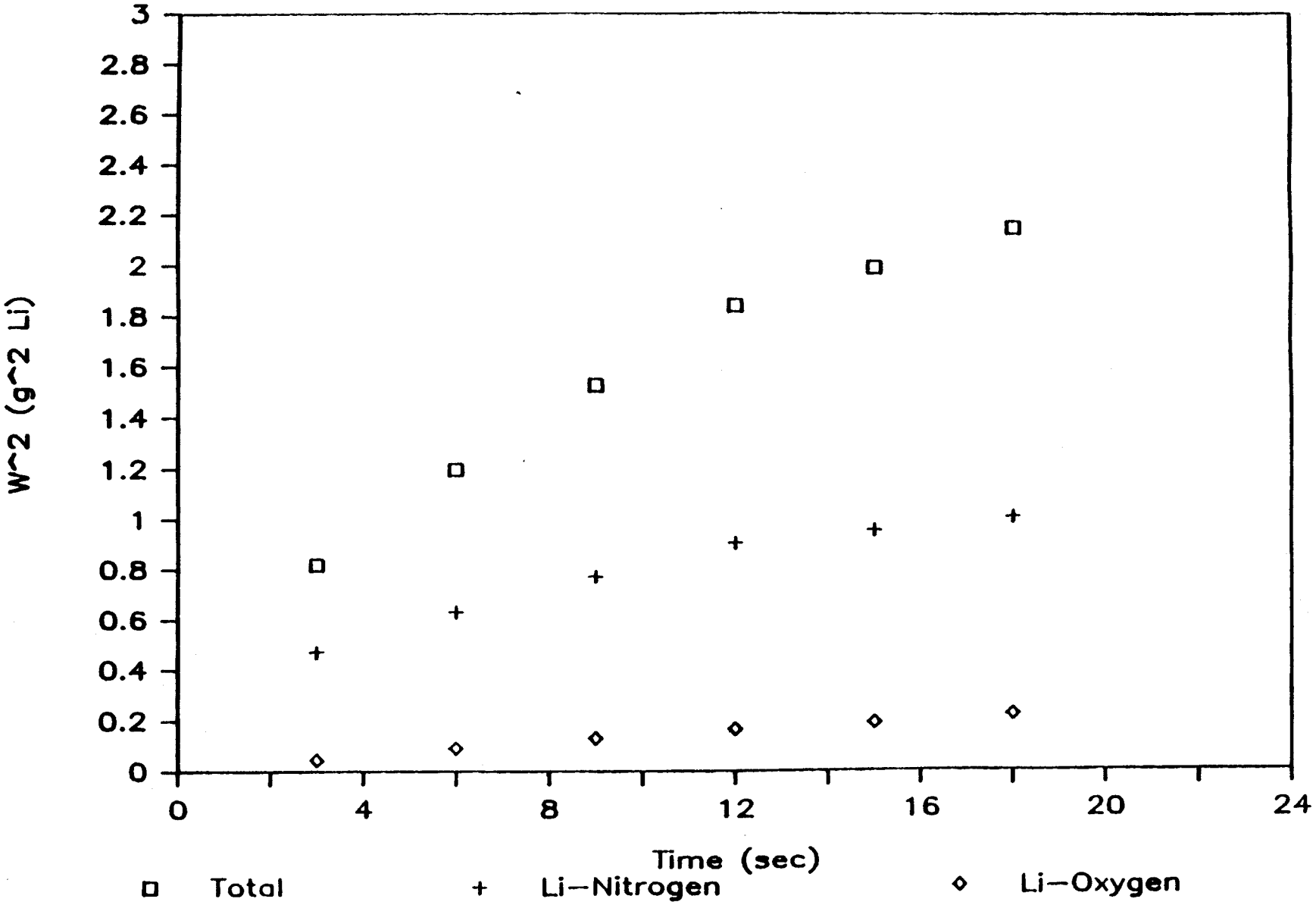

Figure 5.12 Nitride effect on reaction rate (Run No. 8); T_{Li}=865 C and "80-20" composition.

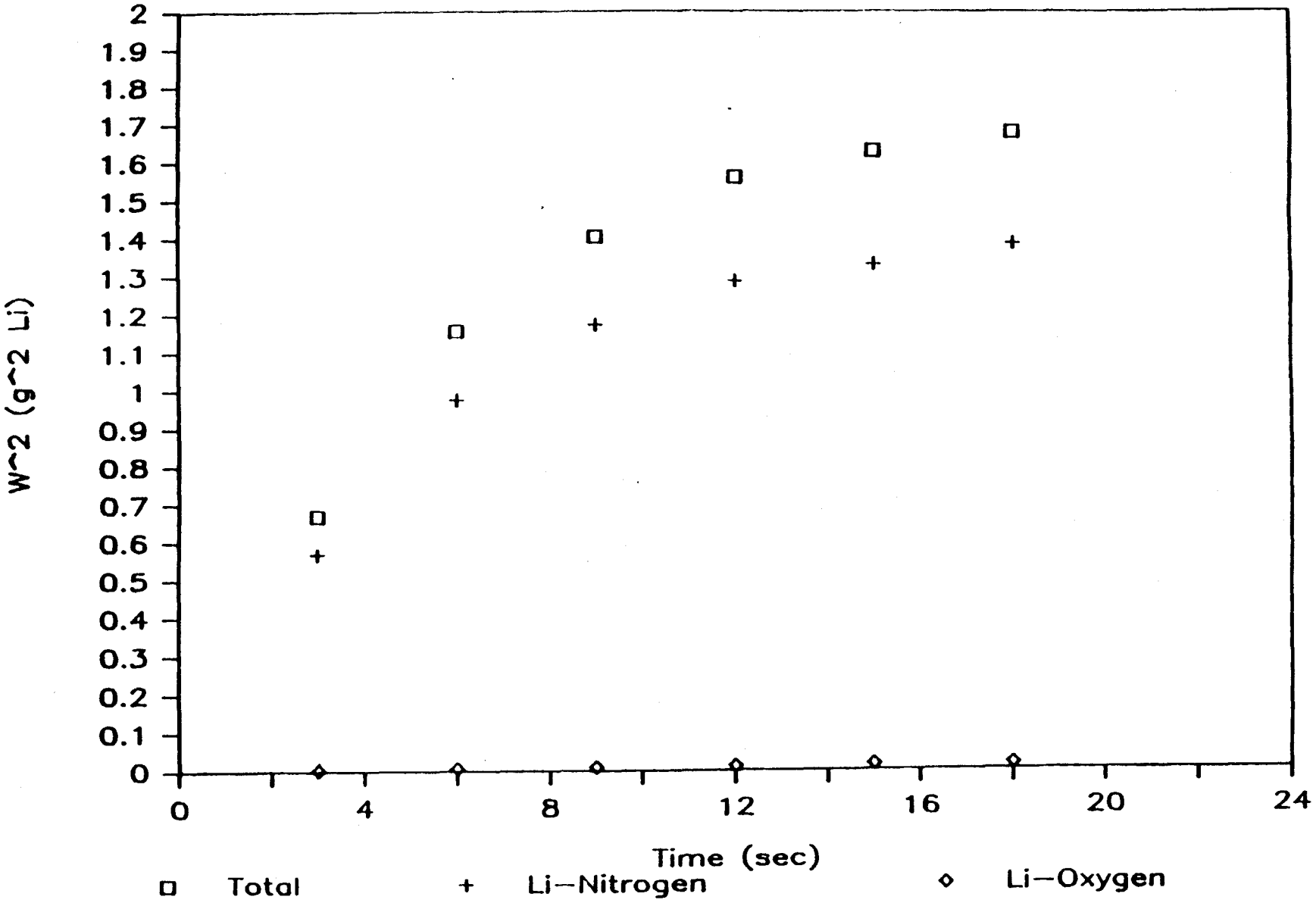

Figure 5.13 Nitride effect on reaction rate (Run No. 13); T_{Li}=912 C and "90-10" composition.

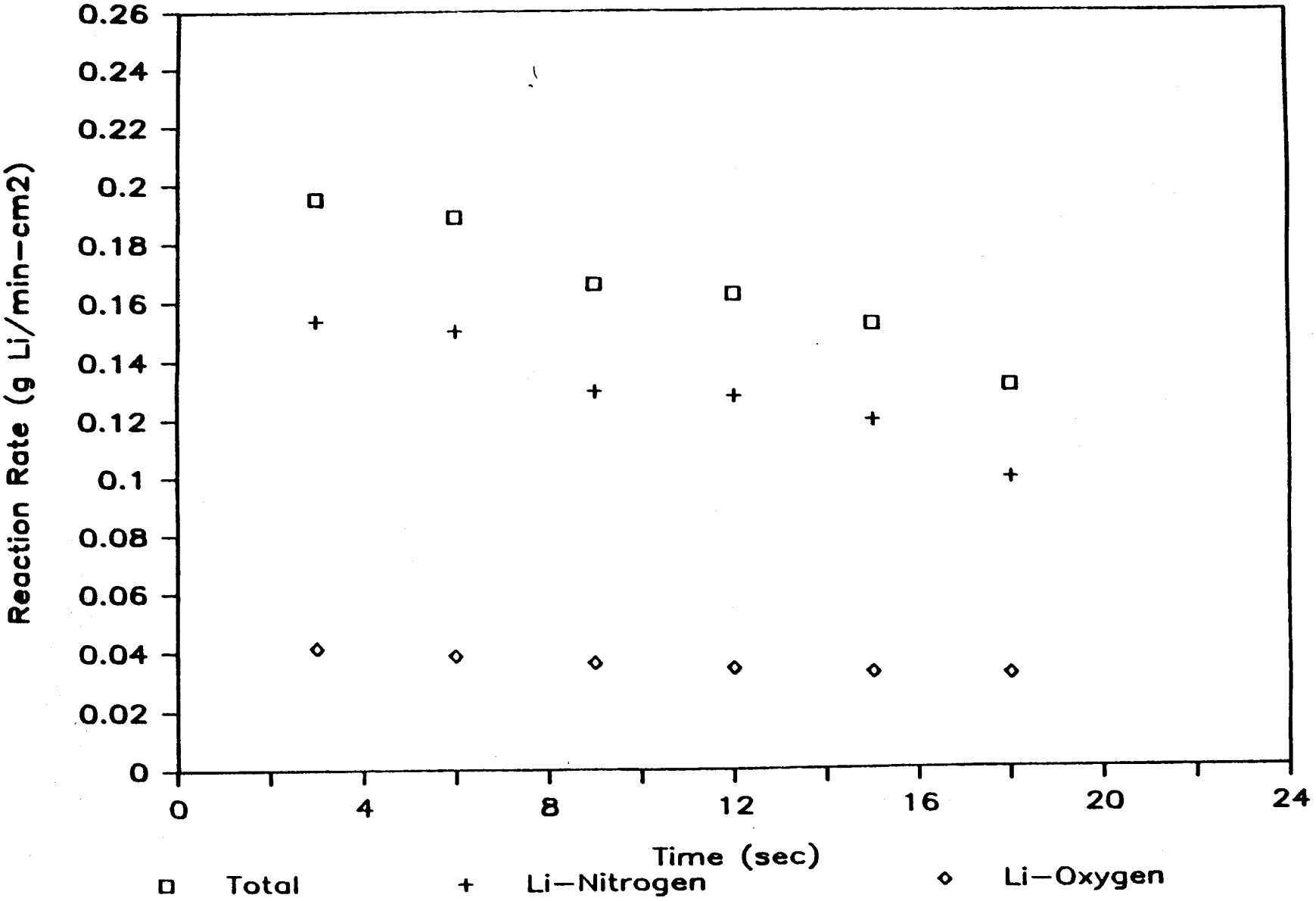

Figure 5.14 Nitride effect on reaction rate (Run No. 14); T_{Li}=690 C and "90-10" composition.

Secondly, Figure 5.9 shows certain jumps in the curve indicating that the reaction rate was actually increasing momentarily. This can be explained in the following way. In this run, the surface of the pool was not smooth, there was a definite indication that some cracks occured during the reaction. And thirdly, the oxygen reaction rate seemed not to be noticeably hindered by the layer.

The cracks seen in Run 9 obviously allowed for an unhindered lithium-nitrogen reaction momentarily. And the cracks were more frequently observed in the runs with 20 percent oxygen. This indicates that the larger heat generated by the lithium-oxygen reaction seemed to create more cracks on the surface of the pool. And also, in the high temperature runs, the cracks were seen more frequently. Therefore, the reaction rate can vary significantly if these cracks were continously formed. However, as the time interval of the reaction increases, the thickness of the nitride layer also will increase. In other words, it will be less probable that the crack will occur as the reaction time increases.

There is a definite indication that when the fraction of oxygen in the gas mixture increases, and the lithium pool temperature is higher than 800°C, the probability of forming cracks will increase. This phenomenon is also seen in Figure 5.10 and 5.11. The initial temperature of both runs are about the same, 850°C. However, about 5 percent oxygen was used in the run of Fig. 5.10, while about 10 percent oxygen was used in the run of Fig. 5.7.

In addition, one more interesting phenomenon was seen in Figures 5.10, 5.11, 5.12, and 5.13, that in high temperature runs, since the reaction rate was much larger, the thickness of the nitride also increased more rapidly and the reaction rate decreased rapidly. However, in the runs in Figures 5.8 and 5.14 with much lower lithium pool temperature, the reaction rate did not decrease so rapidly. Therefore, at lower temperatures below 800°C, the reaction rate seemed to be controlled by the thickness of the layer, while in the higher temperatures (above 800°C), the reaction rate seemed to be controlled by three factors: 1) the

thickness of the layer; 2) the concentration of oxygen; and 3) the cracks on the surface of the pool. However, by far the most influential effect was the thickness of the layer.

As seen from all the figures, the lithium-oxygen reaction rate was not hindered significantly by the formation of the nitride layer. This phenomenon is difficult to explain.

From reference 4, 5, and 8, similar nitride layer effects have been seen. In particular, in HEDL's LN-3 experiment, the reaction actually droped from about 100 gram Li/sec-m^2 to 20 gram Li/sec-m^2 in 1000 seconds [7]. In addition, it can be postulated that there is a relatively significant relationship between the oxygen concentration and the nitride layer effect; since the larger the oxygen concentration is, the greater is the probability of the formation of the cracks. And the greater the probability of occurance of the cracks, the greater is the reaction rate, offseting the effect of the nitride layer to some degree.

CHAPTER VI LITFIRE Modification

6.1 Li-Air Reaction Model

6.1.1 Li-Nitrogen Reaction Kinetics

During the early stage of LITFIRE development, the dependence of lithium-nitrogen reaction rate on lithium temperature was recognized. At that time, HEDL's LN-1, LN-2, and LN-3 experiments were available to generate the lithium-nitrogen reaction rate as a function of lithium temperature. However, due to the scarcity of data, Tillack was forced to guess the reaction rate curve which seemed to be ideal [1]. And until recently, the same reaction rate curve had been used in LITFIRE.

Recently, conducting a series of experiments, Ijams obtained an empirical reaction rate as a function of lithium temperature [7]. So it became necessary to implement his result in LITFIRE, replacing the previous curve generated by Tillack. Figure 6.1 shows the "old" and "new" reaction rate curves used in LITFIRE. Ijams's reaction rate curve in the figure is normalized in order to make a comparison with Tillack's curve. The dissociation temperature of lithium nitride used by Tillack was 1027°C, while Ijams's experimental result indicated that the dissocation temperature was actuallly about 100°C higher.

A Fortran function routine was developed in order to implement Ijams's curve. It is important to recognize that Ijams's curve was obtained from a forced convection experiment while all HEDL's experiments were performed in a natural convection mode. Therefore, when natural convection of nitrogen exists and there is a limited supply of gas available, the reaction rate can be lower. In other words, Ijams's curve provides a maximum possible reaction rate at a given lithium temperature.

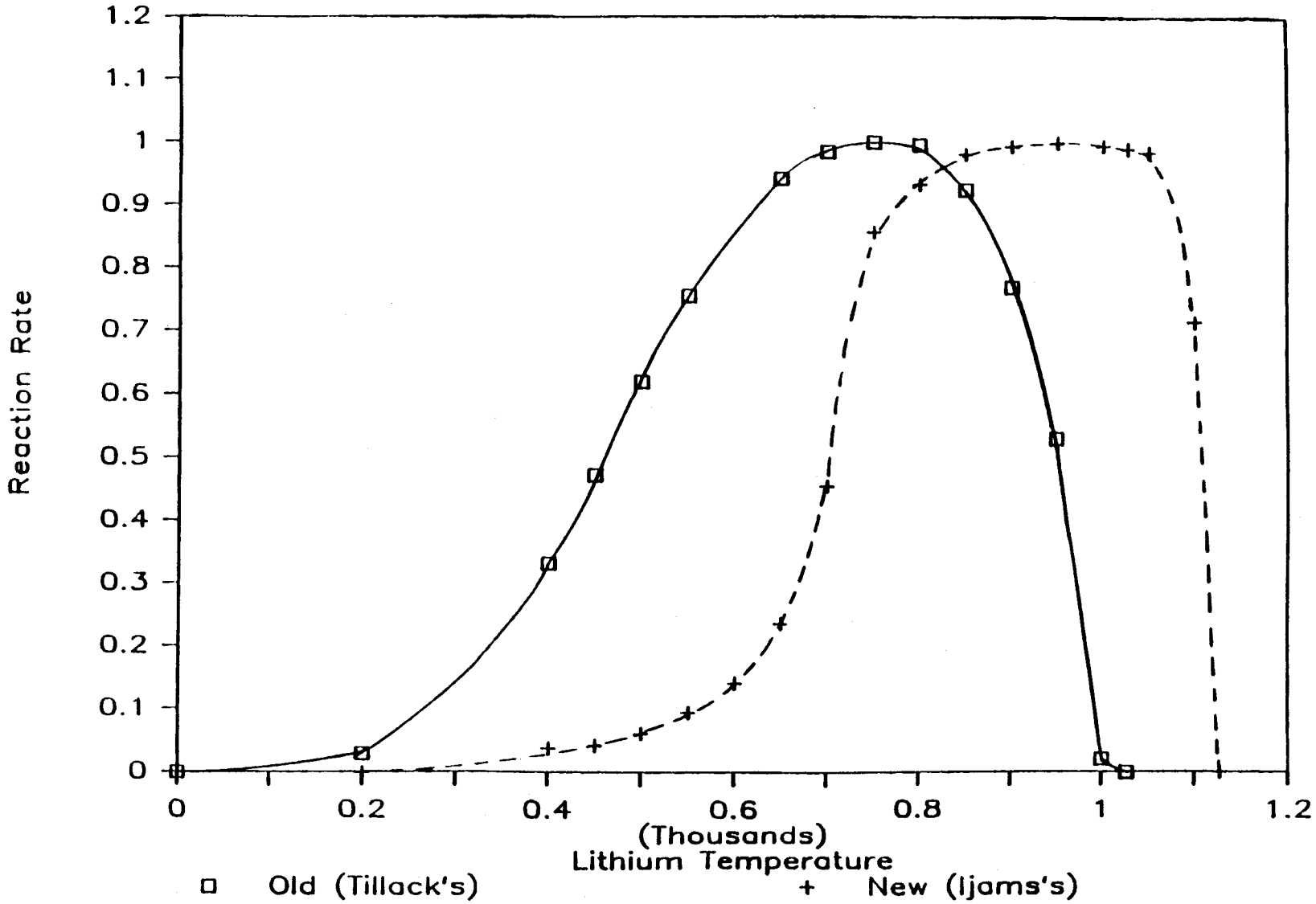

Fig. 6.1 Tillack's and Ijams's version of lithium-nitrogen reaction rate curves.

In the old LITFIRE, no ceiling for the maximum possible reaction rate was provided. The lithium-gas reaction was modeled as a reaction between gas and lithium vapor. It was assumed that the controlling mechanism for the lithium-gas reaction was the rate of arrival of the gas at the reaction site (combustion zone, to be said precisely) by natural convection. The reaction rate was determined by the rate of arrival of the gas to the combustion zone multiplied by the degree of the reaction rate permitted at a given lithium temperature, generated from Tillack's curve. If the gas arrival rate was larger, and all the gas arriving at the zone could not react with the lithium vapor due to a surplus of gas at the zone, the previous model would be incorrect. Because, in the LITFIRE-MOD3, the reaction rate increase with the increase in the amount of gas available near the zone without any limit. Implementing Ijams's curve effectively sets the maximum possible reaction rate at a given lithium temperature regardless of the rate of gas convection.However, the reaction rate in natural convection could be lower than the reaction rate in forced convection because of a limited supply of gas at the reaction site. In this case, the maximum value of the reaction rate is never reached.

After implementing the new reaction rate curve in LITFIRE, HEDL's LA-5 experiment was re-simulated. The result obtained did not significantly differ from the previous result obtained by Gilberti. The average lithium-nitrogen and oxygen reaction rate measured from the experiment were 17.8 and 10.2 Kg Li/hr-m^2 [15], while both the original and the modified LITFIRE predicted 3.6 and 25.3 Kg Li/hr-m^2 respectively. This indicated that the lithium-nitrogen reaction rate inhibition factor, which accounted for the inhibition effect on lithium-nitrogen reaction rate due to the presence of oxygen, was quite conservative. Therefore, it was important to modify the inhibition factor. The next section describes the parametric study performed on the inhibition factor.

6.1.2 Parametric Study on the Inhibition Factors

The lithium kinetics experiments described in Chapters 4 and 5 indicated that the lithium-nitrogen reaction rate mainly depends on four factors: 1) fraction of oxygen in the gas mixture; 2) thickness of the nitride layer; 3) lithium temperature; and 4) number of cracks on the surface of the pool. There is an inter-relationship between all four factors. For example, at high temperature, the nitride layer builds up considerably faster due to the higher reaction rate. And the probability of the cracks occuring would considerably decrease as the reaction time increases.

In order to accurately express the reaction rate, the reaction rate should be in terms of these four variables. However, due to lack of experimental data, it is difficult to express the reaction rate in terms of all four variables. When this study was performed, the result from the lithium-mixed gas experiment was not available. Therefore, the parametric study was only performed on the lithium-nitrogen and lithium-oxygen reaction rate inhibition factors in terms of the fraction of nitrogen and oxygen.

From the experimental results, lithium-nitrogen reaction rate was very vigorous in the temperature range between 800 and 1000°C. Since lithium-nitrogen reaction was significantly inhibited by the presence of oxygen, it may be thought that lithium-oxygen reaction rate would also be inhibited by the presence of nitrogen; particularly, when lithium-nitrogen reaction rate is very vigorous. From HEDL's experiments, the lithium-oxygen reaction rate was not as high as predicted by LITFIRE. This indicates that there may be some inhibition effect on lithium-oxygen reaction rate due to the presence of nitrogen.

In order to select appropriate values for the inhibition factors, a sensitivity study on the inhibition factors was perfomed, selecting HEDL's LA-5 experiment as a reference case. The inhibition factors were expressed in terms of the fraction of oxygen and nitrogen:

$$ro2 = (1 - \frac{F_{N_2}}{F_{N_2} + F_{O_2}})^x \tag{6.1}$$

$$rn2 = 1 - (\frac{F_{O_2}}{F_{N_2} + F_{O_2}})^y \tag{6.2}$$

where $ro2$ and $rn2$ are the inhibition factors, F_{N_2} and F_{O_2} are the fraction of nitrogen and oxygen by weight percent, and x and y are the values of exponents to be selected from the empirical evidence.

As seen from Figure 6.2 and Table 6.1, several values for the exponent x and y were tried in order to select the most ideal case which simulates the LA-5 experiment. By varying x and y, the maximum lithium temperature, time at which the temperature reached its maximum, and time at which the combustion was completed varied considerably. When $rn2$ was higher (Case 1 and 2 in Table 6.1), the time of T_{max} and completion time were much shorter, while T_{max} was much lower. Since more lithium-nitrogen reaction was predicted, T_{max} would be lower due to the lower amount of heat generated by lithium-nitrogen reaction compared to lithium-oxygen reaction. Also the time at T_{max} and completion time were shorter than the cases with lower $rn2$, because three lithium atoms react with one nitrogen atom while only two lithium atoms react with one oxygen atom.

As $ro2$ increased while $rn2$ decreased (Case 3, 4, and 5), the maximum lithium temperature was larger while the time of T_{max} and completion time were longer. The best simulated case was Case 5 in which the simulated maximum temperature and the time of T_{max} were in a reasonable range with the experimental result. The values of x and y found were 0.02 and 0.18. Figure 6.3 shows the selected inhibition factors as a function of the fraction of nitrogen. For 80 percent nitrogen and 20 percent oxygen atmosphere, the corresponding lithium-nitrogen and lithium-oxygen reaction rate inhibition factors were 0.23 and 0.97.

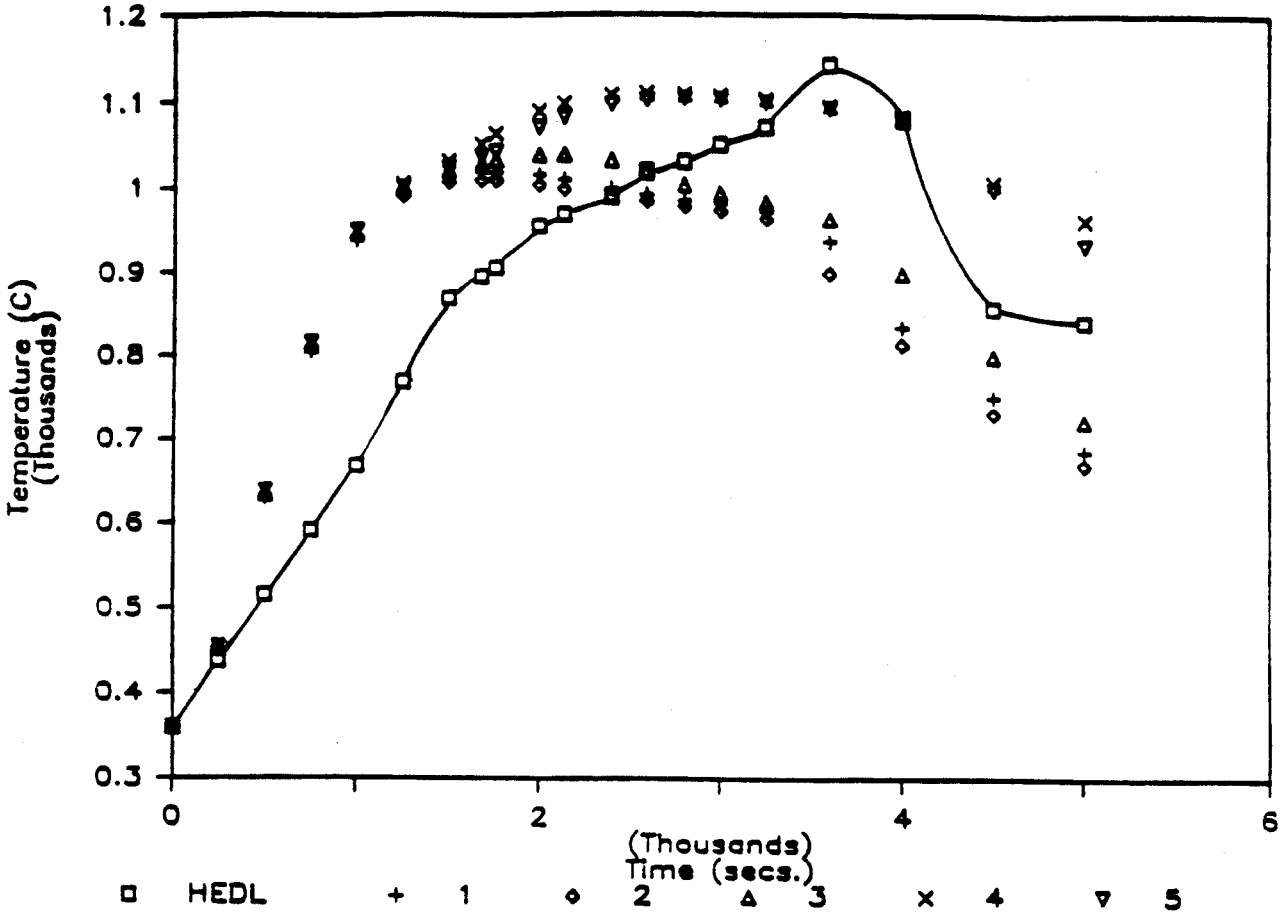

Fig.6.2 Sensitivity on Reaction Rate Inhibition Factors

Table 6.1 Parametric Study on Reaction Rate Inhibition Factors

$Li\text{-}O_2$ R. R. Inhibition Factor

$$ro2 = \left(1 - \frac{F_{N2}}{F_{N2} + F_{O2}}\right)^{x}$$

$Li\text{-}N_2$ R. R. Inhibition Factor

$$rn2 = 1 - \left(\frac{F_{O2}}{F_{N2} + F_{O2}}\right)^{y}$$

Case Number	Exponent of Inhibition Factors (x)	(y)	$T_{max, Li}$ (C)	Time (sec) at T_{max}	Time (sec) at combustion completed
1	0.035	0.185	1018	1760	3440
2	0.035	0.2	1009	1680	3320
3	0.025	0.18	1039	2140	3720
4	0.02	0.17	1109	2590	5000
5	0.02	0.18	1103	2825	4880

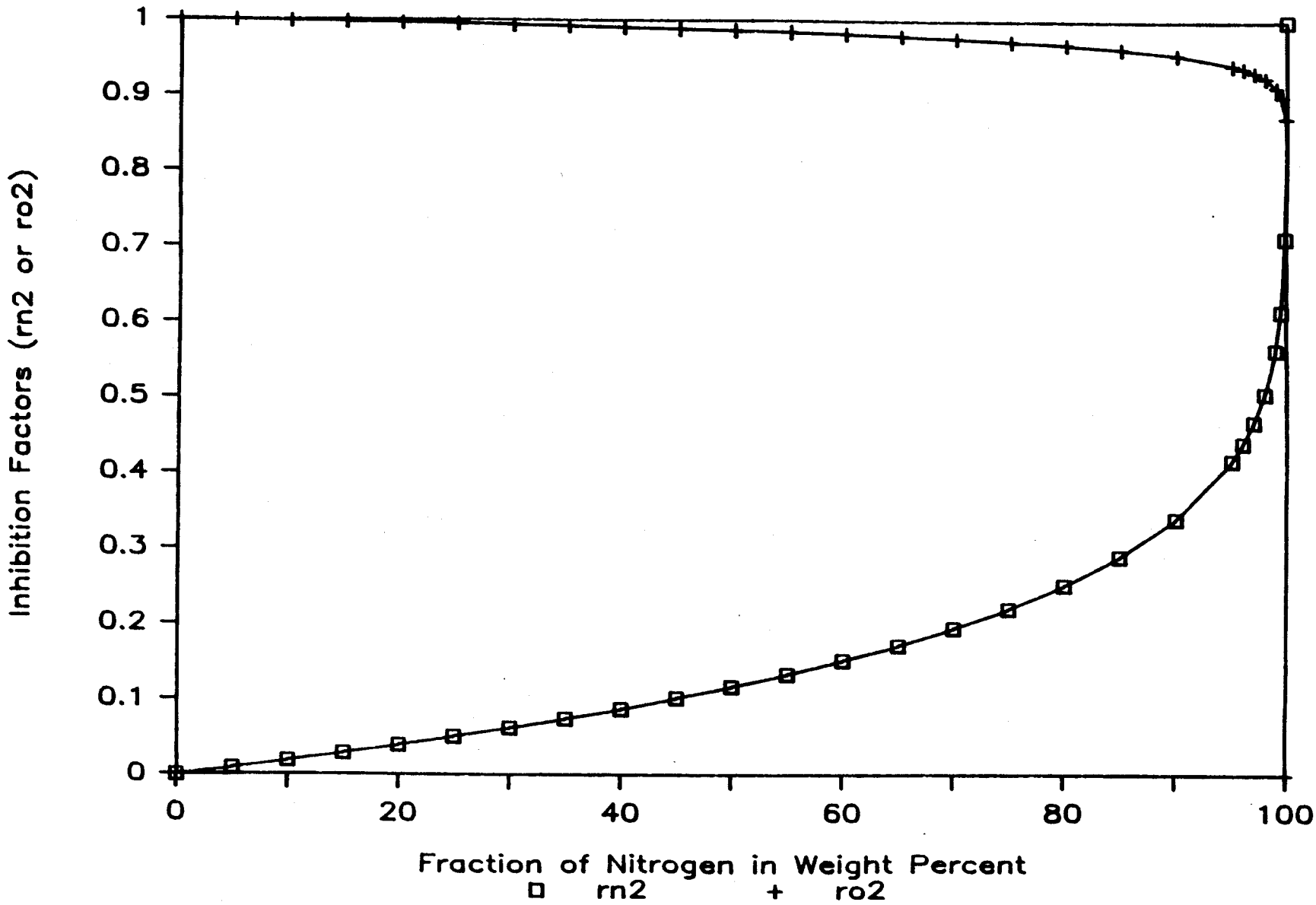

Figure 6.3 Lithium-nitrogen reaction rate inhibition factor selected.

Here, the inhibition factors were only expressed in terms of the fraction of oxygen and nitrogen of the gas mixture. However, the experimental result indicated that the inhibition factors also heavily depend on the temperature. Therefore, it may be necessary to modify the inhibition factors in the future.

6.1.3 Application of LITFIRE to Experiment (HEDL's LA-5)

Several options in LITFIRE were used to simulate the HEDL test. These were the pan geometry, gas injection, and aerosol removal options within a single containment cell. Most of HEDL's experiments were described in Chapter two, and Table 6.2 shows a summary of HEDL test conditions.

With new inhibition factors and newly implemented Ijams's lithium-nitrogen reaction curve, HEDL's LA-5 experiment was re-simulated. Figures 6.4 through 6.7 and Table 6.3 show the result of LITFIRE simulation of LA-5 experiment. The experimental result and "old" LITFIRE prediction are plotted along with the "new" LITFIRE prediction. The output of LITFIRE was newly formatted so that additional information on the reaction rates and weights of reaction products accumulated as solids and aerosols became also available.

As seen in Figure 6.4, "new" LITFIRE predicted slightly lower maximum lithium temperature while the time at which the temperature reached its maximum was much longer than "old" LITFIRE's predicted value. The average lithium-nitrogen reaction rate shown in Table 6.3 indicates that "new" LITFIRE underpredicted it by 20 percent. However, the average lithium-oxygen reaction predicted by LITFIRE is still higher than the experimentally inferred value by a factor of 23 percent. This implies that the code will overestimate the temperature rise due to lithium fires under accident conditions (since O_2 reaction are much more energetic than N_2 reaction).

TABLE 6.2 [15]

Summary of HEDL Test Conditions

	LA-4	LA-5
Containment Vessel		
Diameter (m)	7.62	7.62
Overall Height (m)	20.3	20.3
Volume (m^3)	850.0	850.0
Total Horizontal Surface (m^2)	88.0	88.0
Wall Surface (m^2)	520.0	520.0
Vessel Mass (Rg)	103,000	103,000
Lithium		
Mass of Lithium Spilled (kg)	26.7	100.0
Lithium Reaction Pan Surface (m^2)	0.124	2.0
Initial Lithium Temperature (°C)	600.0	500.0
Depth of Lithium Pool (m)	0.46	0.10
Containment Atmosphere		
Initial Oxygen (mole %)	20.9	20.8
Initial Gas Temperature (°C)	31.0	31.8
Initial Pressure (MPa, absolute)	0.116	0.113
Maximum Temperature (°C)	68	83
Maximum Pressure (MPa, absolute)	0.127	0.127
Final Oxygen Concentration (mole %)	20.0	19.1

Comments

LA-4 Reaction: As a deep pool for ∿3300 sec when the pan integrity failed and all lithium spilled to the floor and reacted within 10 mins. LA-5 Reaction Terminated after 3900 seconds.

Table 6.3

Comparison of LITFIRE and Experimental Combustion Rates

Time (sec)	Lithium Reaction Rate with Nitrogen (Kg-Li/hr-m2)			Lithium Reaction Rate with Oxygen (Kg-Li/hr-m2)		
	HEDL	Old LITFIRE	NEW LITFIRE	HEDL	Old LIFIRE	New LITFIRE
100	4.5	10.9	0.98	1.4	16.9	15.2
300	13.9	14.05	5.65	2.4	23.6	20.4
500	3.4	23.56	19.6	6.8	26.4	24.6
800	37.5	5.22	39.9	9.4	27.4	28.9
1500	32.5	0.0	39.9	12.8	27.0	27.1
2500	16.6	0.0	0.0	12.4	24.9	24.8
3450	1.1	0.0	0.0	9.8	22.5	22.9
Average During 3900 sec.	17.8	3.6	13.0 *	10.2	25.3	23.6 *

* The time it took to complete the combustion. (4880 sec.)

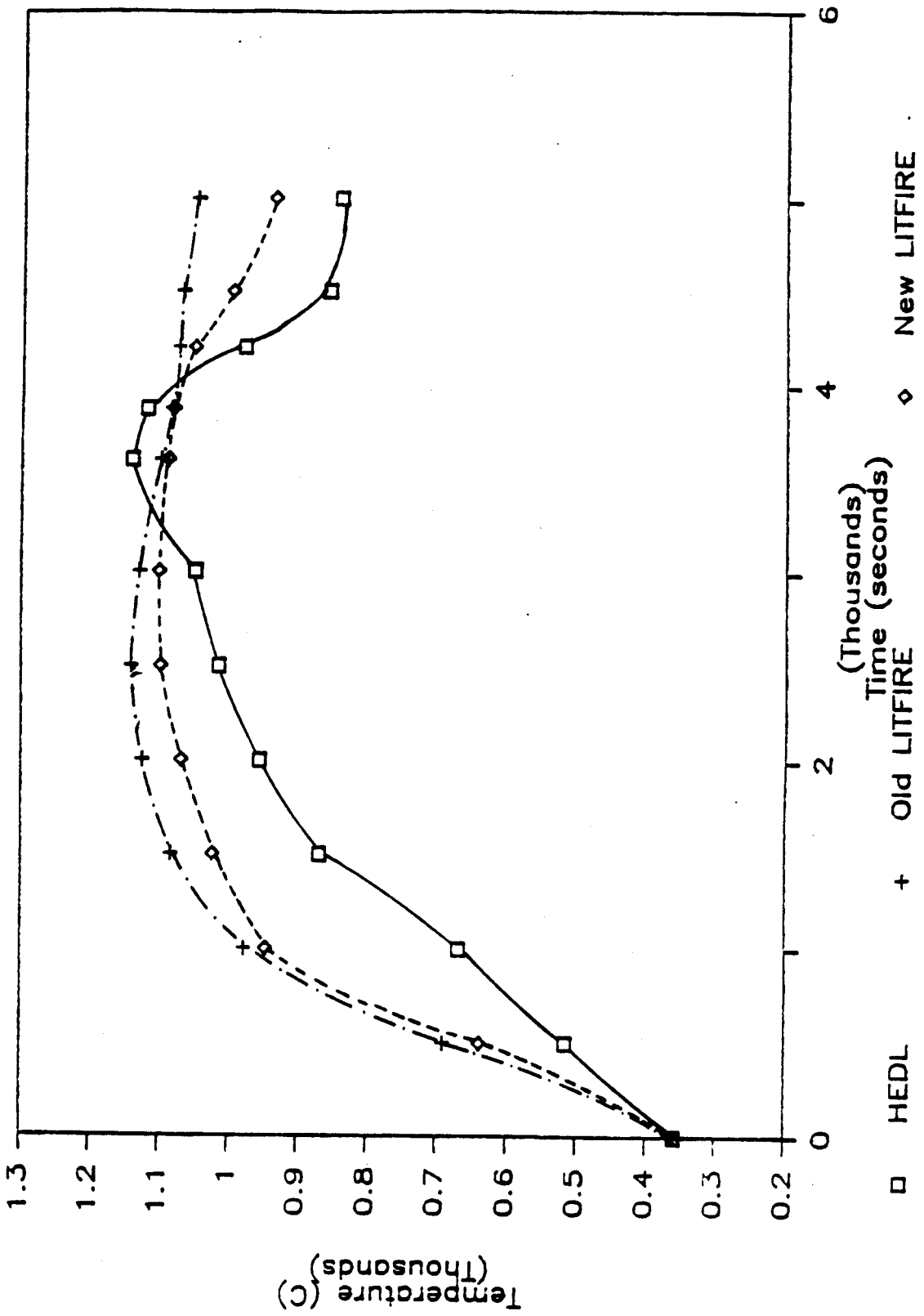

Figure 6.4 Lithium pool temperature for HEDL's LA-5 experiment.

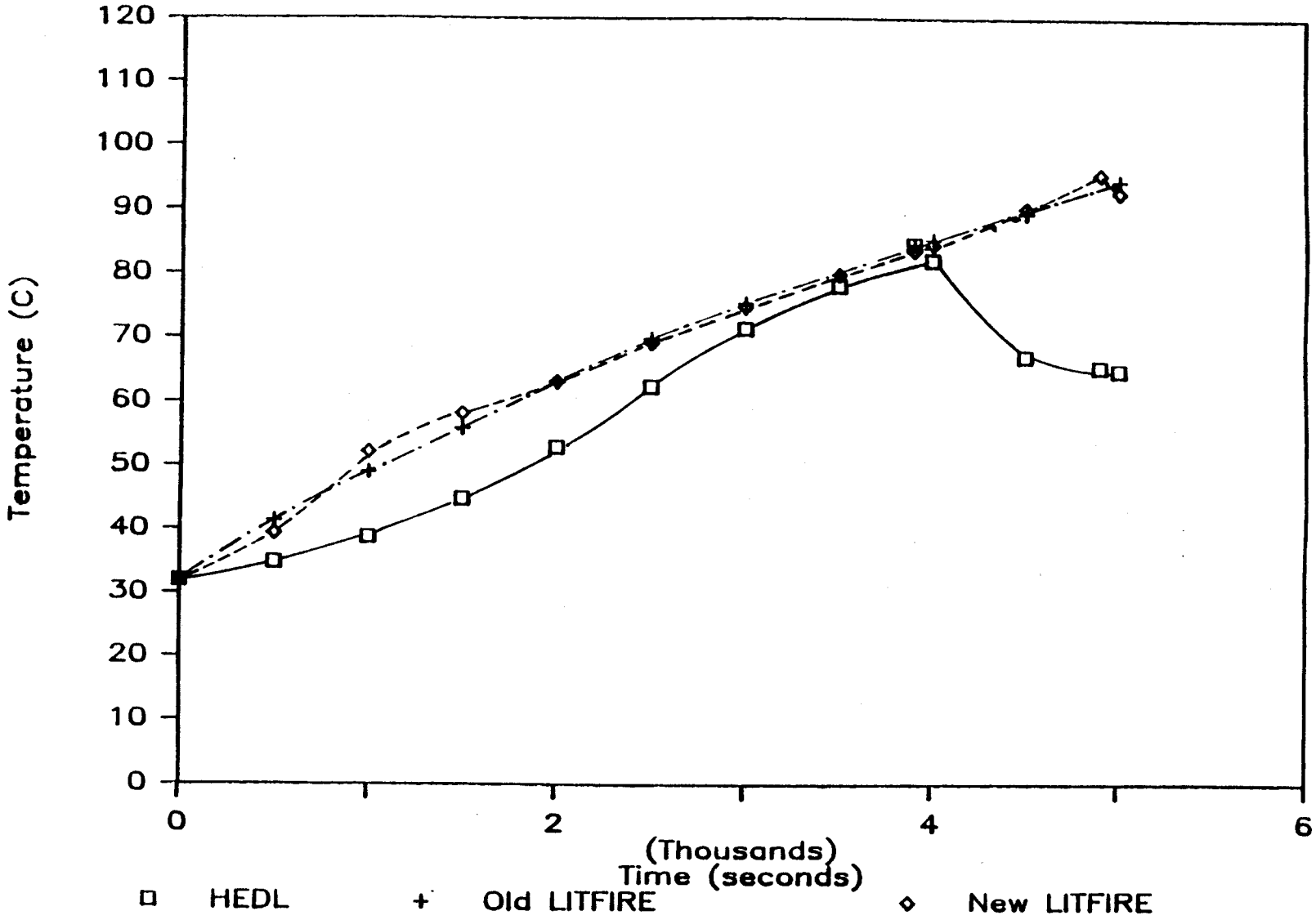

Fig. 6.5 Cell gas temperature for HEDL's LA-5 experiment

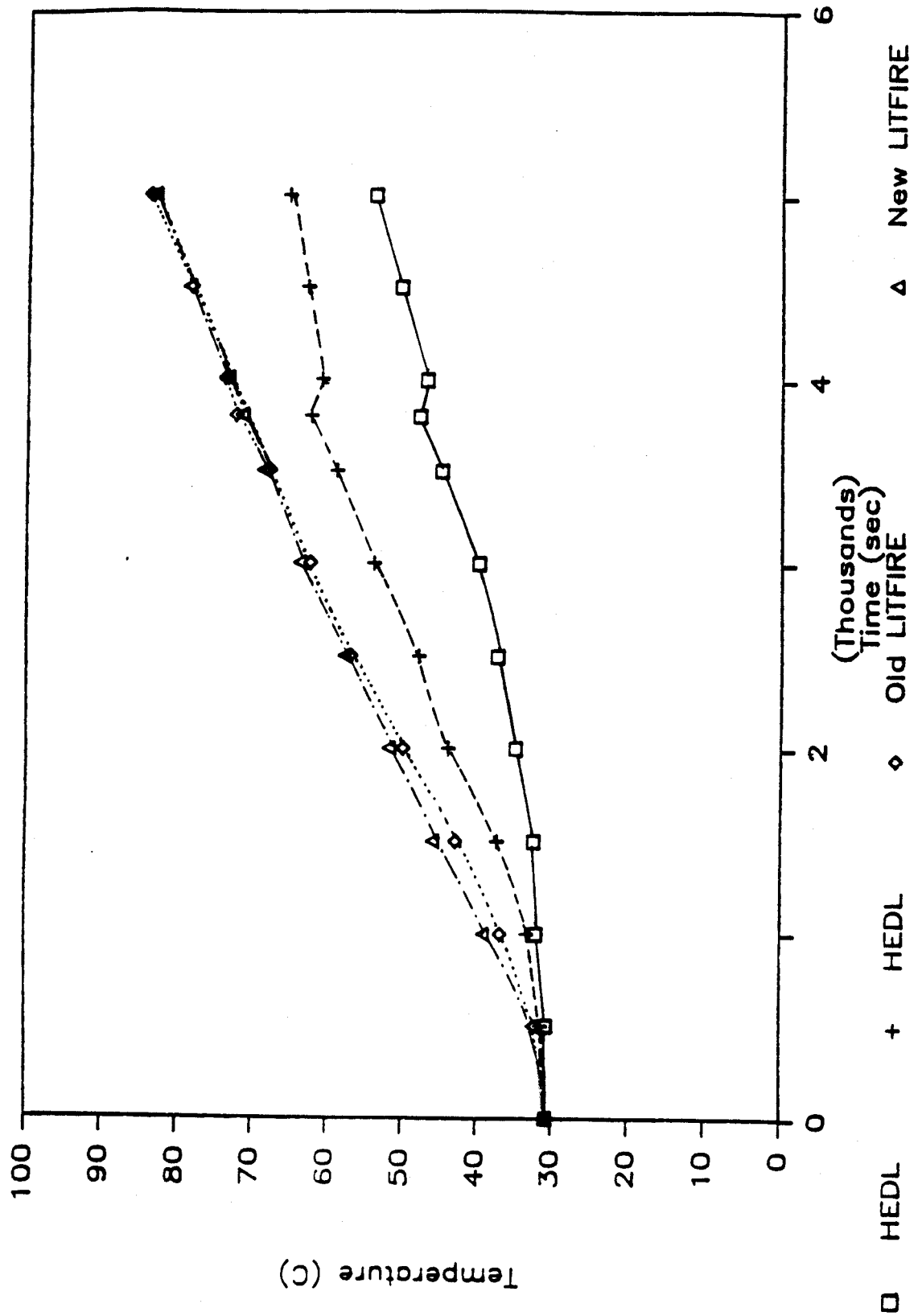

Fig. 6.6 Containment Vessel Wall Temperature for HEDL's LA-5 Experiment

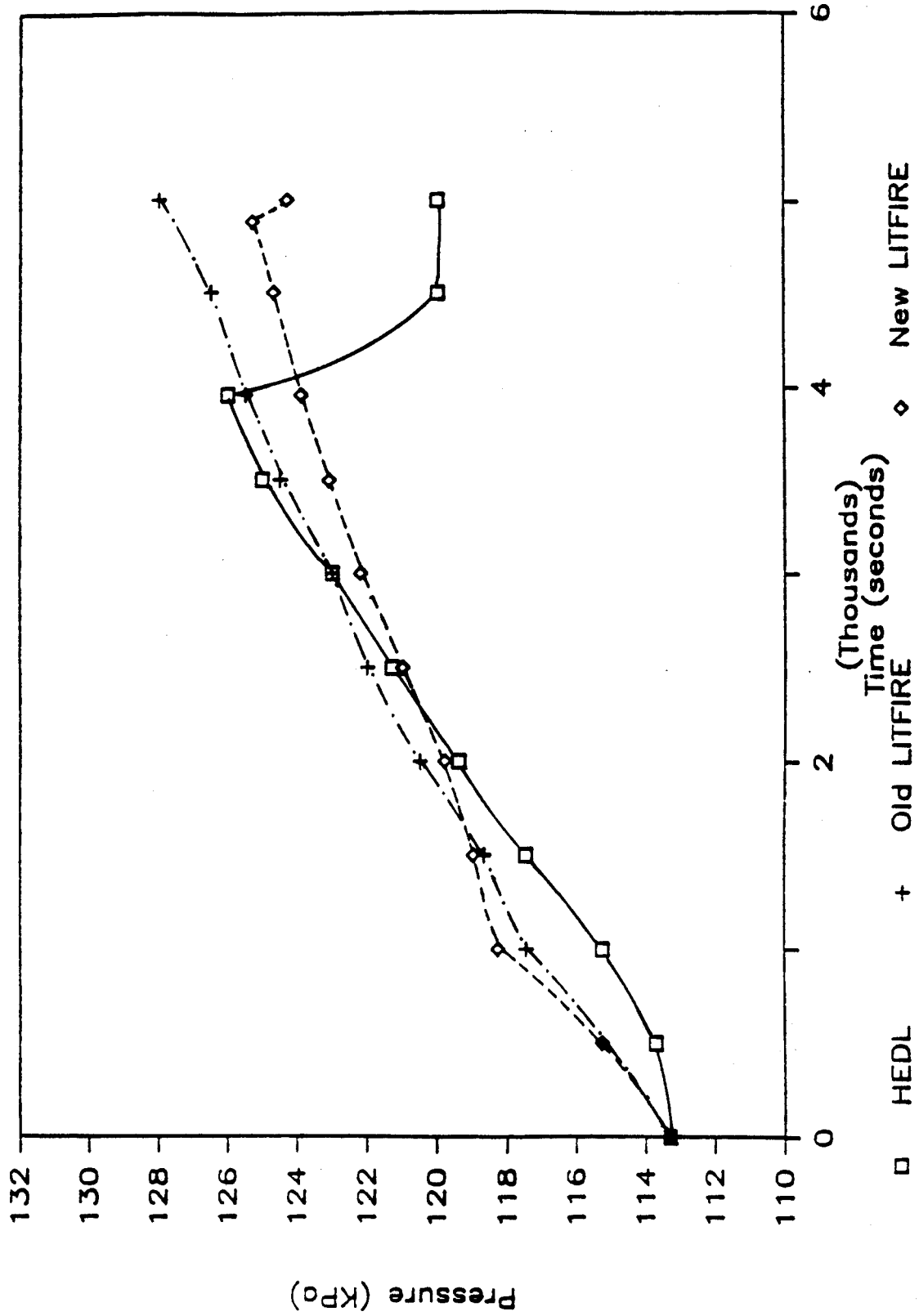

Fig. 6.7 Cell gas pressure for HEDL's LA-5 experiment

The reason for the larger lithium-oxygen reaction rate can be explained in the following way. LA-5 experiment was prematurally terminated at 3900 seconds from the initial reaction. Only 61 percent of the lithium was consumed during 3900 second period. If the reaction were to continue, the lithium-oxygen reaction rate measured may have been much larger since lithium would no longer react with nitrogen above 1127°C while lithium-oxygen reaction would continue until the lithium was completely consumed.

In addition, the reaction rate of lithium with nitrogen and oxygen was not directly measured but was inferred from the data on gas composition and cell temperature and pressure. This was done by applying the ideal gas law. The mole percent concentration of oxygen in the cell gas was measured at various points in the cell and an average of these was used in the calculation. The reaction rate is extrapolated from the change in moles of oxygen and nitrogen at specific intervals and is considered constant between intervals. This way of calculation the reaction rate introduces some error. Therefore, the inferred reaction rates may have been larger than the actual values.

The agreement of the experimental and predicted cell gas and containment vessel wall temperatures was reasonable. If the reaction were not terminated at 3900 seconds, the cell gas temperature prediction would have been quite accurate. The gas pressure predicted was also in a reasonable range with the experimental result. Overall, the "new" prediction did not differ considerably from the "old" prediction which simulated the experiment within a reasonable range. However, the lithium temperature profile shows slight improvement and the average lithium-nitrogen reaction rate predicted shows good agreement with the experimental result.

It is important to recognize that the LA-5 simulation was performed with the changes made relavant to the lithium-nitrogen reaction rate and the inhibition factors. None of physical and chemical properties were changed. In

particular, physical properties of emissivity and transmissivity of the combustion zone, and the lithium film conductance should be experimentally verified since these properties have considerable influence on the accuracy of the code. Reference 15 provides sensitivity analyses on those physical properties.

6.2 Analysis of Lithium Spill in UWMAK-III

The main objective of the development of LITFIRE was to predict the consequences of lithium spills in commercial size reactor containments. The agreement between LITFIRE and HEDL's scale experiments is encouraging, so that larger spills and fires could be reasonably modeled.

6.2.1 Description of UWMAK and LITFIRE Geometries

The prototypical fusion reactor chosen by Dube [14] for his analysis was the UWMAK-III design of which the containment building is shown in Figure 6.8. Dube provided a sensitivity analysis of the relevant parameters for modeling large fires and proposed a base set of parameters as a best guess at predicting the consequences of large fires. Gilberti [15] also applied LITFIRE in order to simulate the consequences of lithium spills in UWMAK-III with modified parameters such as combustion zone emissivity, cell gas emissivity, and steel liner thickness with his upgraded version of LITFIRE. Table 6.4 shows the major parameters used by the present analsyis and Dube's analysis. The present analysis basically retained most of the parameters used by Gilberti. The initial temperature of the spilled lithium was 600°C.

In this case study, both air and nitrogen atmosphere were used in order to observe the advantage of using nitrogen as a cover gas in case of a lithium spill accident. The aerosol removal option was not used in these test cases. In addition, none of the options for mitigating the effects of lithium fires were employed in order to make a conservative best estimate. Furthermore, the selection of the UWMAK-III design would result in a conservative estimate since the amount of lithium spill would be much larger than other conceptual designs of fusion reactor containments.

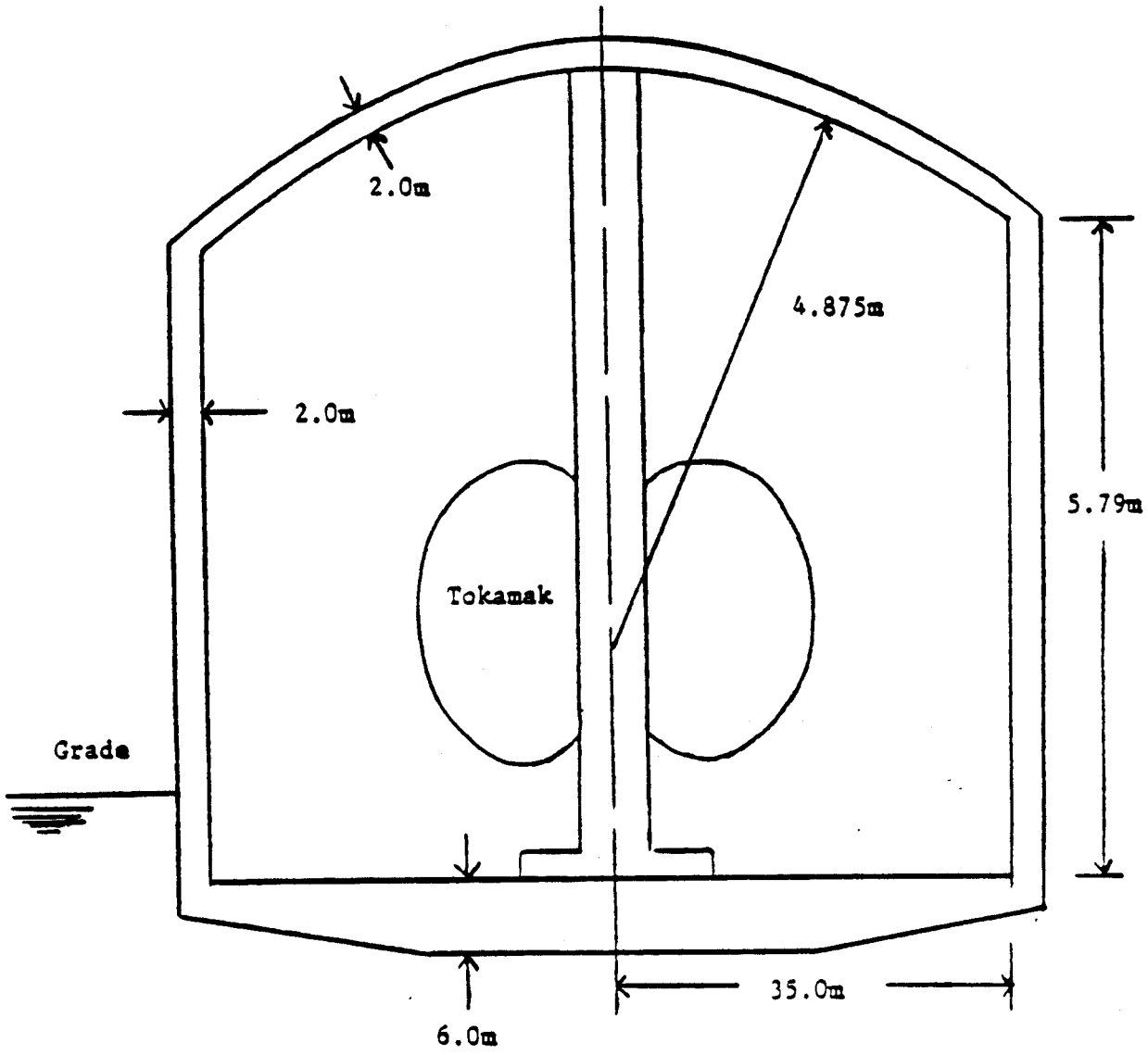

Total Floor Area	$3860m^2$
Total Volume	$250725m^3$
Wall Area	$17050m^2$
Total Lithium Mass	396000kg
Lithium Spilled	22000kg
Ambient Temperature	25.9 °C
Initial Pressure	.101 MPa

Figure 6.8 Cross Section of UWMAK-III Primary Containment Building

TABLE 6.4

Major Parameter Comparison of present and Dube's UWMAK III Input File

Parameter	Dube's	Present
Initial containment pressure	14.7 psia (101.4 KPa)	14.7 psia
Containment volume	8855700 Ft3 (2.5E5 m3)	2.4E5 m3
Containment wall area	183532 Ft2 (1.7E4 m2)	1.7E4 m2
Total floor area	41548 Ft2 (3862 m2)	3862 m2
Spill size	48388 lbm (22000 Kg)	22000 Kg
Li pool area	10387 Ft2 (966 m3)	966 m3
Initial spill temperature	2256 R (1253 K)	873 K
Initial combustion zone temperature	2300 R (1277 K)	1277 K
Oxygen in containment	.231	.2316
Vapor in containment	0.0	0.0
Fraction of combustion products evolved into cell gas	0.75	0.05
Method of Integation	3	3
Lithium pool emissivity	0.2	0.2
Combustion zone emissivity	0.5	0.9
Primary cell gas emissivity	0.0	0.04
Steel liner emissivity	0.9	0.9
Spray	0.01	0.0
Concrete thickness		
wall	.8333 ft	.8333 ft
floor	2.083 ft	2.083 ft
Steel liner thickness	.0208 ft	.0508 ft
Gap between liner and concrete	.00208 ft	.00208 ft
Vaporization temperature of lithium	2949 R (1638 K)	2916 R (1619)
Disassociation temperature of lithium nitride	2340 R (1027 K)	2520 R (1127 K)

6.2.2 Prediction of Lithium Spill Consequences

The results of the lithium spill consequences are plotted in Figures 6.9 through 6.16. In Figures 6.9 through 6.12, present analyses of the lithium spill consequences (based on Gilberti's parameters) are shown and in Figures 6.13 through 6.16, the results based on Dube's parameters were plotted. Table 6.5 shows a comparison of the results using Gilberti's and Dube's parameters under air and nitrogen atmospheres.

In the case with air atmosphere using Gilberti's parameters, the combustion temperature exceeded 1200°C, while in the case with nitrogen atmosphere, the maximum combustion temperature was below 900°C. The floor temperature was significantly lower in nitrogen atmosphere than in air. The peak pressure generated by the spill in air was about 193 KPa compared to 136 KPa in the nitrogen atmosphere case, so that the nitrogen case pressure rise is only 40% of the rise in the air case. Even though the containment atmosphere and structures are much larger than in the HEDL experiments, the predicted consequences in the case of air are much more severe. This is primarily due to the large surface area of the lithium pool in the UWMAK model. This suggests that in order to mitigate the consequences, a proper design of the containement to collect the spilled lithium into the pools with smaller surface area should be taken into consideration.

Table 6.5 shows significant differences in the results between Dube's and Gilberti's case. In Dube's case, the combustion zone and floor temperatures were much higher than Gilberti's case. However, the pressure predicted was lower in Dube's case than Gilberti's case. This is what one might have expected. Since Gilberti's combustion zone emissivity is much larger than Dube's combustion zone emissivity, the radiative heat transfer from the combuston zone to the containment gas and wall was much larger in Gilberti's case than Dube's case. Hence, the combustion zone temperature did not increase as much. Since

Gilberti's parameters were verified to be much more accurate than Dube's in the LA-5 simulation as well as other simulations [15], it would be safe to assume that the prediction based on Gilberti's parameters would be more realistic.

This result is quite encouraging to the fusion reactor designers who consider liquid lithium as a breeder blanket and primary coolant. The pressurization of the containment was not considerably large and the floor temperature was relatively low. If nitrogen were to be used as a cover gas on top of the lithium pool in the lithium spill condition, the conquences of the accident could be significantly reduced. Furthermore, if the initial lithium temperature were to be limited below 500°C, the consequence of the accident would be minimum; the nitride formed on the surface of the pool would effectively prevent any further reaction.

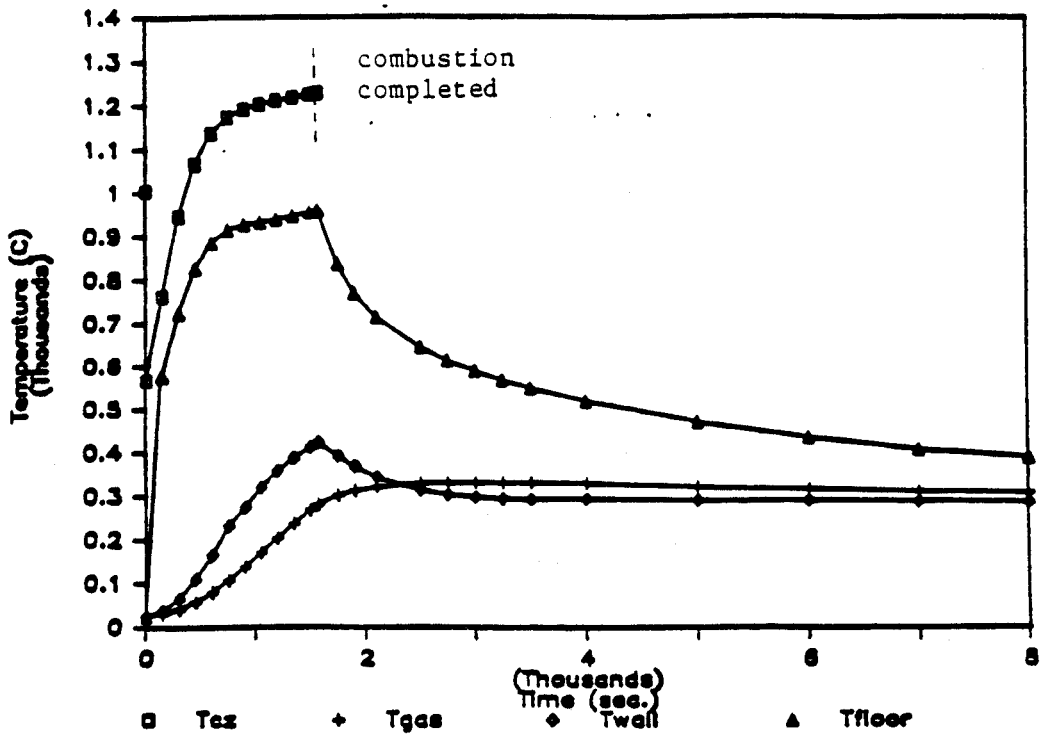

Fig. 6.9 UWMAK-III Thermal history under air atmosphere at the initial temperature of 600 C.

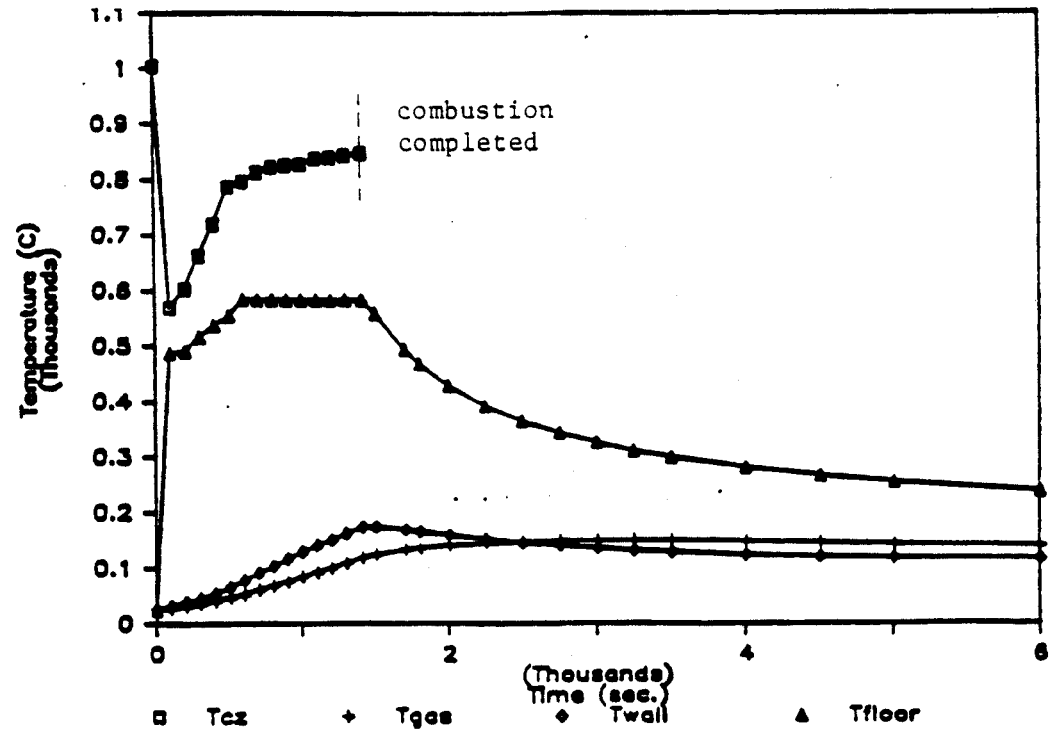

Fig. 6.10 UWMAK-III thermal history under nitrogen atmosphere at the initial temperature of 600 C.

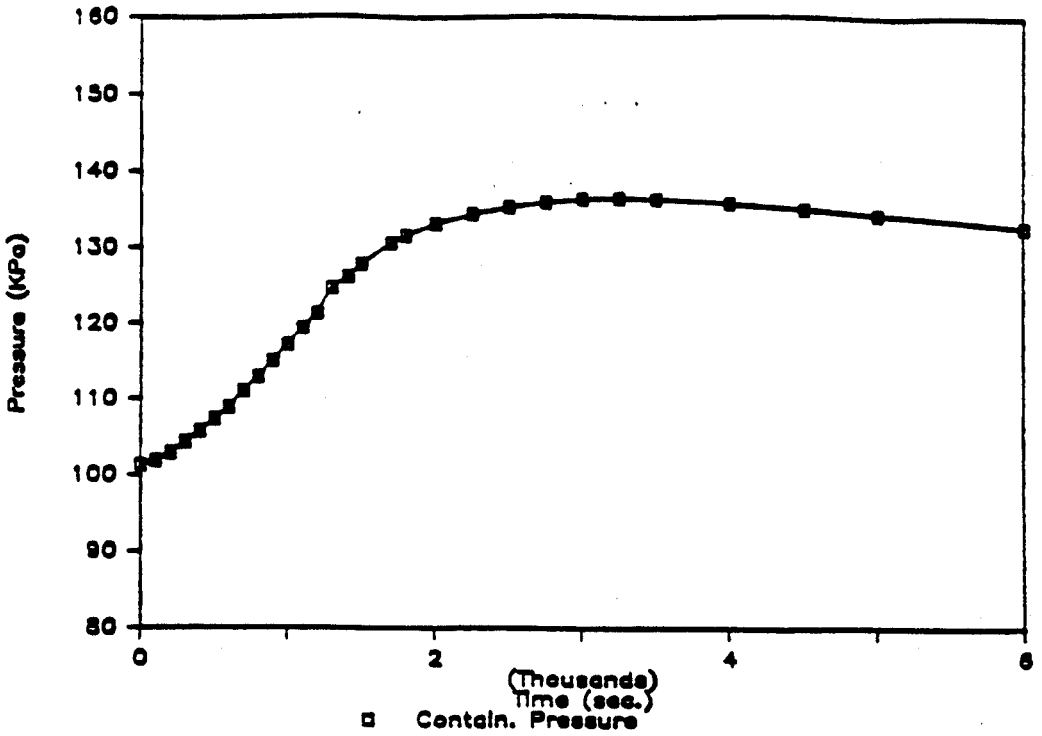

Fig. 6.11 UWMAK-III containment pressure prediction under nitrogen atmosphere with an initial lithium temperature of 600 C.

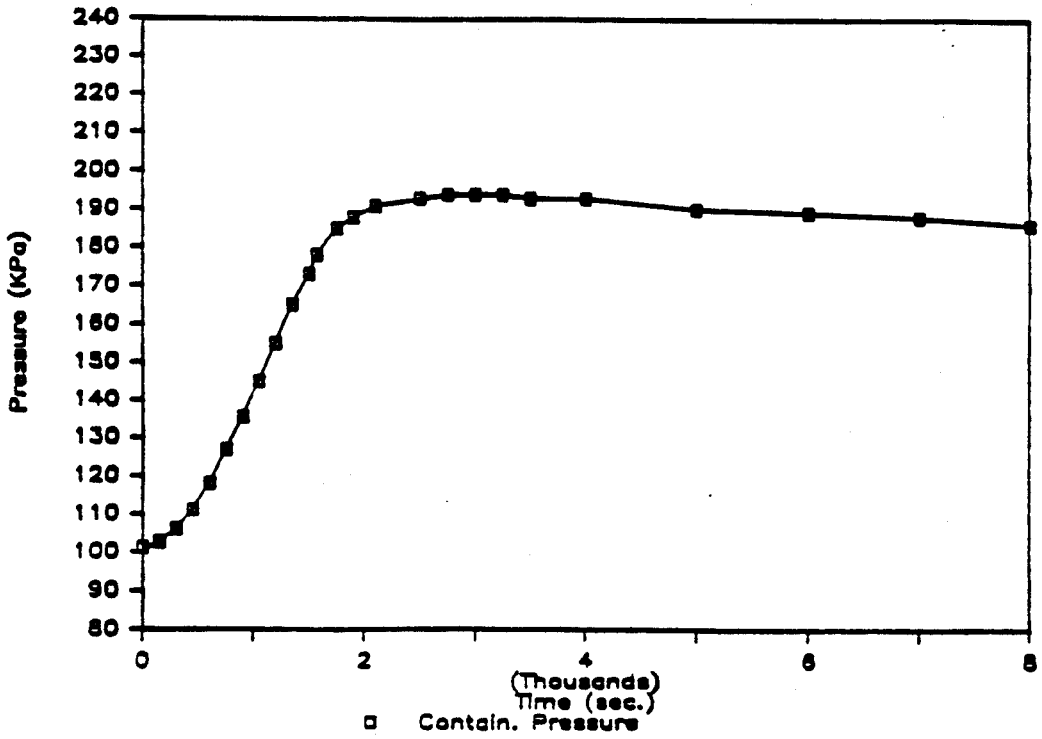

Fig. 6.12 UWMAK-III containment pressure prediction under air atmosphere with an initial temperature of 600 C.

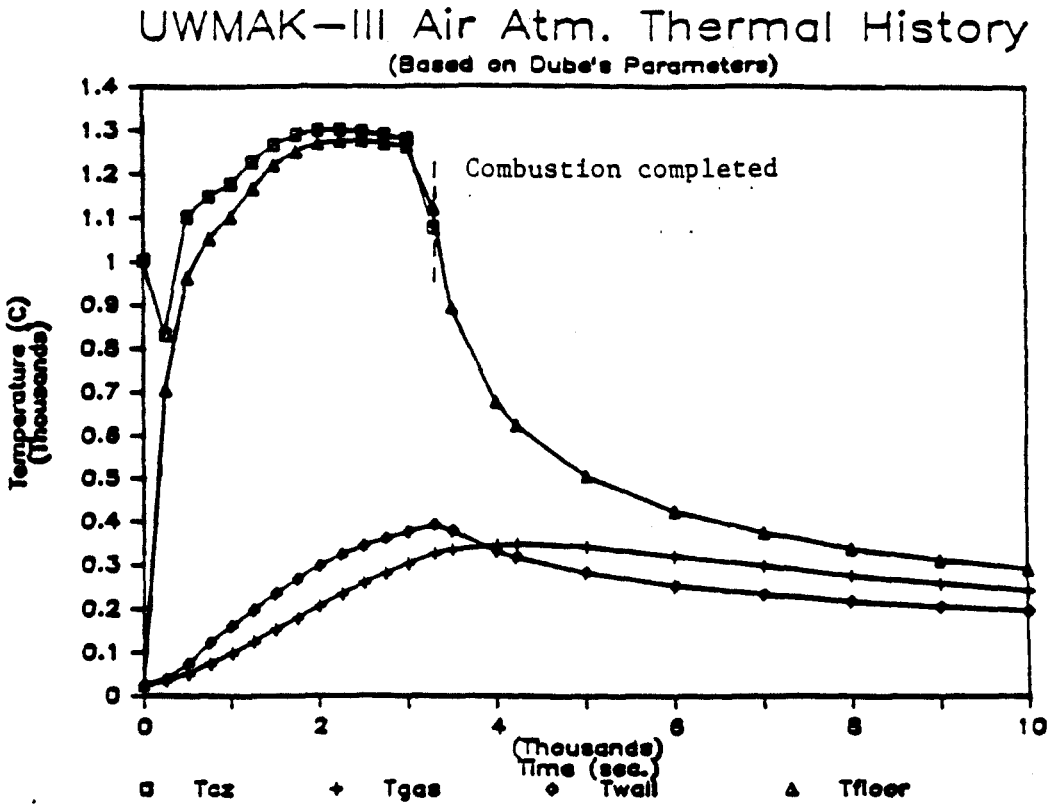

Fig. 6.13 UWMAK-III Thermal history under air atmosphere at the initial lithium temperature of 600 C.

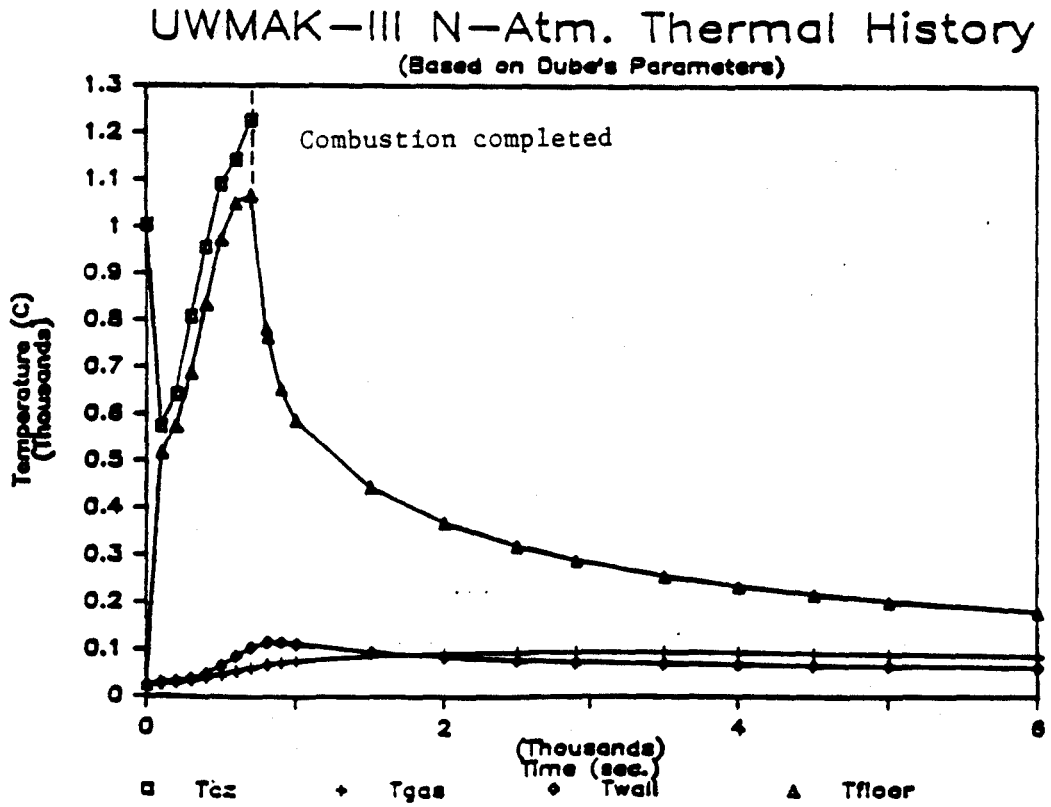

Fig. 6.14 UWMAK-III thermal history under nitrogen atmosphere at the initial lithium temperature of 600 C.

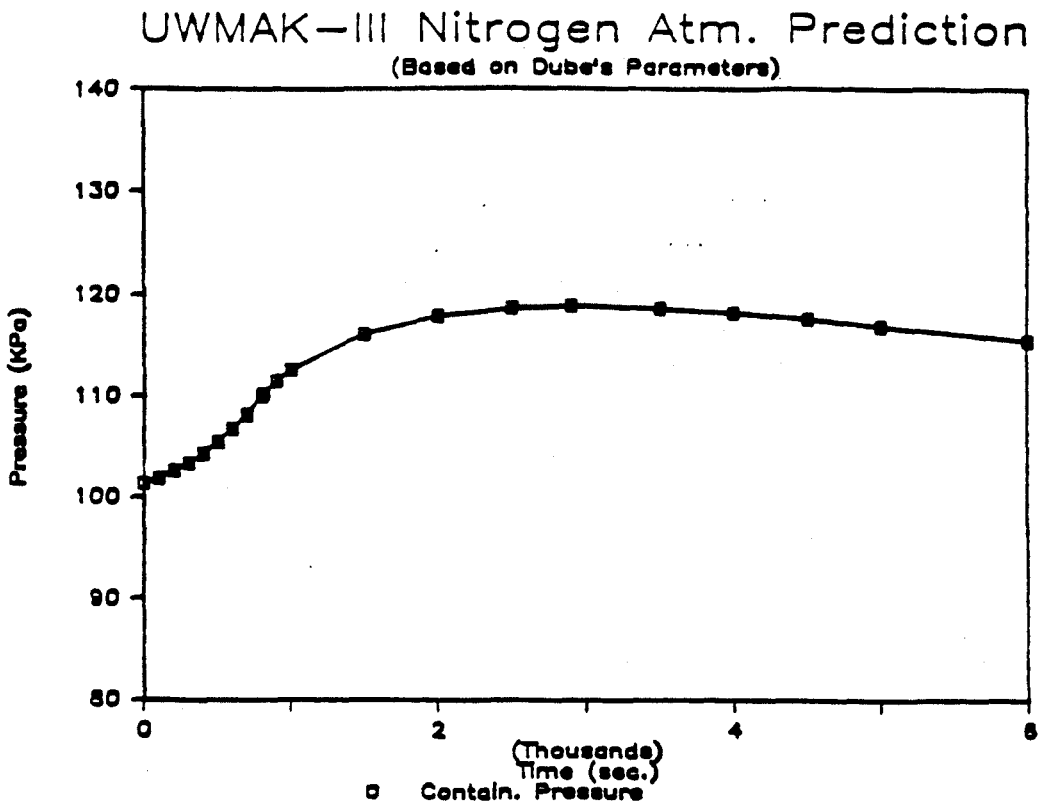

Fig. 6.15 UWMAK-III containment pressure prdiction under nitrogen atmosphere with an initial lithium temperature of 600 C.

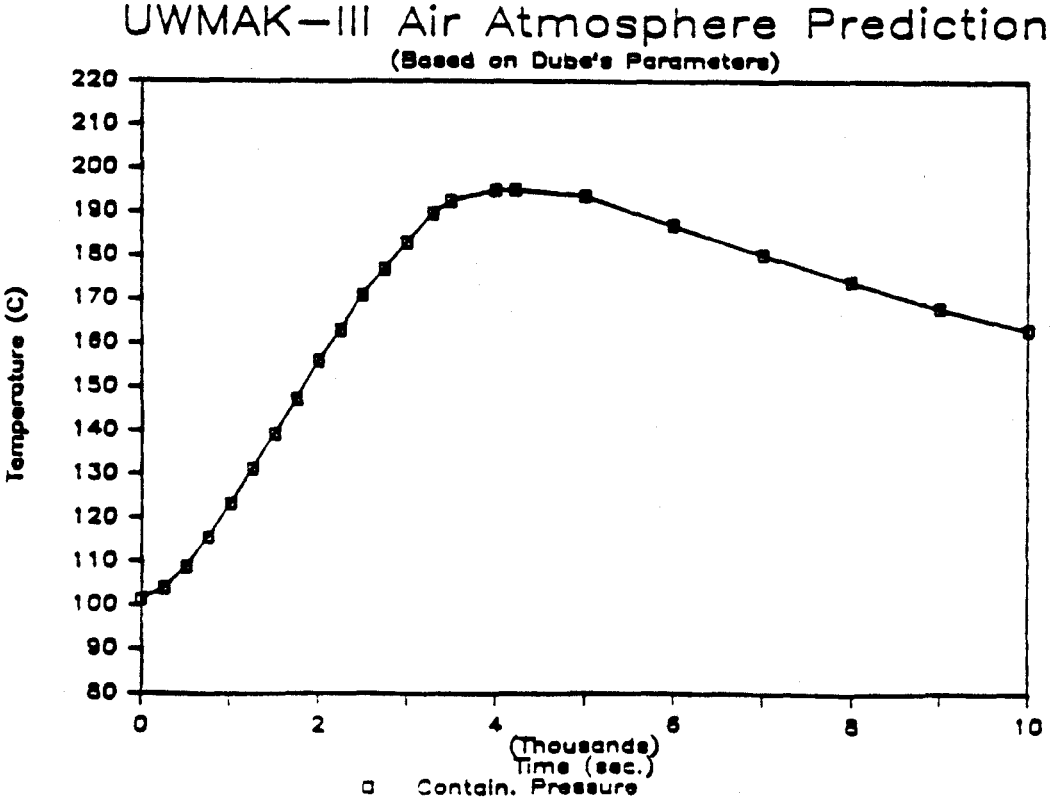

Fig. 6.16 UWMAK-III containment pressure prediction under air atmosphere with an initial lithium temperature of 600 C.

TABLE 6.5

Simulated Consequences of Lithium Spills in UWMAK-III

	Gilberti's Case		Dube's Case	
	Air	Nitrogen	Air	Nitrogen
Max. combustion zone temp. (C)	1215	830	1300	1225
Max. floor temp. (C)	930	585	1270	1050
Max. containment gas temp. (C)	334	162	350	93
Max. containment wall temp. (C)	425	182	394	112
Max. containment pressure (KPa absolute)	193	136	195	119

6.3 Li-CO_2 Reaction Model

The LITFIRE-MOD3 allows the following lithium-gas reactions: 1) lithium -nitrogen; 2) lithium-oxygen; and 3) lithium-water vapor. The above reactions produce lithium hydroxide, lithium nitride, lithium oxide, and hydrogen. There are mainly two reasons for developing a Li-CO_2 reaction model in LITFIRE. First, from HEDL's experiments, some of the test results indicated that lithium carbonate was one of the major constituents of aerosols generated from the various gas reactions under air. The result suggested that lithium aerosol is more stable as lithium carbonate than as lithium oxide or lithium hydroxide. Even though the fraction of CO_2 is quite insignificant compared to the fraction of oxygen and nitrogen present in normal atmosphere, the amount of lithium carbonate aerosols generated is quite significant. If an unlimited amount of normal air is supplied, the contribution of lithium-CO_2 reaction to the total aerosols generated would be even more significant. Second, CO_2 has been suggested as a cover gas for lithium in some conceptual studies. This model will help assess the consequences of CO_2-Li reaction. These are major motivations for developing a Li-CO_2 reaction model in LITFIRE.

6.3.1 Model Description

At present, only a few lithium-CO_2 reaction experiments have been performed. HEDL's LC-1 and LC-2 experiments were used as reference cases for developing the lithium-CO_2 reaction model. However, in the LC-1 test, only surface reaction was observed and the lithium temperature decreased slowly from the initial lithium temperature of 238°C [9]. One report indicated that the carbonate layer buildup effect could effectively inhibit lithium-CO_2 reaction below the lithium temperature of 300°C [3]. Therefore, lithium-CO_2 reaction rate was assumed to be inhibited by the carbonate layer below 400°C. LC-2 experiment also suggested that the ignition temperature of lithium under CO_2 atmosphere is below 540°C and there was no carbonate layer inhibition effect observed above

540°C. Tables 2.1 and 2.2 show a summary of the LC-1 and LC-2 experiments.

In addition, in the LC-2 experiment, the preferred reaction was lithium -oxygen rather than lithium-CO_2. Approximately 83 percent of lithium reacted with CO_2 to produce solid lithium oxide while only about one percent of lithium reacted with CO_2 to produce solid lithium carbonate. However, most of the aerosols generated were of lithium carbonate. Therefore, it was appropriate to assume that all the aerosol generated is lithium carbonate. Lithium takes one of the two following reaction paths when it reacts with CO_2. One path produces lithium oxide and carbon. The other path results in lithium carbonate and carbon. Lithium reacting with carbon, produced by both paths, forms lithium carbide. From the LC-2 experiment, the reaction product was composed of 91.3% lithium oxide, 5.7% lithium carbonate, and 3.0% lithium carbide in weight fraction excluding carbon.

Since there is no knowledge concerning exactly what percent of lithium-CO_2 reaction will produce lithium oxide or lithium carbonate, a "combustion branching ratio" was defined. This is defined as the ratio of the reaction preferred by lithium when it reacts with CO_2. The ratios used for lithium- CO_2 reaction to produce lithium oxide and lithium carbonate were 87 and 13%. And lithium-carbide reaction rate was assumed to be 1 percent of the total reaction rate at a given time. Since lithium-oxygen reaction rate depends on the lithium temperature, the ratio may vary depending on the temperature. However, due to the scarcity of experimental data, the ratios were assumed to be constant regardless of the lithium temperature.

An option in LITFIRE was developed in order to allow lithium-CO_2 reaction under CO_2 atmosphere. Also, lithium-CO_2 reaction is allowed in normal atmospheric conditions as one of the gas constituents. The fraction of lithium carbonate aerosols generated from the lithium-CO_2 reaction was assumed to be 0.05. In order to allow the lithium-CO_2 reaction, mass flows in LITFIRE

was modified, which is shown in Figure 3.5. Most of the options of LITFIRE including gas injection, aerosol removal, secondary cell, and pan were modified in order to allow added mass flows introduced by lithium-CO_2 reaction. Also, the heat balance equations were modified. Furthermore, the lithium spray fire calculation was modified in order to allow instantaneous lithium spray fire prior to pool lithium-CO_2 reaction.

In the lithium-CO_2 reaction model, three reactions were allowed: 1) lithium-CO_2 reaction forming lithium oxide; 2) lithium-CO_2 reaction forming lithium carbonate: and 3) lithium-carbon reaction forming lithium carbide. The heat of reaction of forming lithium oxide is 143 Kcal/mole, 148.6 Kcal/mole for the reaction forming lithium carbonate, and 14.2 Kcal/mole for the lithium-carbon reaction forming lithium carbide [3].

In addition, in order to simulate HEDL's LC-2 experiment, a routine that simulates lithium relocation from the lithium transfer pot to the reaction pan was developed. In LC-2, it took approximately two and one-half minutes before 10 Kg of liquid lithium was transferred to the pan. That proved to be a significant fraction of the total reaction time.

6.3.2 Application of the Model to Experiment (HEDL's LC-2)

The model developed was applied to HEDL's LC-2 experiment in order to verify the accuracy of the model. Figures 6.17 through 6.20 show the results of the simulation. A detailed description of the experiment was given at the section 2 of Chapter two. After about three minutes from the beginning of the reaction, the reaction pan failed and the lithium fell to the catch pan. This caused a huge pressure and temperature peak in the containment vessel atmosphere. At about 5 minutes of the reaction time, argon was added in order to terminate the reaction. And at near 7 minutes of the reaction time, venting began. Since LITFIRE does not have an option which can simulate the corrosion of the pan, the simulation is only valid for the time until the pan failed.

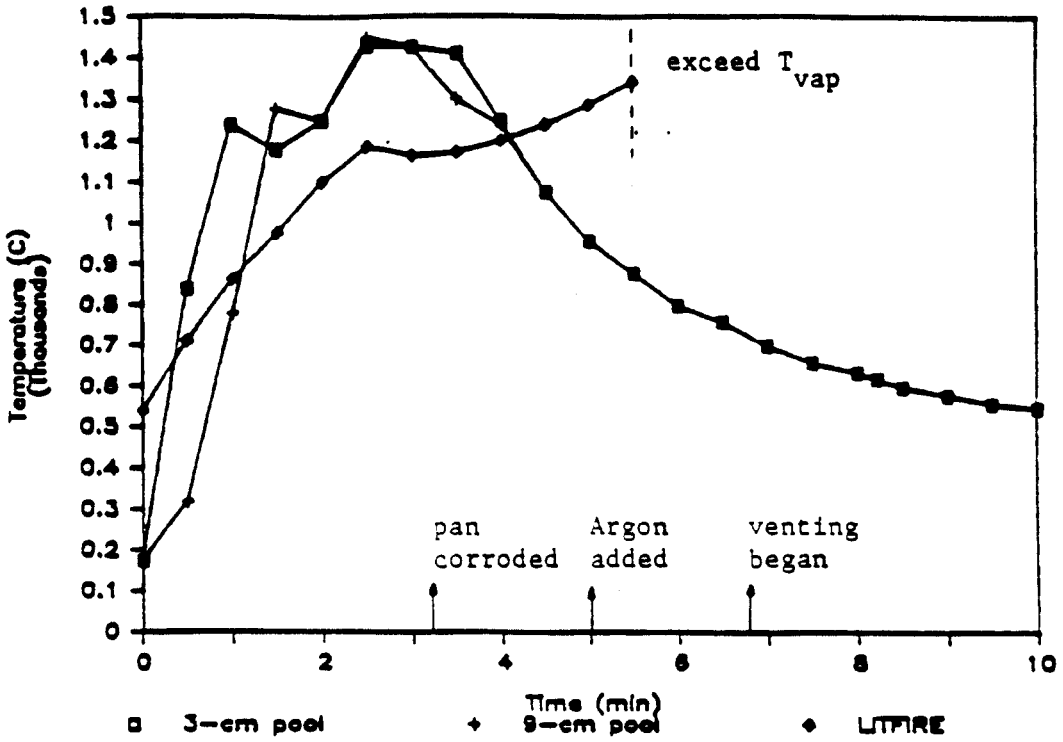

Fig. 6.17 Lithium pool temperature for HEDL's LC-2 experiment

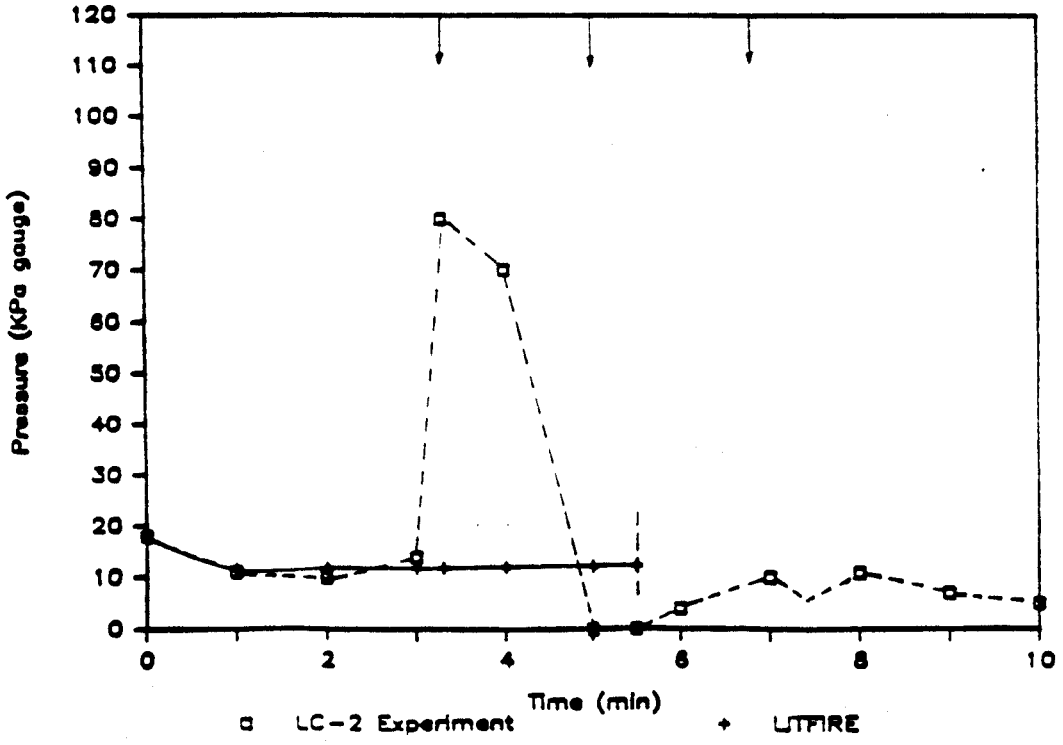

Fig. 6.18 Containment pressure for HEDL's LC-2 experiment

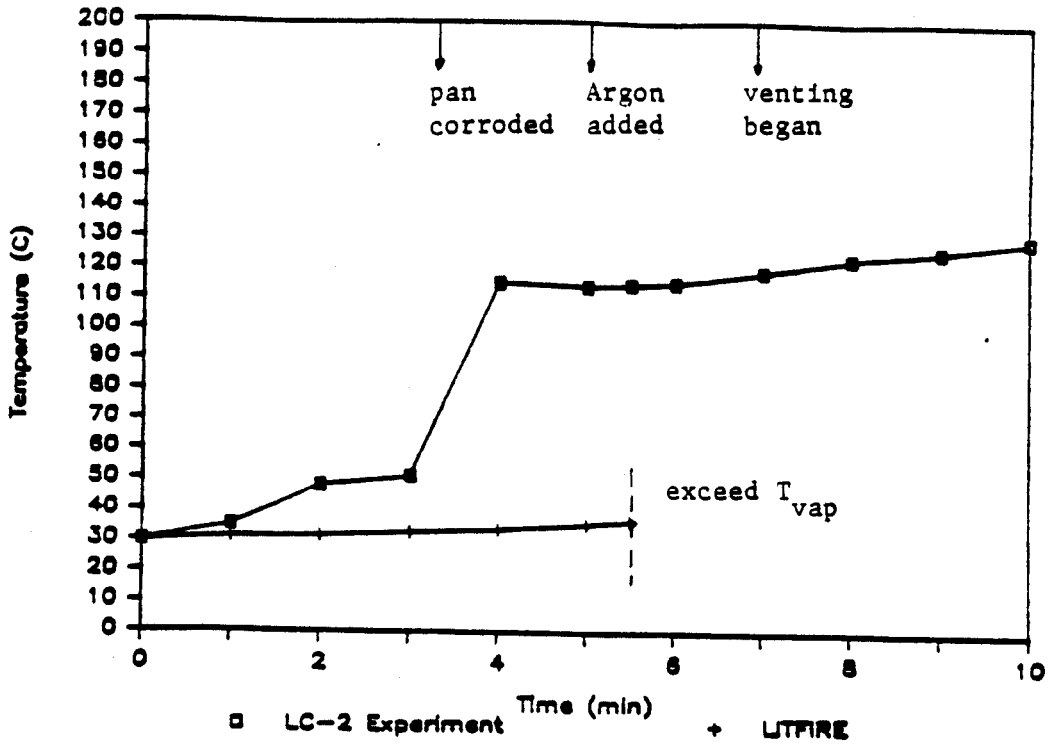

Fig. 6.19 Wall Temperature for HEDL'sLC-2 experiment

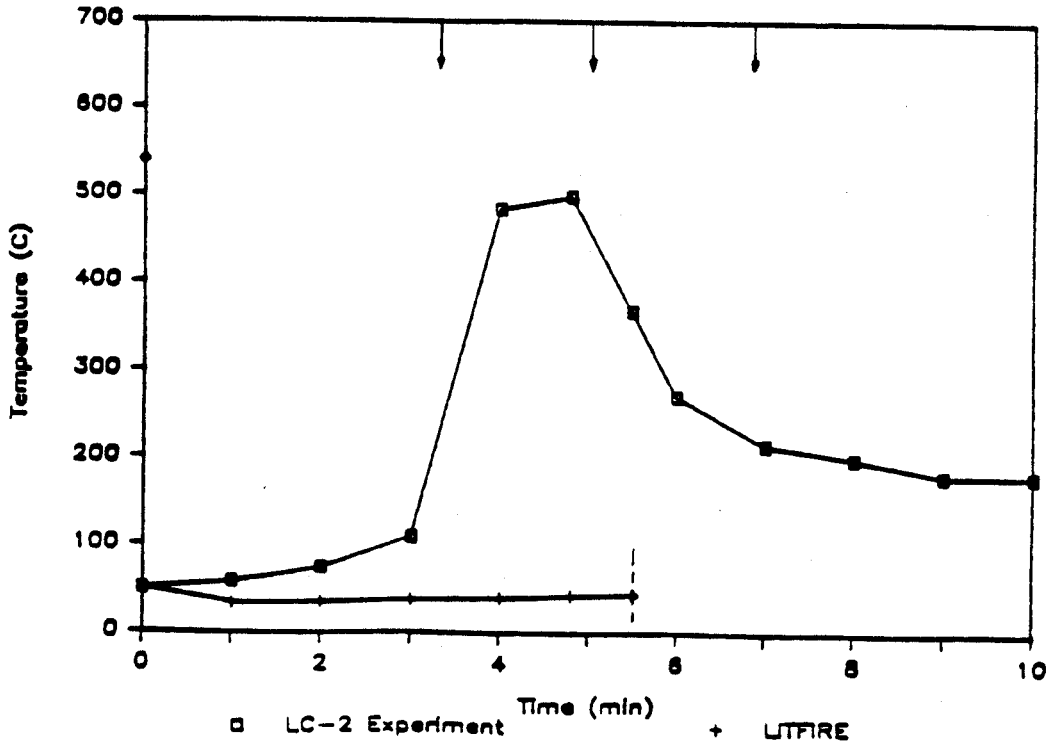

Fig. 6.20 Containment gas temperature for HEDL's LC-2 experiment

Since there was no provision in LITFIRE to compute the pressure and thermal history beyond the vaporization temperature of lithium, LITFIRE computation stopped when the lithium temperature exceeded the vaporization temperature. The initial lithium temperature of the experiment seen in Figure 6.13 was not the actual lithium pool temperature. It was the pan temperature and at that time, the thermocouples were not in direct contact with liquid lithium. As more liquid lithium was transferred to the pan, the thermocouple temperature increased instantaneously by contacting hot liquid lithium. That is why the temperature of the thermocouple located at 9 cm above the bottom of the pan increased instantaneously shortly after the thermocouple located at 3 cm contacted with the lithium. The actual lithium temperature was 540°C.

The predicted lithium temperature is in a rough agreement with the experimental result. The predicted lithium temperature was about few minutes delayed compared with the experimental result. Since the reaction was more vigorous than the lithium-air reaction experiments, the reaction occurred much faster and the peak lithium temperature was much higher. The containment pressure predicted was in good agreement while the wall and gas temperatures were underpredicted. A possible explanation for the underprediction may be due to incorrect flame temperature and its emissivity and percent of the aerosols generated by the reaction.

HEDL's experiment indicates that lithium-CO_2 reaction is similar to lithium- oxygen reaction, which can be more vigorous than Li-air. In fact, most of the solid reaction product produced was lithium oxide. This also indicates that lithium-oxygen reaction is a preferred reaction. The heat of reaction generated by forming lithium oxide and lithium carbonate is approximately the same. From the simulation, the products were composed of 91.2% lithium oxide, 6.7% lithium carbonate, and 2.1% lithium carbide, in good agreement with the experimental values.

References

1) M. S. Tillack and M. S. Kazimi, "Development and Verification of the LITFIRE Code for Predicting the Effects of Lithium Spills in Fusion Reactor Containments," MIT, Plasma Fusion Center, Report No. PFC-RR-80-11, July 1980.

2) D. Smith, et. al.. "Blanket Comparison and Selection Study," ANL/FPP-84-1, 1984.

3) D. W. Jeppson, et. al., "Lithium Literature Review: Lithium's Properties and Interaction," HEDL-TME-78-15, April, 1978.

4) E. F. McFarlane and F. C. Tompkins, "Nitridation of Lithium," "Trans. Faraday Society," Volume 58, 1962.

5) C. C. Addison and B. M. Davies, "Reaction of Nitrogen with Stirred and Unstirred Lithium," "J. Chemical Society (A)," page 1822, 1969.

6) J. O. Cowles and A. D. Pasternak, "Lithium Properties Related to Use as a Nuclear Reactor Coolant," UCRL-50647, Lawrence Radiation Laboratory, Ca., April 18, 1969.

7) W. J. Ijams and M. S. Kazimi, "Temperature Effects on Lithium-Nitrogen Reaction Rates," MIT PFC/RR-85-7, Jan. 1985.

8) D. W. Jeppson, et al., "Interaction of Liquid Lithium with Various Atmospheres, Concretes, and Insulating Materials; and Filtration of Lithium Aerosols," HEDL-TME-79-7 UC 20, June 1979.

9) D. W. Jeppson et al., "Scoping Studies: Behavior and Control of Lithium and Lithium Aerosols," HEDL-TME 80-79 UC 20. Jan. 1982.

10) L. D. Muhlestein et al., "Summary of HEDL Fusion Reactor Safety Support Studies," HEDL-SA-2360, 1981.

11) D. W. Jeppson et al., A draft report of "Results and Code Prediction Comparisons of Lithium-Air Reaction and Aerosol Behavior Tests," HEDL-TME-85-25, Jan. 16, 1986.

12) D. W. Jeppson, Personal conversation made in December 1985.

13) I. Charak and L. W. Person, "SPOOL-FIRE: Analysis of Spray and Pool Sodium Fire," Argonne National Laboratory, October 1976.

14) D. A. Dube and M. S. Kazimi, "Analysis of Design Strategies for Mitigating the Consequences of Lithium Fire Within Containment of Controlled Thermonuclear Reactors," MITNE-219, July 1978.

15) V. J. Gilberti and M. S. Kazimi, "Modeling of Lithium and Lithium-Lead Reactions in Air Using LITFIRE," MIT PFC/RR-83-08, Jan. 1983.

16) E. Yachimiak et al., "LITFIRE User's Guide," MIT PFC/RR-83-11, June 1983.

17) R. Rozier, "A Study Lithium-Oxygen Reactions," B.S. Thesis, Dept. of Nucl. Eng., MIT, Feb. 1986.

APPENDIX 1

Summary of Experimental Runs

Run No.	Pool Temp. (C)	Initial Gas Comp.(%)		Final Gas Comp.(%)		Gas Flow (liters/min)
		N2	O2	N2	O2	
80-20%						
1	discarded due to impurity problem.					
2	discarded due to impurity problem.					
3	discarded due to impurity problem.					
11	383	79.9	20.1	82.7	17.3	2.0
4	493	80.9	19.1	82.8	17.2	2.0
7	592	82.5	17.5	86.5	13.5	2.5
6	663	81.9	18.1	87.9	12.1	3.5
5	760	82.9	17.1	89.2	10.8	3.5
8	865	78.9	21.1	95.5	4.5	3.5
18	943	79.4	20.6	93	7	5.5
9	960	78.4	21.6	95.5	4.5	3.5
17	1051	78.6	21.4	96.9	3.1	5.5
10	1070	78.2	21.8	98.4	1.6	3.5
16	1090	78.6	21.4	97.6	2.4	5.5
	1110	78.6	21.4	97.6	2.4	5.5
90-10%						
21	1033	89.3	10.7	99.2	0.8	5.5
20	947	87.6	12.4	97.9	2.1	5.5
13	912	90.7	9.3	99	1	3.5
12	air filter cloaked.					
19	823	89.4	10.4	96.5	3.5	5.5
14	689	89.9	10.1	95	5	3.5
15	488	88.6	11.4	94	6	3.0
95-5%						
24	1004	94.1	5.9	100	0	5.5
23	930	94.2	5.8	100	0	5.5
25	842	94.9	5.1	99	1	5.5
26	668	94.1	5.9	97.3	2.7	4.5
22	514	95.4	4.6	96.3	3.7	3.0

Run No.	Reaction Rate* (g Li/min-cm2)		Total RR*	Initial Press.** (Psi)	Reacted Press.** (Psi)
	Li-Nitrogen	Li-Oxygen			
80-20%					
1	Discarded due to lithium impurity.				
2	Discarded due to lithium impurity.				
3	Discarded due to lithium impurity.				
11	0.0056	0.0036	0.0091	0.0451	0.0083
4	0.028	0.005	0.033	0.1892	0.0121
7	0.031	0.0209	0.052	0.1994	0.0178
6	0.0715	0.0468	0.1183	0.2591	0.0341
5	0.089	0.079	0.167	0.2586	0.0406
8	0.3064	0.1107	0.4171	0.3051	0.1305
18	0.4675	0.1861	0.6536	0.3713	0.1719
9	0.5443	0.1869	0.7312	0.3173	0.1899
17	0.2972	0.2255	0.4128	0.4062	0.1483
10	0.2301	0.183	0.4131	0.3242	0.121
16	0.1023 0.0134	0.2301 0.2334	0.3324 0.2468	0.3968 0.3875	0.103 0.0786
90-10%					
21	0.452	0.12	0.572	0.40887	0.14704
20	0.5905	0.131	0.7211	0.40660	0.18351
13	0.5988	0.0526	0.6514	0.2067	0.1460
12	air filter cloacked.				
19	0.447	0.086	0.533	0.3674	0.1343
14	0.1522	0.0402	0.1924	0.2190	0.0487
15	0.063	0.008	0.071	0.034	0.0175
95-5%					
24	0.689	0.0676	0.7566	0.40114	0.1845
23	0.662	0.0674	0.7294	0.40690	0.1780
25	0.5912	0.0483	0.6395	0.37143	0.1548
26	0.2573	0.0207	0.278	0.1698	0.0673
22	0.0851	0.00934	0.09444	0.2682	0.02312

* Averaged Reaction Rate

** Pressure measurement not averaged. (one of the values averaged.)